

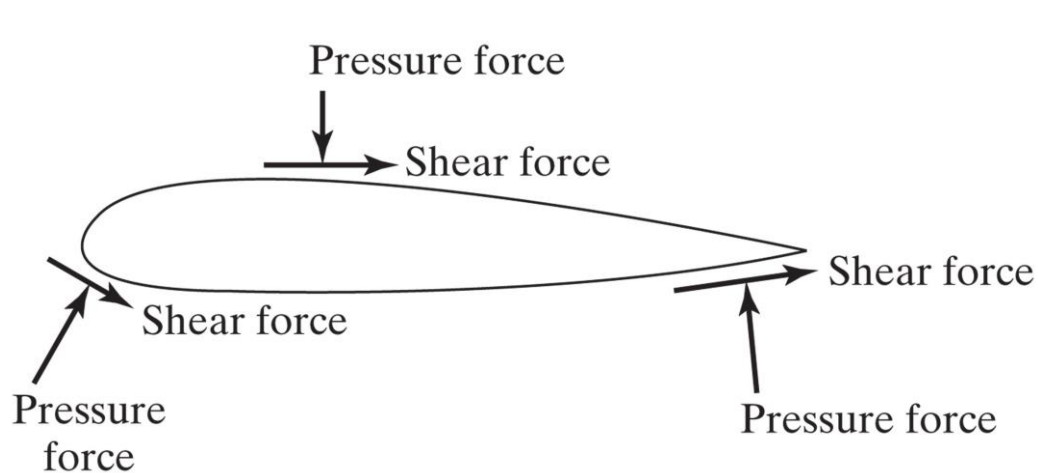
Part 2.

Anatomy of the wing and its performance

A reminder on the notation and
how forces are computed

A reminder on the notation and how forces are computed

- Aerodynamic forces acting on a body.
 - The aerodynamic forces acting on a body are due to the action of pressure and shear stresses on the surface of the body.
 - The aerodynamic forces can be decomposed into two main contributions, namely,
 - Pressure contribution and viscous contribution (shear stresses).
 - The balance between both contributions can change according to the application or working conditions.
 - Sometimes the pressure contribution is larger than the viscous contribution, and sometimes the viscous contribution can be larger than the pressure contribution



$$\mathbf{F} = \int_{\partial S} \left(\overset{\substack{\text{Pressure contribution} \\ \downarrow}}{-p\mathbf{I}} + \overset{\uparrow}{\text{Viscous contribution}} \boldsymbol{\tau} \right) \cdot \mathbf{n} dS$$

A reminder on the notation and how forces are computed

- If the force coefficients are known, the forces and moments acting on an airfoil (2D) can be computed as follows,

$$L = \frac{1}{2} \times \rho \times V^2 \times c \times c_l$$

where c_l is the airfoil lift coefficient, c the airfoil chord, V is the free-stream velocity and ρ is the air density

$$D = \frac{1}{2} \times \rho \times V^2 \times c \times c_d$$

where c_d is the airfoil drag coefficient, c the airfoil chord, V is the free-stream velocity and ρ is the air density

$$M = \frac{1}{2} \times \rho \times V^2 \times c \times c_{ref} \times c_m$$

where c_m is the airfoil pitching moment coefficient (usually computed at $c/4$), c the airfoil chord, c_{ref} is the reference arm, V is the free-stream velocity and ρ is the air density

- Notice that the forces and moments are computed per unit depth in 2D.
- Remember, the force coefficients contain the information related to the dependence on the angle of attack, Reynolds number and Mach number.

A reminder on the notation and how forces are computed

- If the force coefficients are known, the forces and moments acting on a wing (3D) can be computed as follows,

$$L = \frac{1}{2} \times \rho \times V^2 \times S_{ref} \times C_L$$

where C_L is the wing lift coefficient, S_{ref} is the wing reference area, V is the free-stream velocity and ρ is the air density.

$$D = \frac{1}{2} \times \rho \times V^2 \times S_{ref} \times C_D$$

where C_D is the wing drag coefficient, S_{ref} is the wing reference area, V is the free-stream velocity and ρ is the air density.

$$M = \frac{1}{2} \times \rho \times V^2 \times S_{ref} \times c_{ref} \times C_M$$

where C_M is the wing pitching moment coefficient (usually computed at $c/4$ of the MAC), c_{ref} is the reference arm, S_{ref} is the wing reference area, V is the free-stream velocity and ρ is the air density.

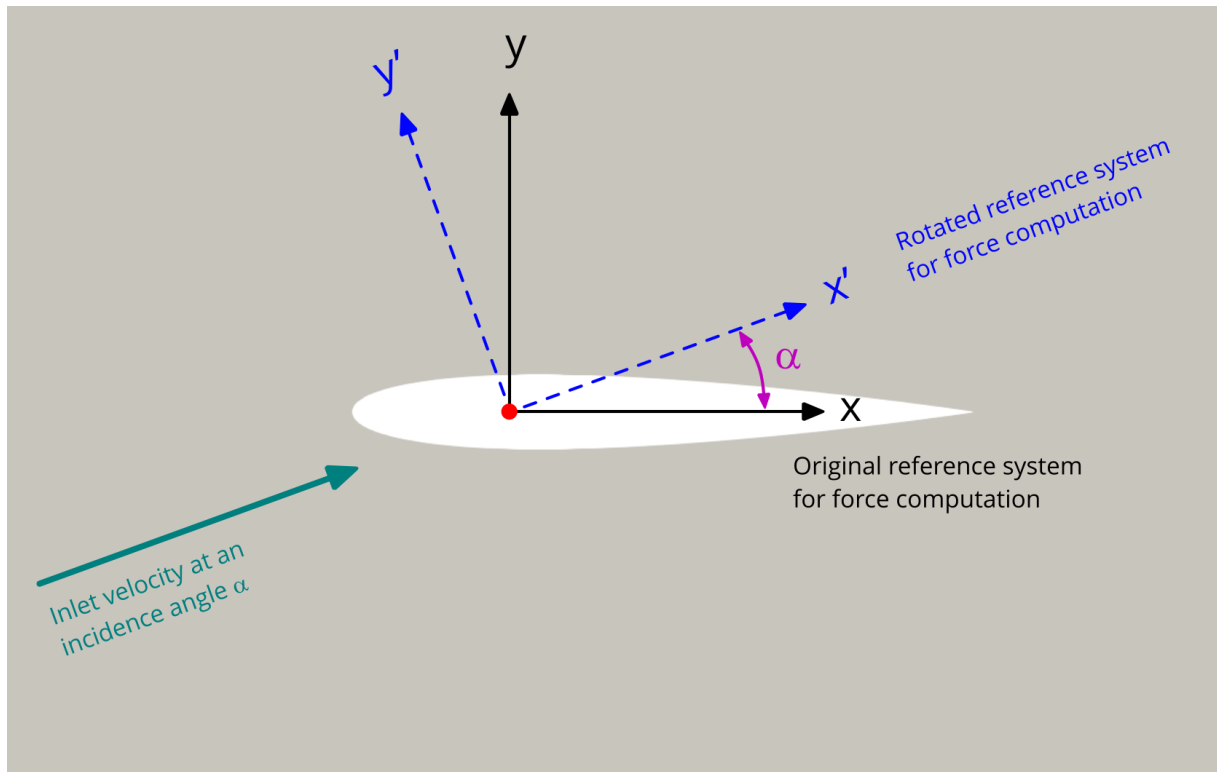
- Remember, the force coefficients contain the information related to the dependence on the angle of attack, Reynolds number and Mach number.

A reminder on the notation and how forces are computed

- The previous equations are used to get the forces and moments if the force coefficients are known.
- The coefficients contain all the information related to angle of attack, wing/airfoil geometry, Reynolds number, and compressibility effect.
- If you are doing CFD, you can directly compute the forces and moments by integrating the pressure and viscous forces over the body surface.
- In 2D we use the airfoil chord to normalize the coefficients, and in 3D we use the wing planform area.
- Some people might use the wetted surface for C_D (I usually do it in CFD).

A reminder on the notation and how forces are computed

- Remember, lift and drag acting on an airfoil or a wing are perpendicular and parallel to the incoming flow, respectively.
- So, if the inlet velocity is entering at a given angle, you should adjust the vectors lift and drag vectors, so they are aligned with the incoming flow (rotation matrix).



$$\text{liftDir } (-\sin(\alpha), \cos(\alpha), 0)$$

$$\text{dragDir } (\cos(\alpha), \sin(\alpha), 0)$$

A reminder on the notation and how forces are computed

- A final reminder about notation:

- The following notation refers to wing coefficients:

C_L C_D C_M  All in uppercase letters

- The following notation refers to wing section coefficients:

C_l C_d C_m  The subscripts are in lowercase letters

- The following notation refers to airfoil coefficients:

c_l c_d c_m  All in lowercase letters

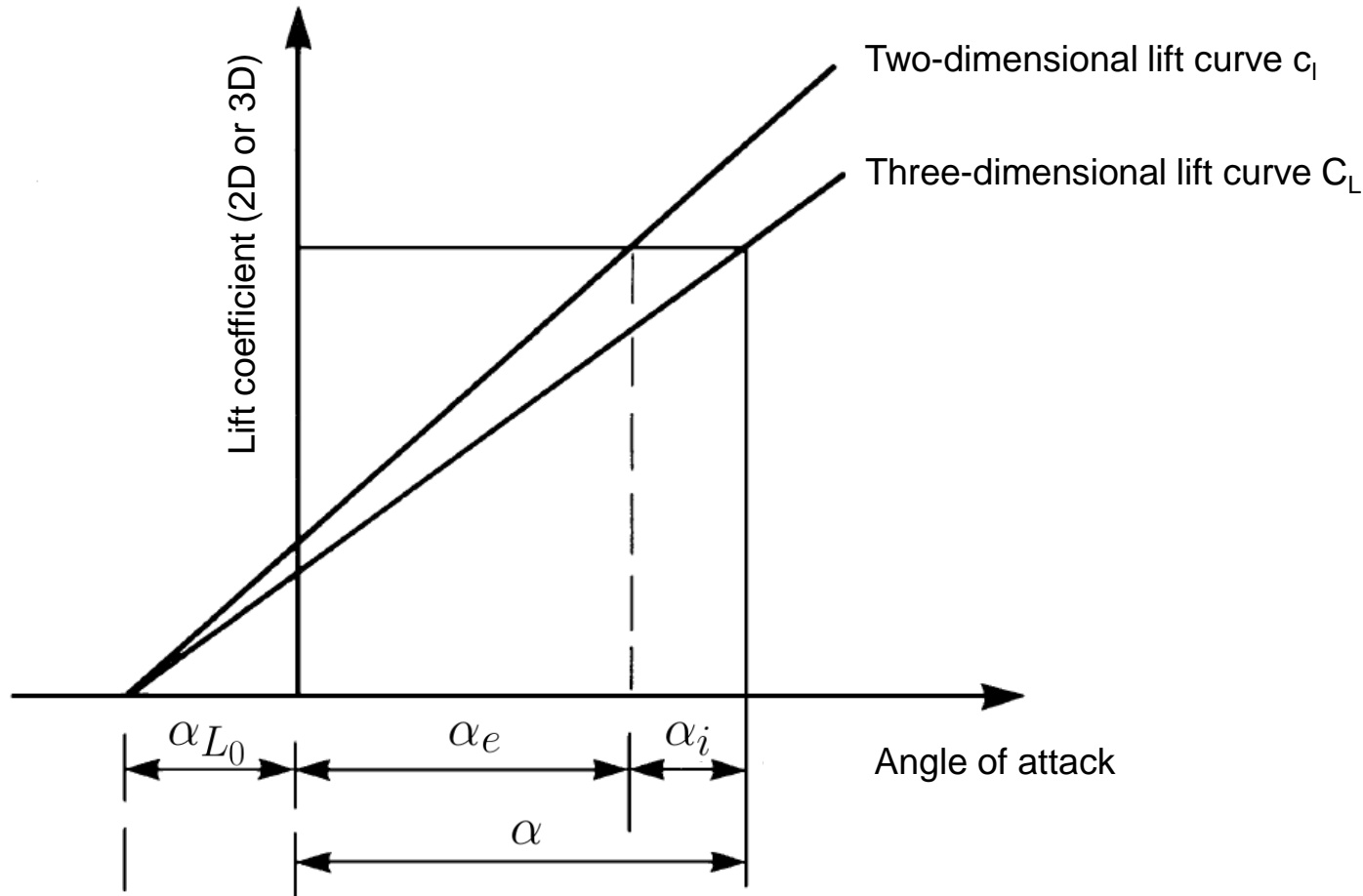
Lift curve slope of an airfoil and a finite-span wing

Lift curve slope of an airfoil and a finite-span wing

- Due to three-dimensional effects, the behavior of wings is slightly different from that of airfoils.
- The difference in the aerodynamic behavior is more evident when three-dimensional effects are larger.
 - Usually, this is the case of low aspect ratio wings.
- For very large aspect ratios, the behavior of wings is close to that of airfoils.
 - After all, airfoils can be seen as wings with infinity aspect ratio.
- What is aspect ratio? It will be covered in the next section.
- It is clear that we cannot use the same design criteria used for airfoils when working with wings.
 - For example, the slope of lift curve of wings is not anymore 2π .

Lift curve slope of an airfoil and a finite-span wing

- Comparison of the lift-curve slope of a two-dimensional airfoil with that for a finite-span wing.
 - The lift slope of finite-span wing becomes less as the wingspan becomes smaller.
 - For a wing with α_{L_0} , the effective angle of attack α_e is reduced by the induced angle α_i .
 - The angle α_i is induced by the downwash along the wingspan.



Airfoil lift curve slope

$$C_{L_\alpha} = a = \frac{a_0}{1 + \frac{a_0}{\pi AR} (1 + \tau)}$$

Wing efficiency, zero for elliptical lift distribution

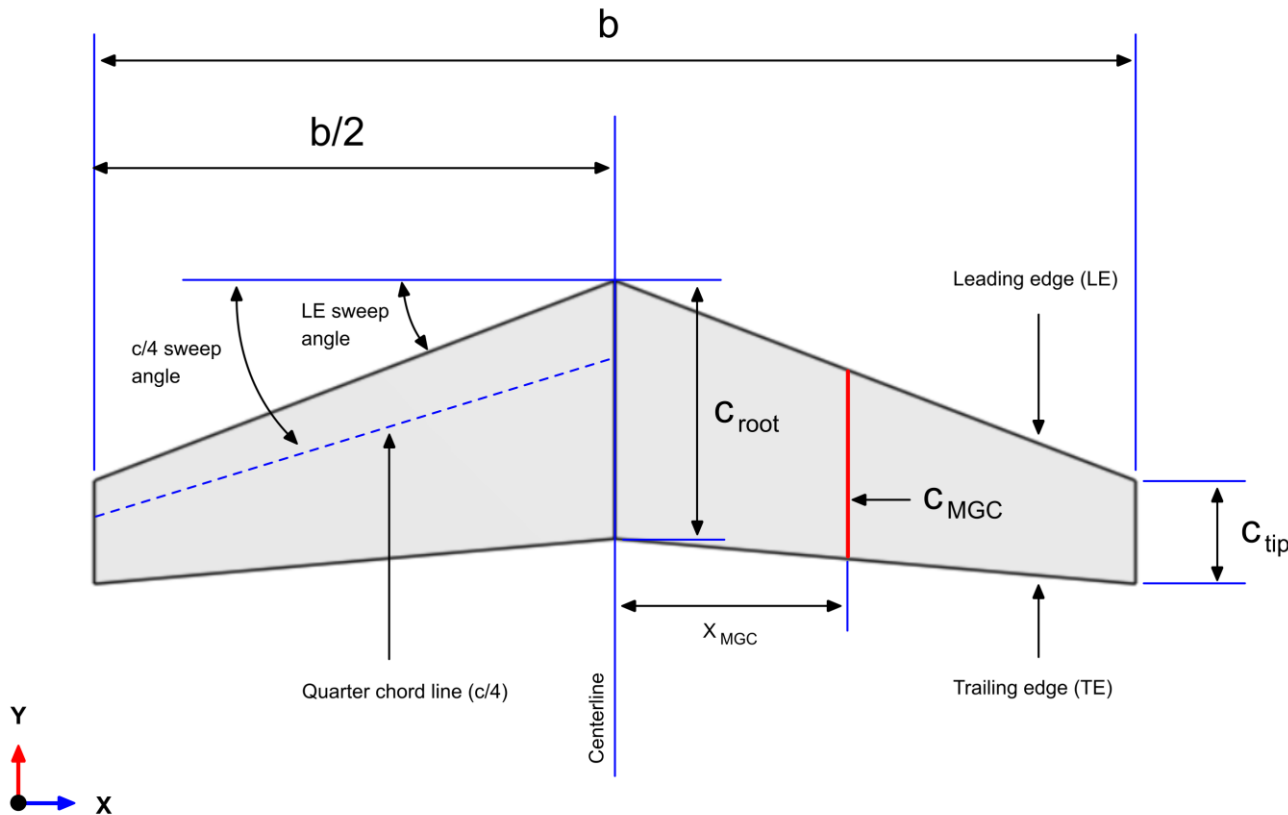
$$C_L = a(\alpha - \alpha_{L_0})$$

$$\alpha_e = \alpha - \alpha_i - \alpha_{L_0}$$

Anatomy of the wing

Anatomy of the wing

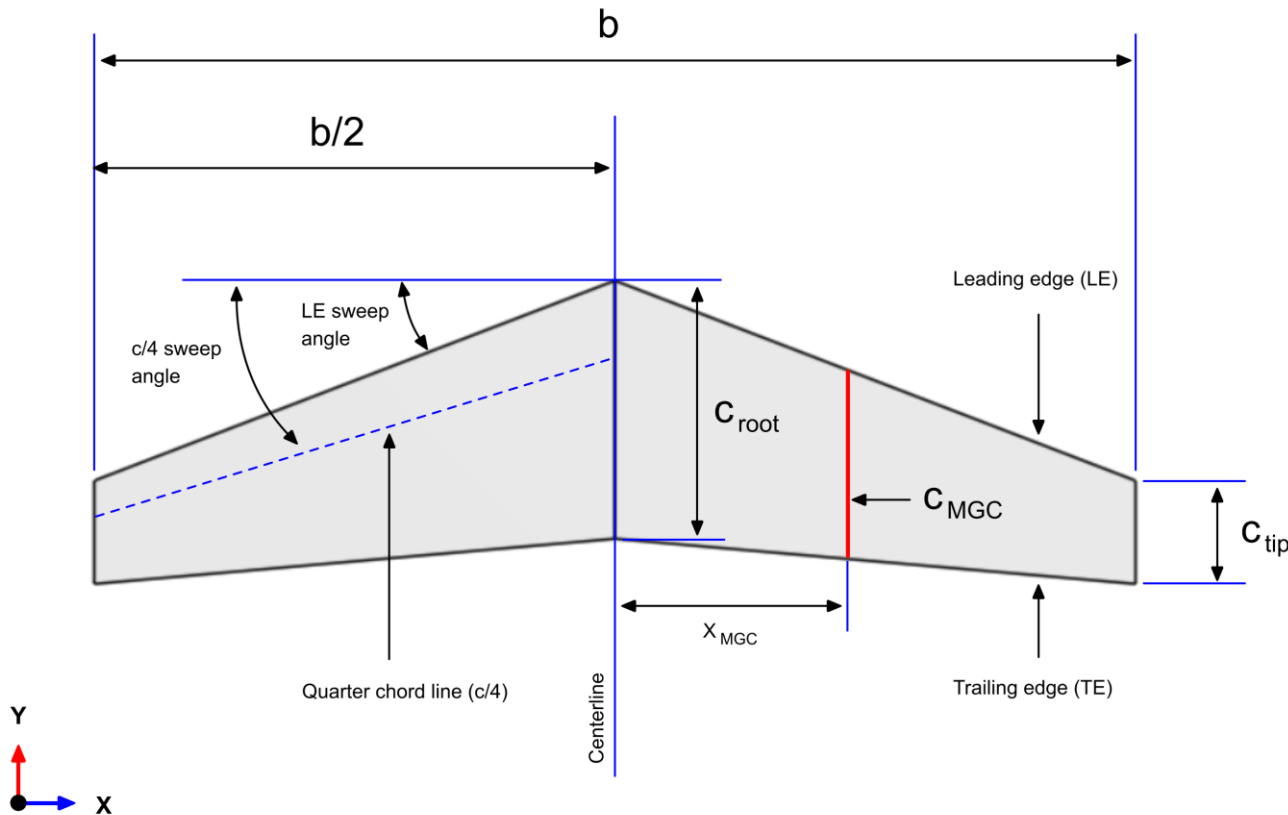
- Main geometrical definitions of a trapezoidal wing planform.



- The wingspan, b , is the straight-line distance measured from wing tip to wing tip.
- The quantity $b/2$ is called wing semi-span (the span of one single wing).
- The root chord, C_{root} , is the chord at the wing centerline
- The tip chord, C_{tip} , is the chord at the wing tip.
- The ratio of the tip chord to the root chord is the taper ratio (**TR** or λ).
- The sweep angle, **SA** or Λ , is usually measured as the angle between the quarter chord line and a perpendicular to the root chord.
- Sweep angles of the leading edge (**LE**) or trailing edge (**TE**) are also often used.

Anatomy of the wing

- Main geometrical definitions of a trapezoidal wing planform.



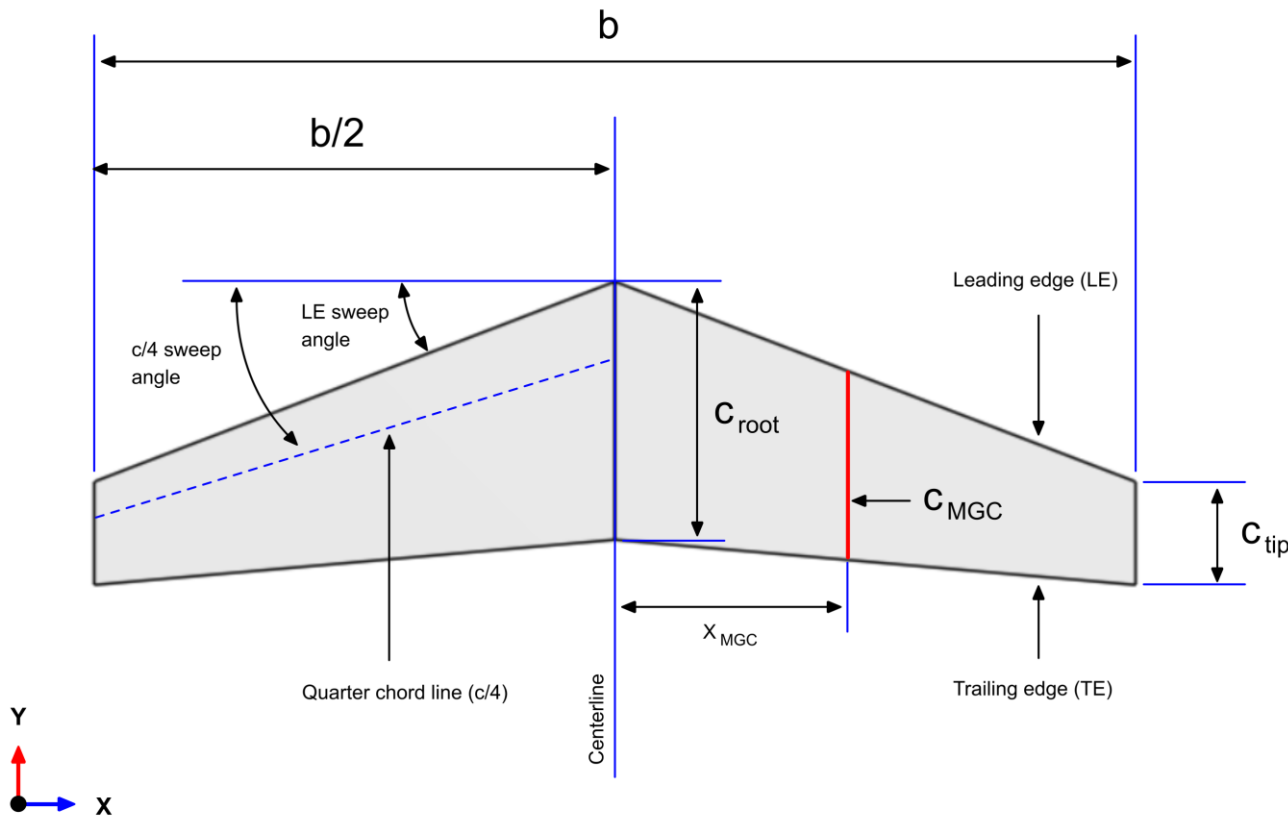
- C_{MGC} is the mean geometrical chord, which can be computed as follows,

$$C_{MGC} = \left(\frac{2}{3}\right) C_{root} \left(\frac{1 + \lambda + \lambda^2}{1 + \lambda}\right)$$

- The mean geometrical chord (C_{MGC}) can be used to compute the wing Reynolds number.
- To compute the local Reynolds number, or the Reynolds number at a given cross-section, you need to use the local airfoil chord.
- You can also use the mean aerodynamic chord (MAC) to compute the wing Reynolds number.
- By the way, do not confuse the mean geometrical chord MGC with the MAC.

Anatomy of the wing

- Main geometrical definitions of a trapezoidal wing planform.



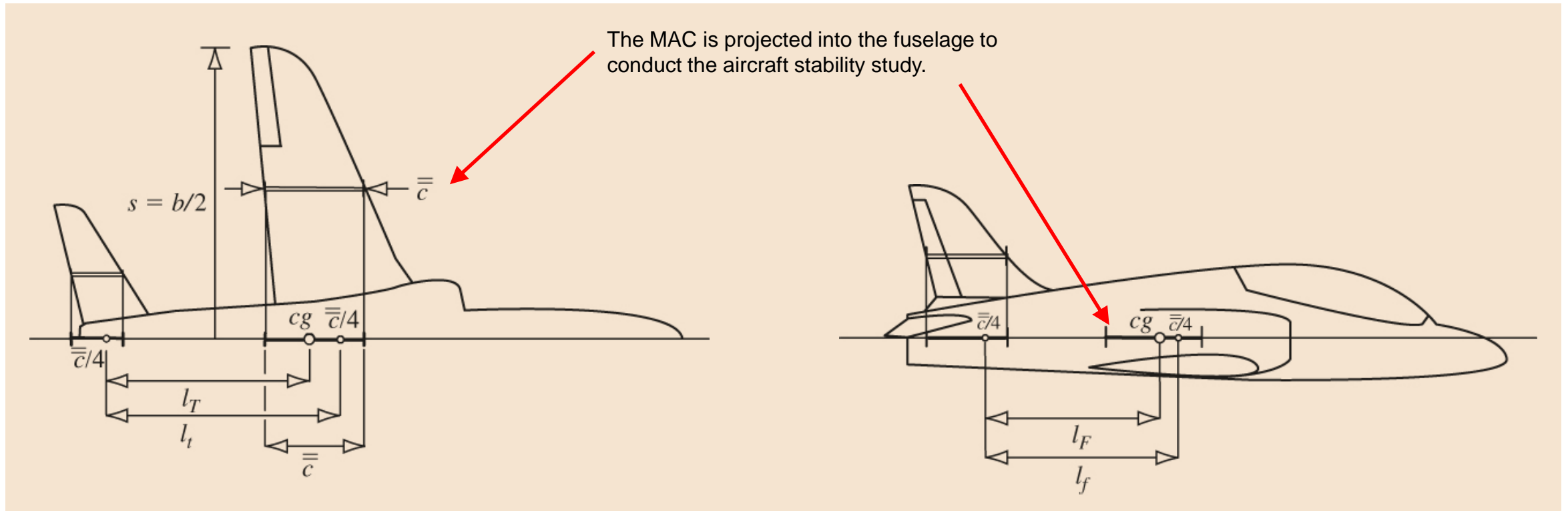
- The MAC is defined as follows,

$$mac = \frac{1}{S} \int_{-b/2}^{+b/2} [c(y)]^2 dy$$

- In few words, the MAC is a two-dimensional representation of the whole wing.
- The MAC is a very important quantity used for aircraft stability.
- Aircraft center of gravity limitations and the actual center of gravity CG are often expressed in terms of percent of the MAC.
- This is not strictly true, but the mean geometrical chord (C_{MGC}) is approximately the same as the MAC.

Anatomy of the wing

- A description of the geometric layout of an aircraft is fundamental to conduct an aircraft stability study.
- It is convenient that the geometry of the aircraft can be adequately described by a small number of dimensional reference parameters, as shown in the figures below.
- Many of the variables used in aircraft stability are common to wing aerodynamics.



Anatomy of the wing

- **Wing aspect ratio (AR).**
- Wing **AR** is a measure of how wide is the wing compared to its chord.
- The wing aspect ratio can be computed as follows,

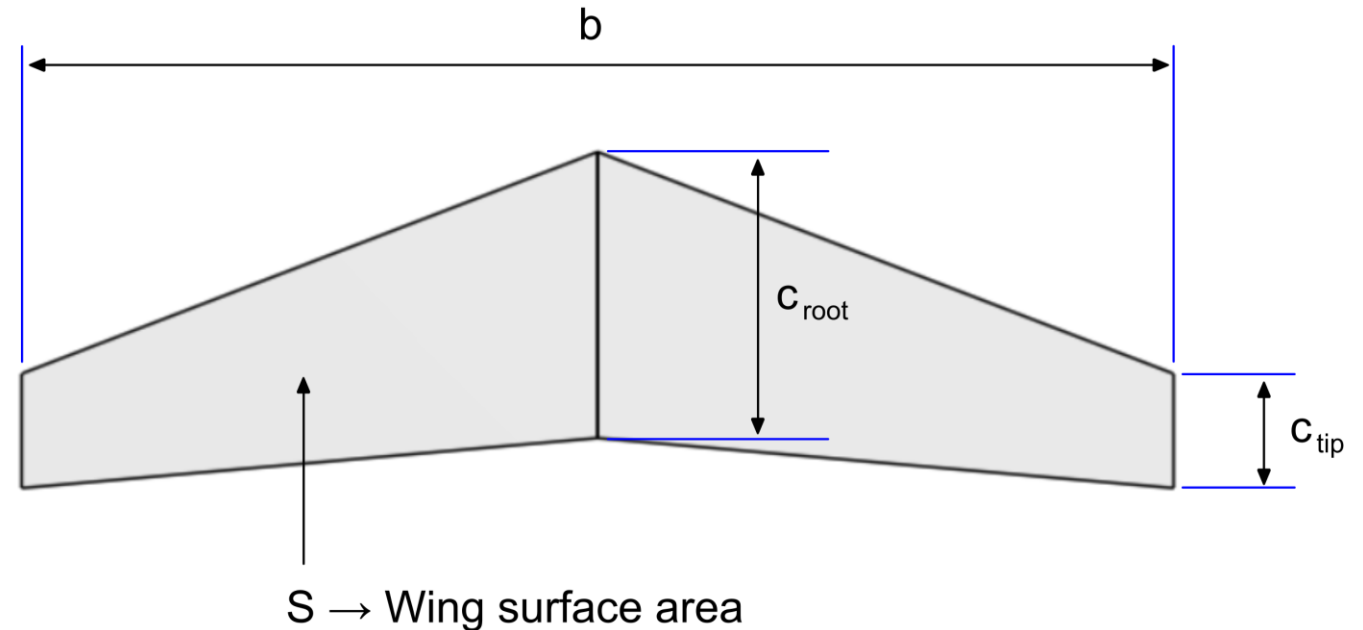
$$AR = \frac{b^2}{S}$$

- **AR** is used when determining the aerodynamic characteristics and structural weight of the wing.
- For a constant-chord wing of chord **c** and span **b**, the aspect ratio is given by:

$$AR = \frac{b}{c}$$

- **AR** is related to induced drag as follows,

$$C_{D_{ind}} = \frac{C_L^2}{\pi AR e}$$

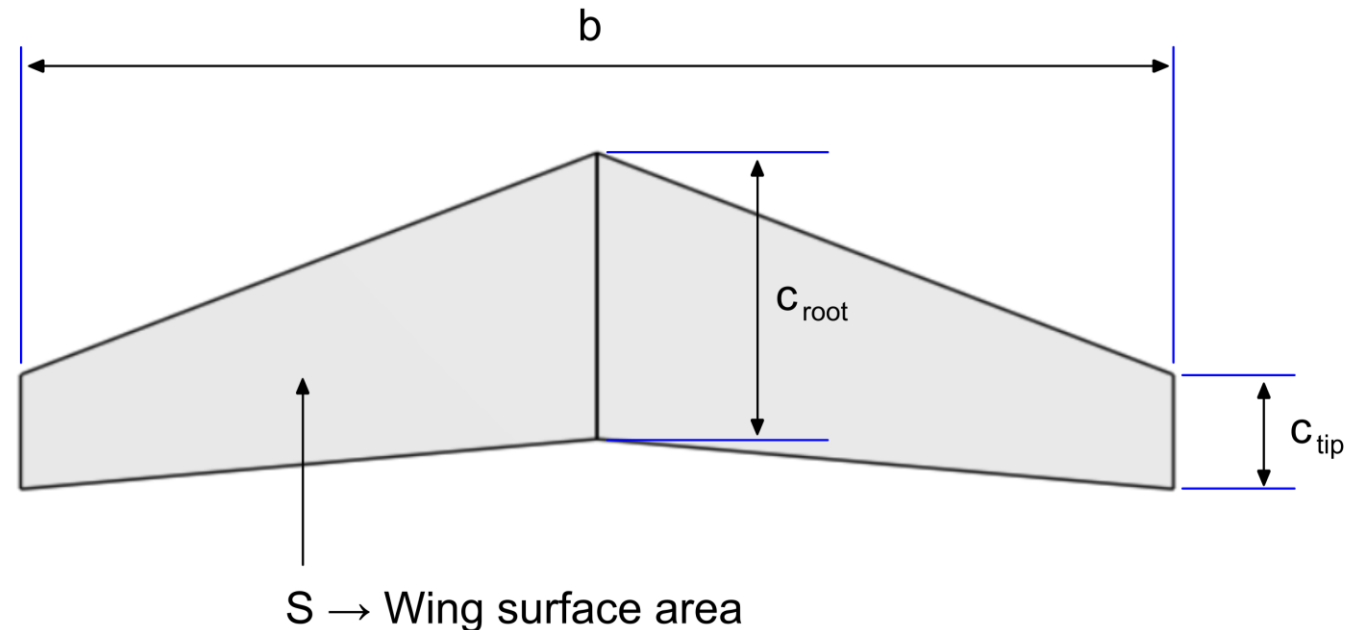


Anatomy of the wing

- The wing taper ratio (TR or λ).
- The ratio of the tip chord to the root chord is the taper ratio.
- The wing taper ratio can be computed as follows,

$$TR = \lambda = \frac{C_{tip}}{C_{root}}$$

- The taper ratio affects the lift distribution and structural weight of the wing.
- A rectangular wing has a taper ratio of 1 while a pointed tip delta wing has a taper ratio of 0

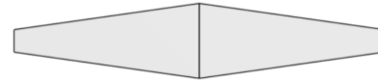


Anatomy of the wing

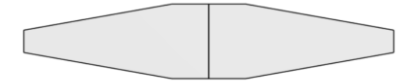
- Different wing planforms – A selection of the most common ones.
- Each one has different aerodynamic characteristics.



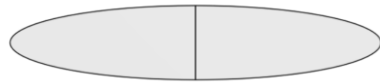
Rectangular wing



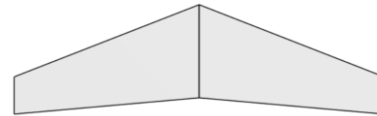
Trapezoidal wing



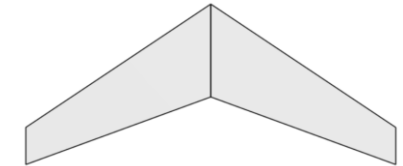
Compound tapered wing



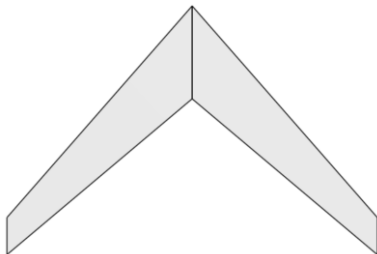
Elliptical wing



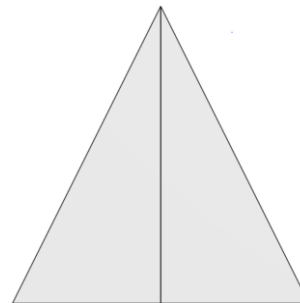
Slightly swept wing



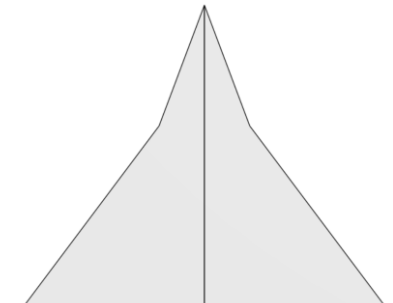
Moderately swept wing



Highly swept wing



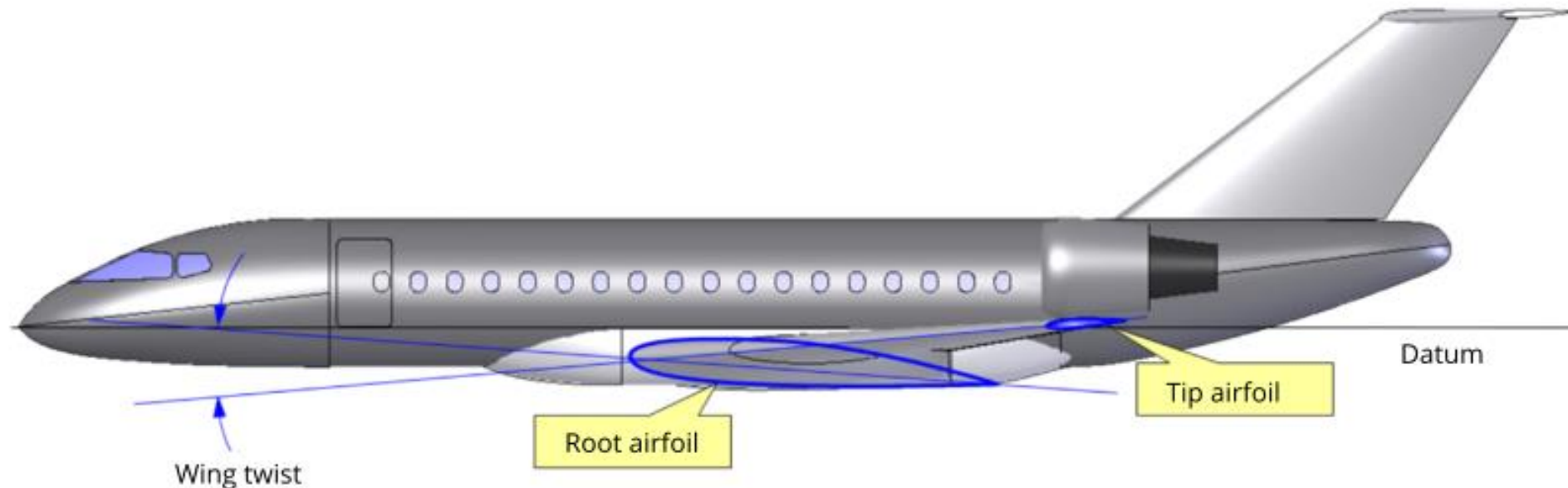
Delta wing



Double delta wing

Anatomy of the wing

- And of course, the wing has a cross section, which can be different along the wingspan and can have different incidence angles.
- From the 2D lectures, we know the aerodynamic properties of airfoil sections.
- It is important to know that the wing will inherit most of the properties of the airfoil section.
- However, due to three-dimensional effects, the performance of wings is different from that of airfoil sections.



Anatomy of the wing

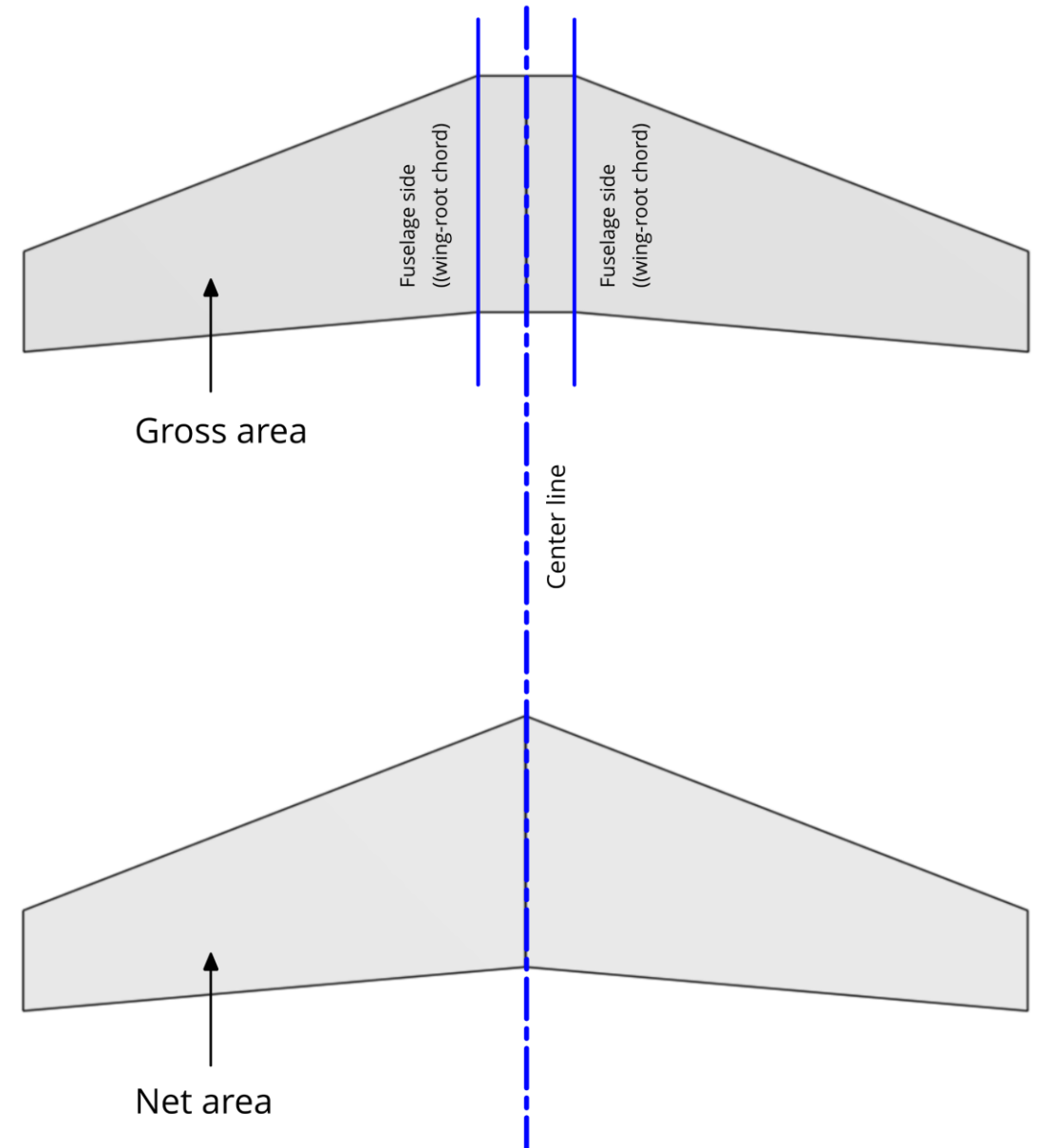
- The wing planform area (including the continuation of the fuselage) is the wing gross area,

$$S_{gross}$$

- The exposed wing planform area is the net area (area excluding the continuation of the fuselage),

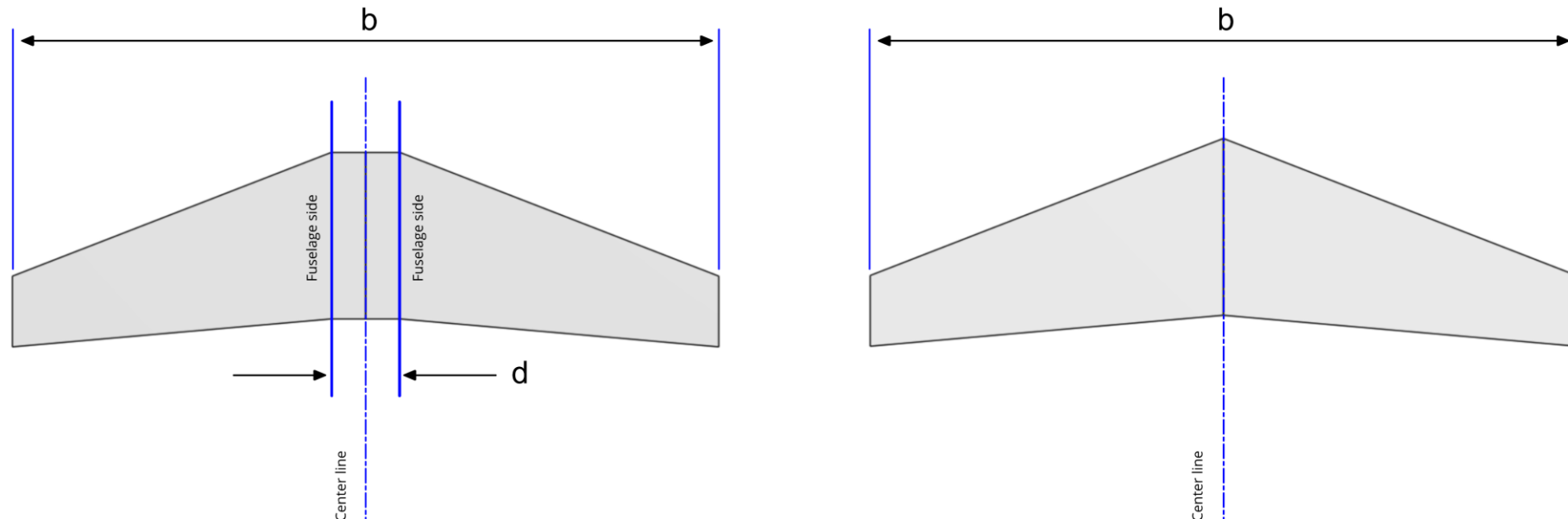
$$S_{net}$$

- Note that the specifics of the method used to estimate the gross area or net area are irrelevant.
- The wing area serves as the reference area for most aerodynamic coefficients.
- When choosing the gross area or net area you must be consistent.
- Consistency is as important as precision.



Anatomy of the wing

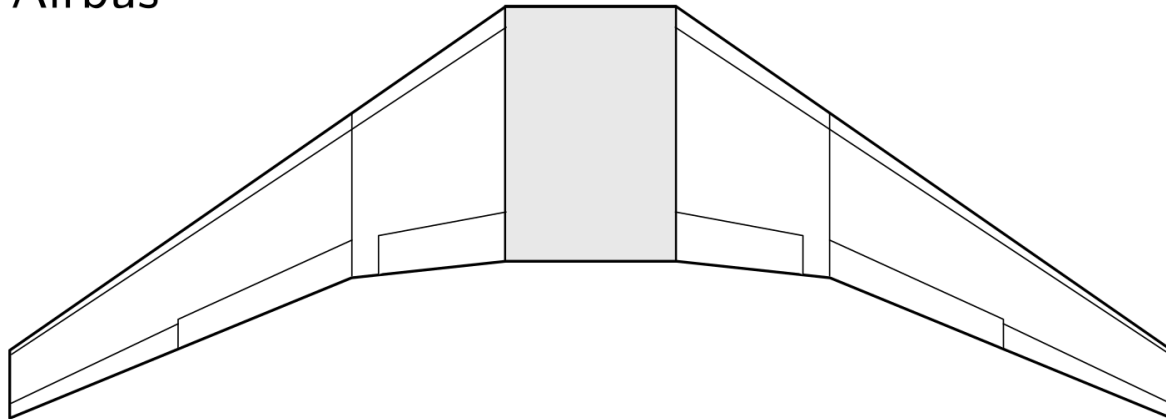
- There is no accurate analytical method that can predict the lift of the wing-fuselage combination.
- Either the configuration must be tested in a wind tunnel, or a computational fluid dynamic calculation must be made.
- We cannot even say in advance whether the combined lift will be greater or smaller than the sum of the two parts.
- For subsonic speeds, however, data obtained using different fuselage thicknesses, d , mounted on wings with different spans, b , show that the total lift for a wing-fuselage combination is essentially constant for d/b ranging from 0 (wing only) to 6 (fat fuselage with a short, stubby wing) [1].
- Hence, the lift of the wing-fuselage combination can be treated as simply the lift on the complete wing by itself, including that portion of the wing that is masked by the fuselage.
- Therefore, we will consistently use the gross area S_{gross} .



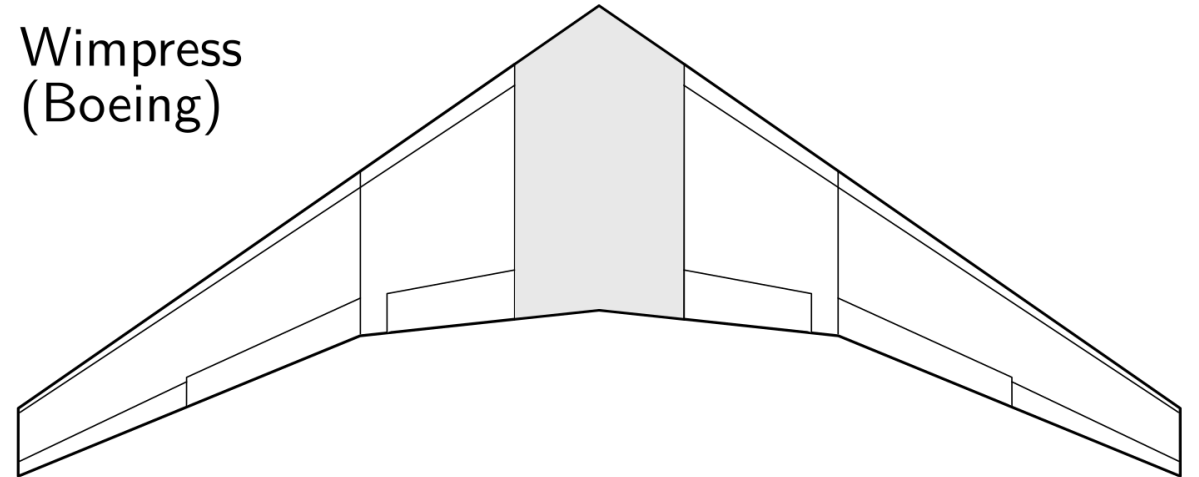
Anatomy of the wing

- A little note on how to estimate the gross area.
 - To estimate the gross area, the two most important methods are the Wimpress method (used by Boeing) and the Airbus method.
 - Either method is acceptable.
 - You must be consistent with the method used.
 - Remember, the wing area only serves as the reference area for most aerodynamic coefficients.

Airbus



Wimpress
(Boeing)

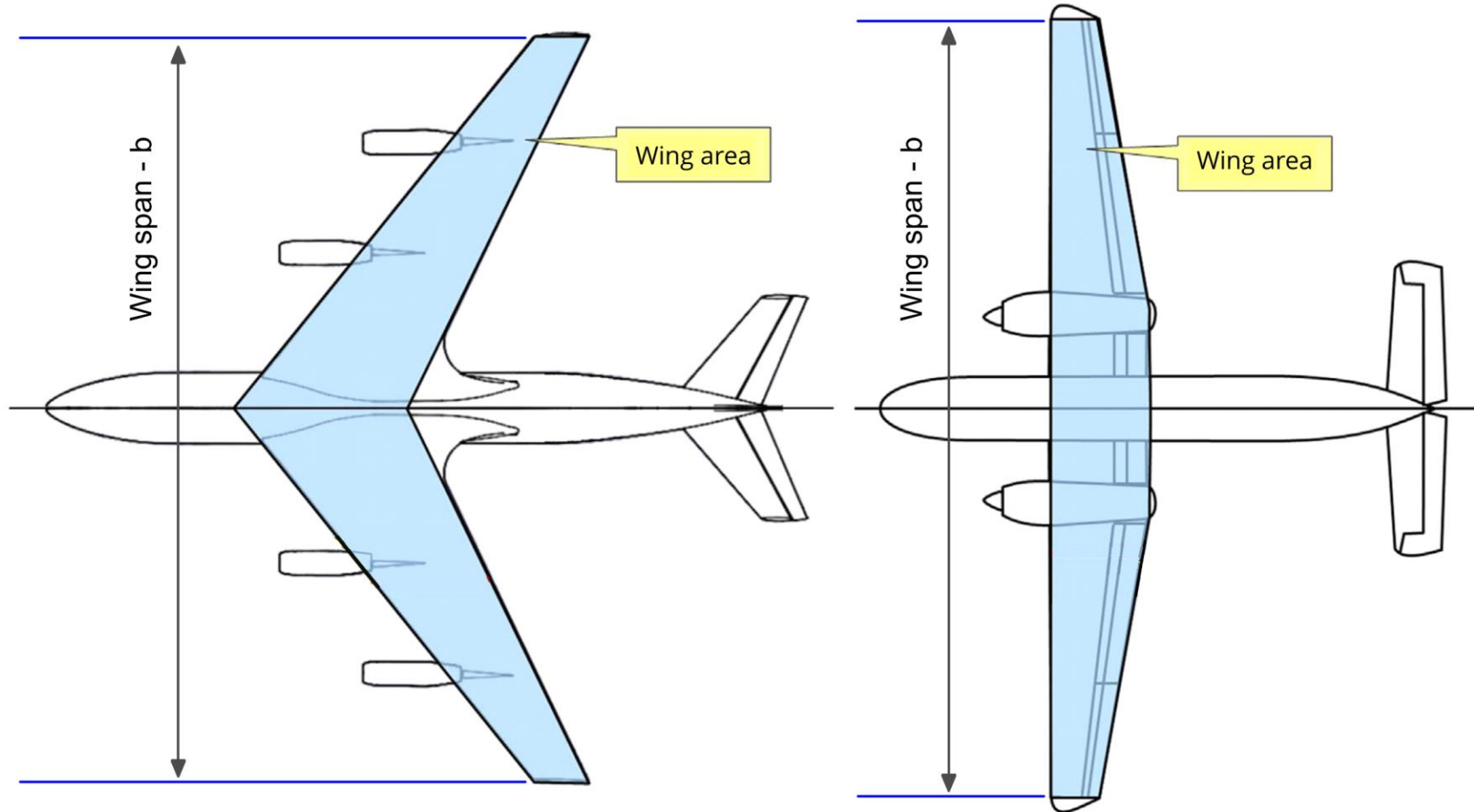


- Obtained by connecting using straight lines the points where the leading and trailing edges meet the fuselage on both sides.

- Obtained by extending the wing's leading and trailing edges forward into the fuselage.

Anatomy of the wing

- Just to be loud on this.
- When computing the aspect ratio, you use the wing area (gross area) and wingspan (tip to tip distance).

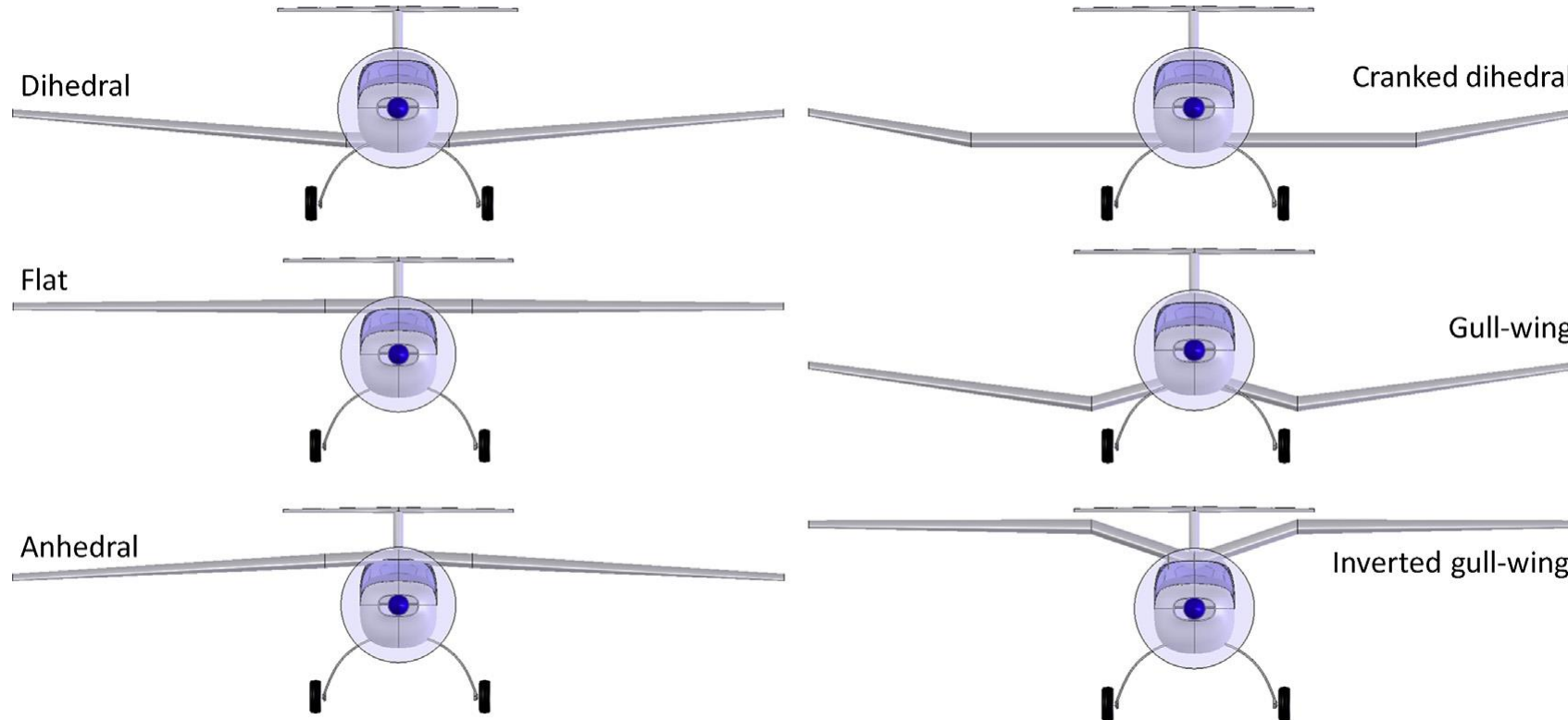


Other wing parameters

Dihedral angle and wing location

Anatomy of the wing

- The dihedral angle is the angle between a horizontal plane containing the root chord and a plane midway between the upper and lower surfaces of the wing.
- If the wing lies below the horizontal plane, it is termed as the anhedral angle.
- The dihedral/anhedral angle affects the lateral stability characteristics of the airplane.



Anatomy of the wing

- **Technical note.**

- The main purpose of the gull wing is to have more clearance. For example, propeller clearance.
- They are also used to have a shorter and stronger landing gear strut.
- From the aerodynamic point of view, when the angle between the root of the wing and the fuselage is the ideal, they reduce interference drag.



Vought F4U Corsair with gull wing

<https://www.beale.af.mil/News/Photos/igphoto/2000940168/>



Vought F4U Corsair with folded wings

https://commons.wikimedia.org/wiki/File:F4U-4_Bu97388_folding_wings.jpg

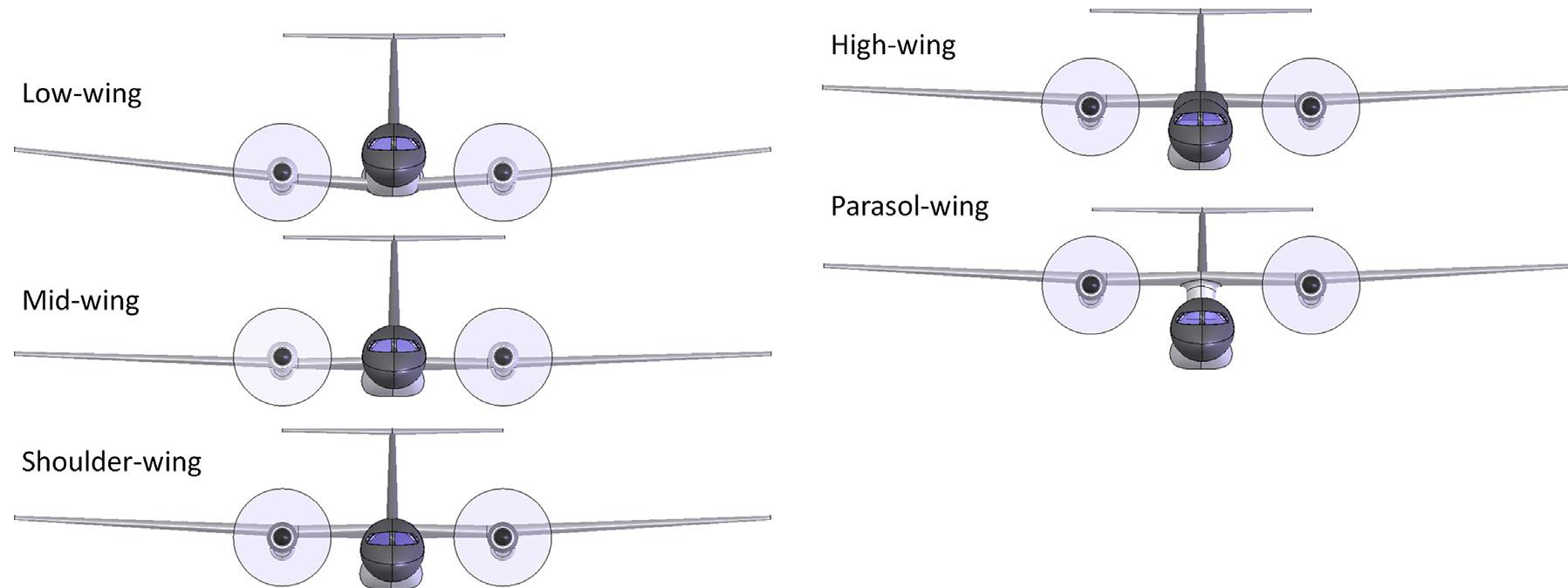


Beriev Be-12 seaplane with gull wing profile

https://en.wikipedia.org/wiki/Gull_wing#/media/File:Beriev_Be-12_Gelenzhik_2Sept2004.jpg

Anatomy of the wing

- Vertical position of the wing.
 - When it comes to wing location, there is nothing written saying that one configuration is better than the other.
 - The vertical wing location may end up being based on a number of factors such as:
 - Accessibility, field of vision, length of landing gear, stability and control, aesthetics, amphibian or land operation, ground clearances, manufacturing and structural issues, designer preference, mission type, and so on.



Anatomy of the wing

- Same design concepts also applies for jet engines.



Boeing 737-800

<https://www.pinterest.com/pin/841117667895977414/>



Bae 146

<https://spottair.com/british-aerospace-bae-146-300qt-by-tnt/>

Anatomy of the wing

- Same design concepts also applies for jet engines.
- And the engines not necessarily need to be located under the wing.



Embraer ERJ-145XR

<https://www.flickr.com/photos/28042007@N07/4088339293>



Cirrus SF50 Vision Jet G2+

<https://flyer.co.uk/cirrus-reveals-g2-vision-jet-with-extra-takeoff-power/>



Honda Jet

<https://cutteraviation.com/aircraft-charter/charter-aircraft-fleet/hondajet-ha-420/>

Wing geometry parameters of some actual airplanes

Anatomy of the wing

- Wing geometry parameters of some actual airplanes.

TABLE 5.1 Wing-Geometry Parameters

<i>Type (Original and Current Manufacturer Names Are Given)</i>	<i>Wing Span [m(ft)]</i>	<i>Aspect Ratio, AR</i>	<i>Sweep Angle</i>	<i>Dihedral</i>	<i>Airfoil Section</i>	<i>Speed [km/h (mi/h)]</i>
a. Four-Place Single-Engine Aircraft						
Socata Rallye (France)	9.61 (31.52)	7.57	None	7°	63A414(mod), 63A416, inc. 4°	173–245 (108–152)
Ambrosini NF 15 (Italy)	9.90 (32.5)	7.37	None	6°	64–215, inc. 4°	325 (202)
Beechcraft Bonanza V35B	10.20 (33.46)	6.30	None	6°	23016.5 at root, 23012 at tip, inc. 4° at root, 1° at tip	298–322 (185–200)
Beechcraft Sierra	9.98 (32.75)	7.35	None	6°30'	63 ₂ A415, inc. 3° at root, 1° at tip	211–281 (131–162)
Cessna 172	10.92 (35.83)	7.32	None	1°44'	NACA 2412, inc. 1°30' at root, –1°30' at tip	211 (131)
Piper Commanche	10.97 (36.0)	7.28	2°30' forward	5°	64 ₂ A215, inc. 2°	298 (185)
Bellanca, Model 25	10.67 (35.0)	6.70	None	2°	NACA 63 ₂ – 215, inc. 2°	458–499 (285–310)
Piper Warrior II	10.67 (35.0)	7.24	None	7°	NACA 65 ₂ – 415, inc. 2° at root, –1° at tip	191–235 (119–146)

Anatomy of the wing

- Wing geometry parameters of some actual airplanes.

TABLE 5.1 Wing-Geometry Parameters

<i>Type (Original and Current Manufacturer Names Are Given)</i>	<i>Wing Span [m(ft)]</i>	<i>Aspect Ratio, AR</i>	<i>Sweep Angle</i>	<i>Dihedral</i>	<i>Airfoil Section</i>	<i>Speed [km/h (mi/h)]</i>
b. Commercial Jetliners and Transports						
Caravelle 210 (France)	34.3 (112.5)	8.02	20° at $c/4$	3°	NACA 65 ₁ 212	790 (490)
BAC 111 (UK)	26.97 (88.5)	8.00	20° at $c/4$	2°	NACA cambered section (mod.), $t/c = 0.125$ at root, 0.11 at tip, inc. 2°30'	815 (507)
Tupolev 204 (Russia)	41.84 (137.3)	9.10	28° at $c/4$	—	$t/c = 0.14$ (inboard) to 0.09 (outboard), inc. twist	850 (528)
Boeing 737	28.35 (93.0)	8.83	25° at $c/4$	6°	$t/c = 0.129$ (av.)	848 (527)
Boeing 747	59.64 (195.7)	6.95	37°30' at $c/4$	7°	$t/c = 0.134$ (inboard), 0.078 (midspan), 0.080 (outboard), inc. 2°	958 (595)

Anatomy of the wing

- Wing geometry parameters of some actual airplanes.

TABLE 5.1 Wing-Geometry Parameters

Type (Original and Current Manufacturer Names Are Given)	Wing Span [m(ft)]	Aspect Ratio, AR	Sweep Angle	Dihedral	Airfoil Section	Speed [km/h (mi/h)]
Boeing 777	64.80 (212.6)	8.68	25° at $c/4$			Mach 0.77
Lockheed C-5A	67.88 (222.8)	7.75	25° at $c/4$	Anhedral 5°30'	NACA 0011 (mod.) near midspan, inc. 3°30'	815 (507)
McDonnell Douglas (Boeing) C-17	50.29 (165)	7.2	25° at $c/4$	Anhedral 3°30'	$t/c = 0.153$ (inboard), 0.122 (outboard)	Mach 0.74–0.77
Airbus A310 (International)	43.89 (144.0)	8.8	28° at $c/4$	11°8' (inboard at the trailing edge)	$t/c = 0.152$ at root, $t/c = 0.108$ at tip, inc. 5°3' at root	667–895 (414–556)
Airbus A380 (International)	79.80 (261.8)	7.5	35° at $c/4$ (average)	5.5° (outboard)		945 (587)

Anatomy of the wing

- Wing geometry parameters of some actual airplanes.

TABLE 5.1 Wing-Geometry Parameters

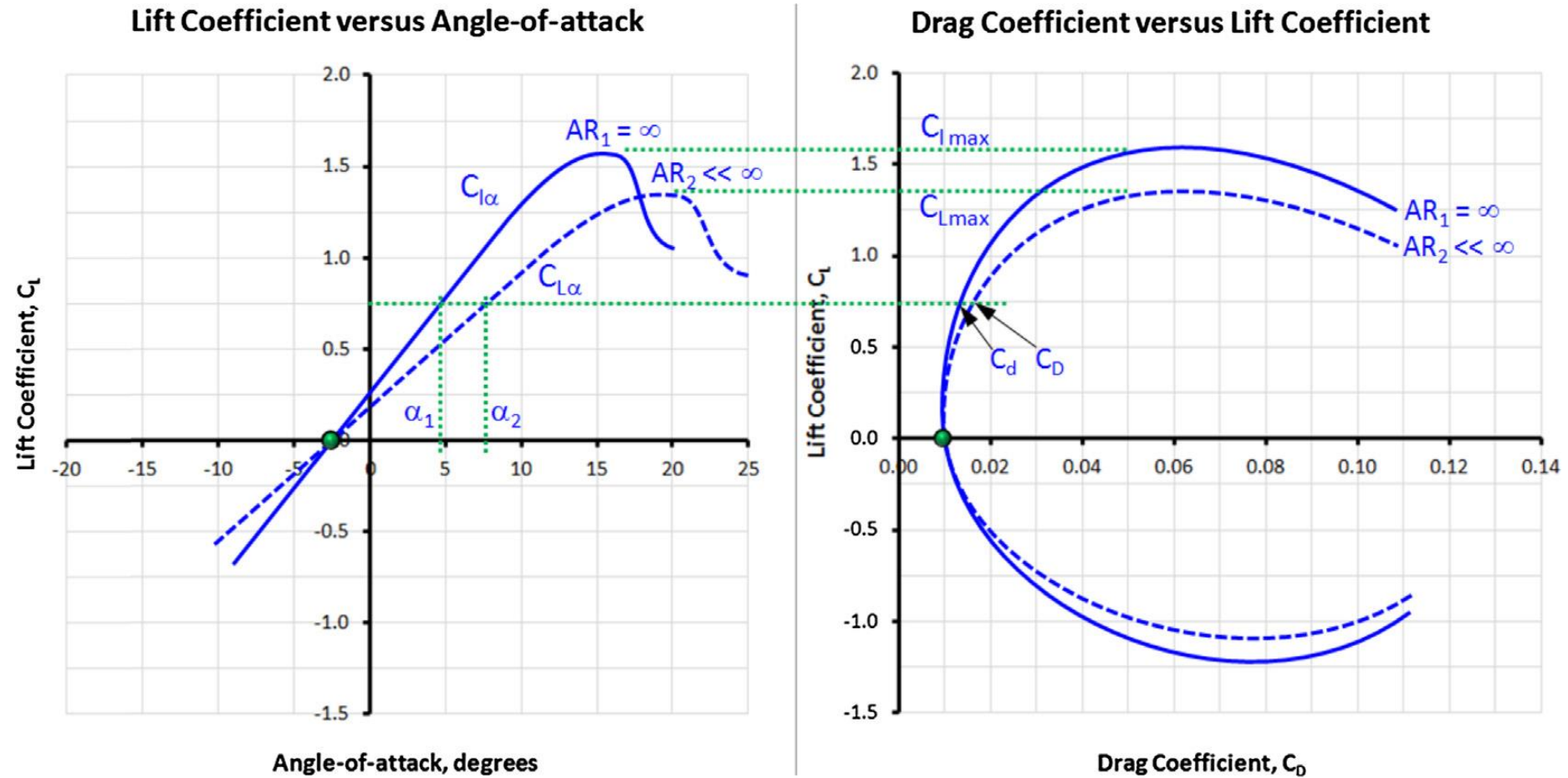
Type (Original and Current Manufacturer Names Are Given)	Wing Span [m(ft)]	Aspect Ratio, AR	Sweep Angle	Dihedral	Airfoil Section	Speed [km/h (mi/h)]
c. High-Speed Military Aircraft						
SAAB-35 Draken (Sweden)	9.40 (30.8)	1.77	Central: leading edge 80° outer: leading edge 57°	—	$t/c = 0.05$	Mach 1.4–2.0
Dassault Mirage III (France)	8.22 (27.0)	1.94	Leading edge 60°34'	Anhedral 1°	$t/c = 0.045–0.035$	Mach 2.2
Northrop F-5E	8.13 (26.67)	3.82	24° at $c/4$	None	65A004.8 (mod.), $t/c = 0.048$	Mach 1.23
McDonnell-Douglas F-4	11.70 (38.4)	2.78	45°	Outer panel 12°	$t/c = 0.051$ (av.)	Over Mach 2.0
LTV F-8	10.81 (35.7)	3.39	35°	Anhedral 5°	Thin, laminar flow section	Nearly Mach 2
LTV A-7	11.80 (38.75)	4.0	35° at $c/4$	Anhedral 5°	65A007, inc. –1°	1123 (698)
Mitsubishi T2 (Japan)	7.88 (25.85)	2.93	35°47' at $c/4$	Anhedral 9°	NACA 65 series (mod.), $t/c = 0.0466$	Mach 1.6
General Dynamics (Lockheed Martin) F-16	9.14 (30.0)	3.0	40° on leading edges	—	NACA 64A-204	Mach 2.0 +
Lockheed Martin F-22	13.56 (44.5)	2.4	42° on leading edges	Anhedral 3.25°	$t/c = 0.0592$ (inboard) and 0.0429 (outboard); –3.1° at tip	Mach 2.0 +
Eurofighter (International)	11.09 (35.35)	2.5	53° on leading edges	1°	NACA 66 (mod.)	Mach 2.0
Sukhoi Su-27 (Russia)	14.70 (48.2)	3.5	37° at $c/4$	0°	$t/c = 0.05$	Mach 2.35

Source: Data from *Jane's All the World's Aircraft* (1973, 1966, 1984, and 2011).

Wing performance in function of the main geometric parameters

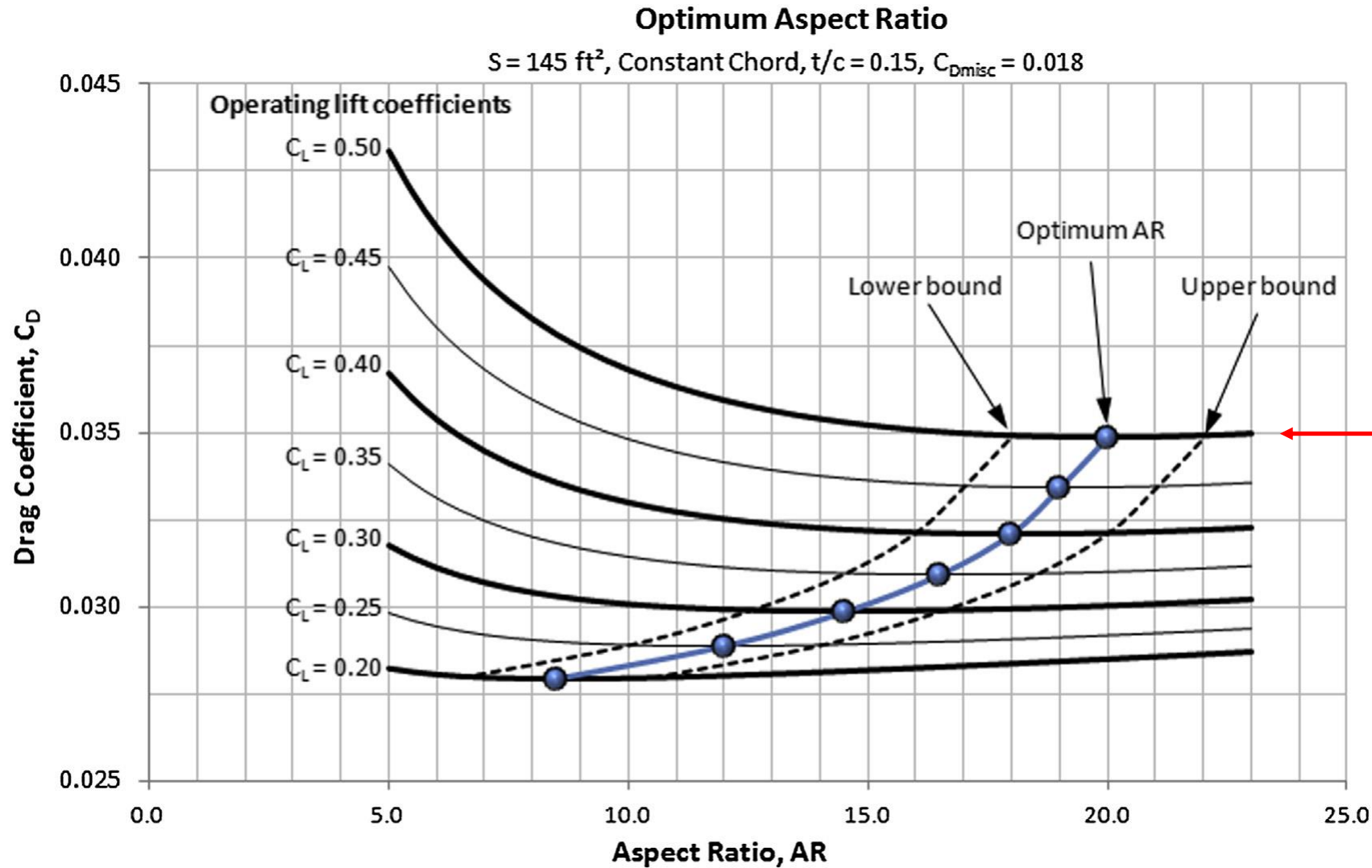
Wing performance in function of the main geometric parameters

- Comparison of finite-span wings (3D case) and infinite span wings (2D case – airfoils).



Wing performance in function of the main geometric parameters

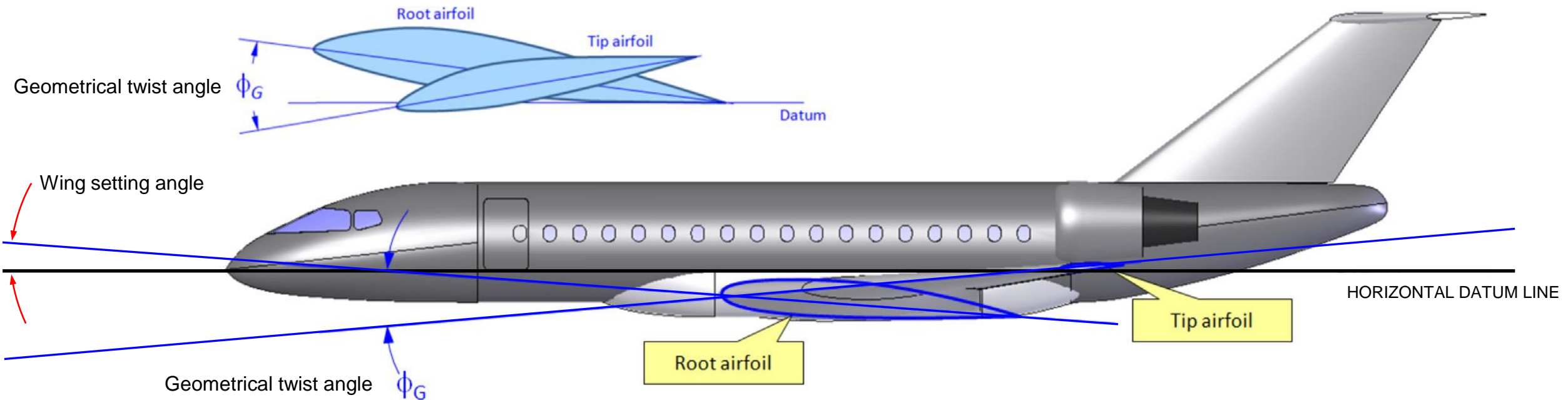
- Effect of aspect ratio on the drag coefficient of a hypothetical airplane.



The optimum AR corresponds to the minimum C_D value of the iso C_L curve

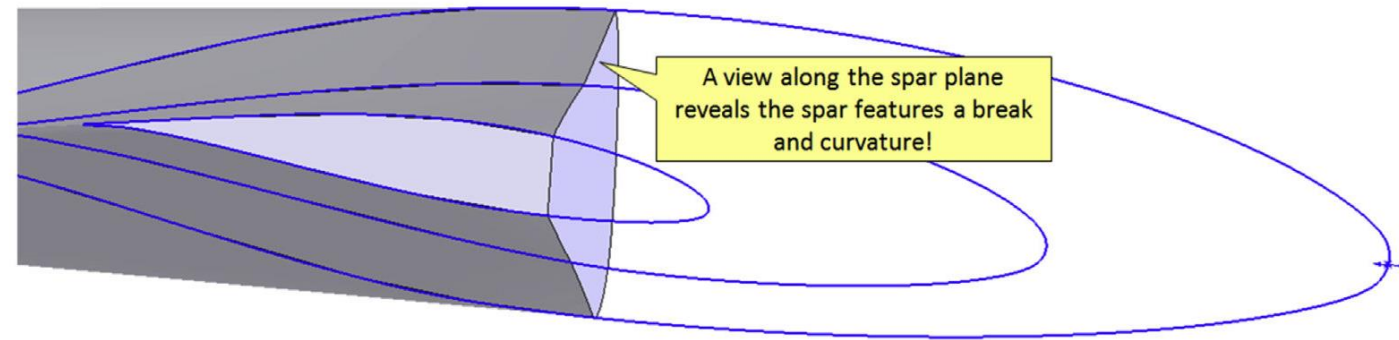
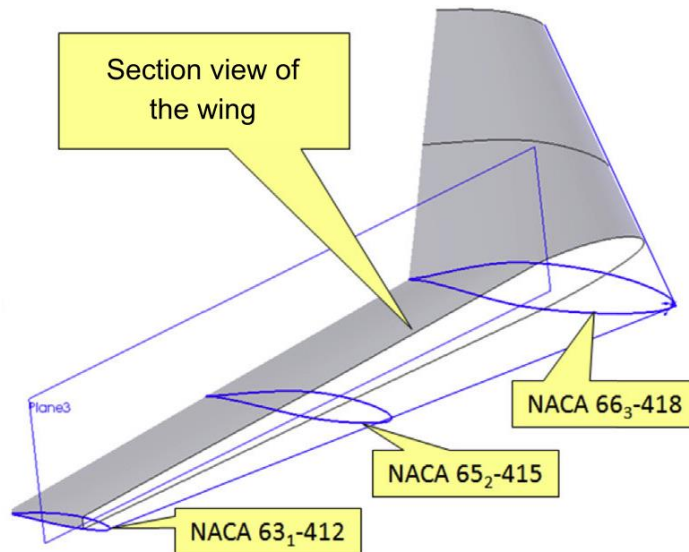
Wing performance in function of the main geometric parameters

- Wing twist – Geometrical twist.
 - When we change the angle of incidence of the wing sections, we call it geometrical twist.
 - When the root airfoil AOA is larger than that of the tip airfoil, we call it wash-out.
 - The opposite scenario is called wash-in.
 - The angle between the root airfoil and the datum line is known as wing incidence angle or setting angle (datum-root airfoil decalage).



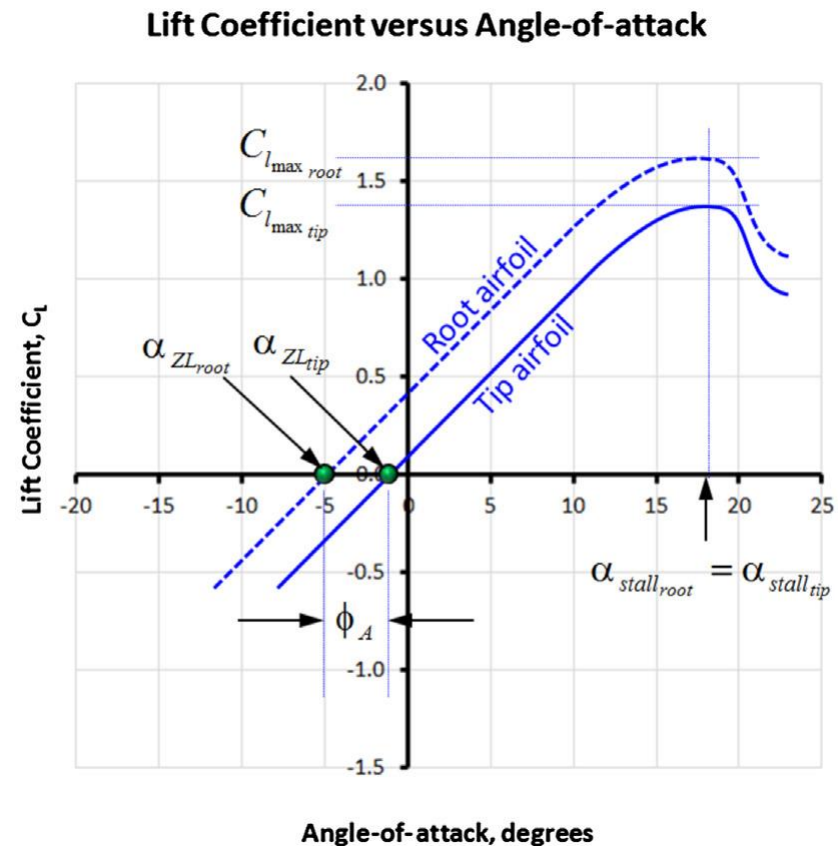
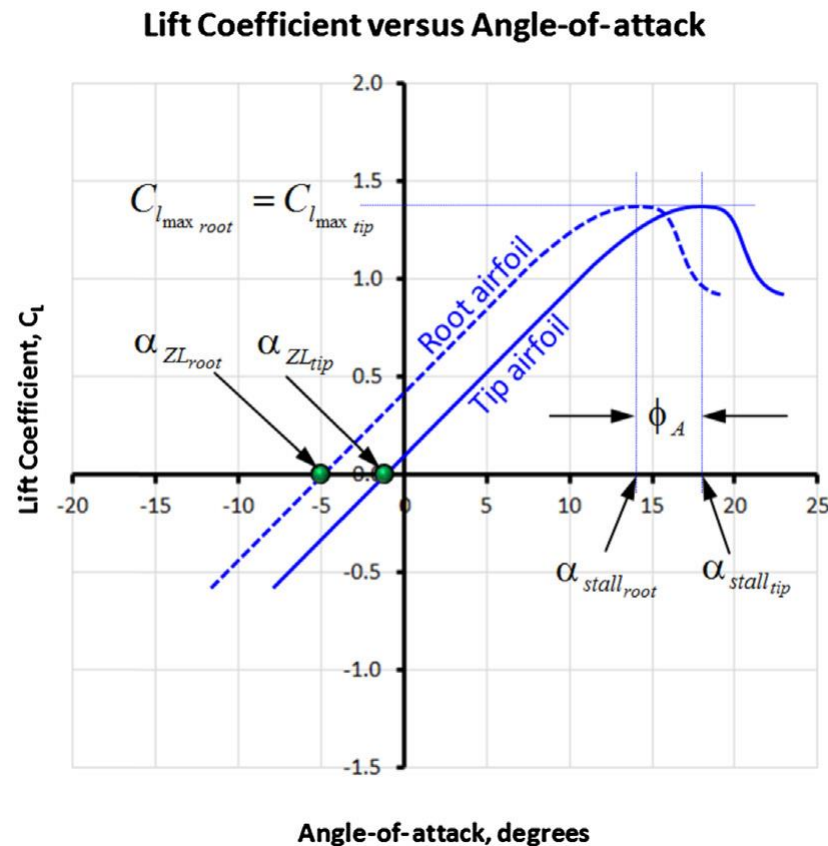
Wing performance in function of the main geometric parameters

- Wing twist – Aerodynamic twist.
 - When we change the airfoil sections, we call it aerodynamic twist.
 - Geometrical twist and aerodynamic twist can be used together.



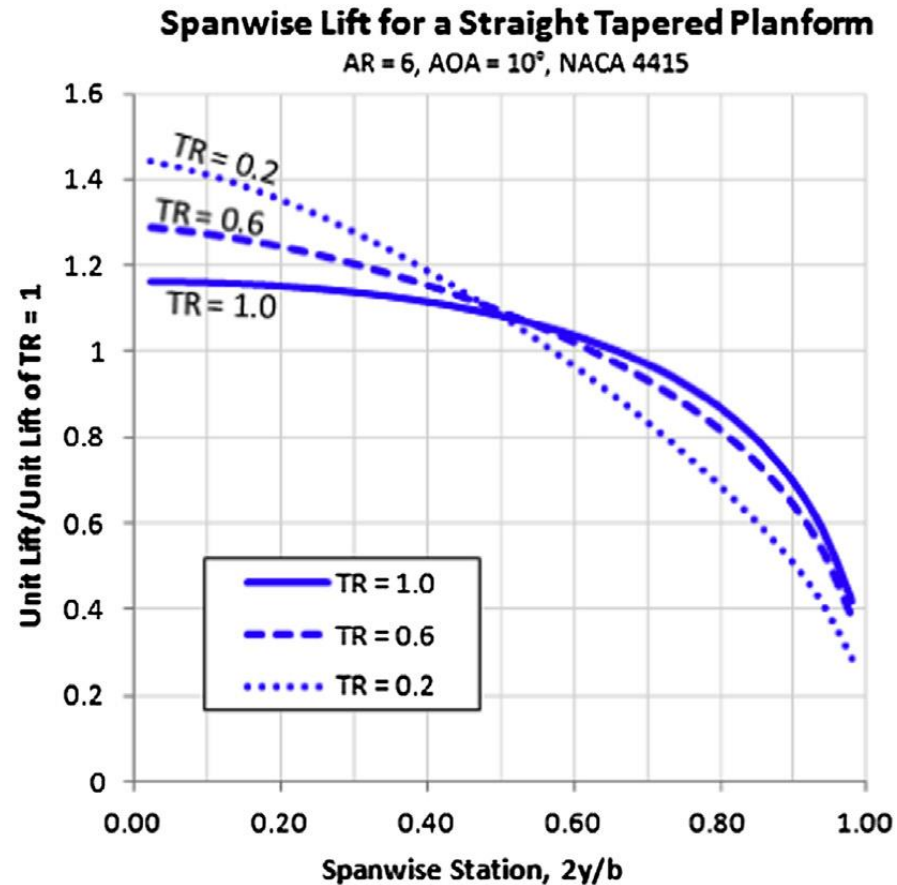
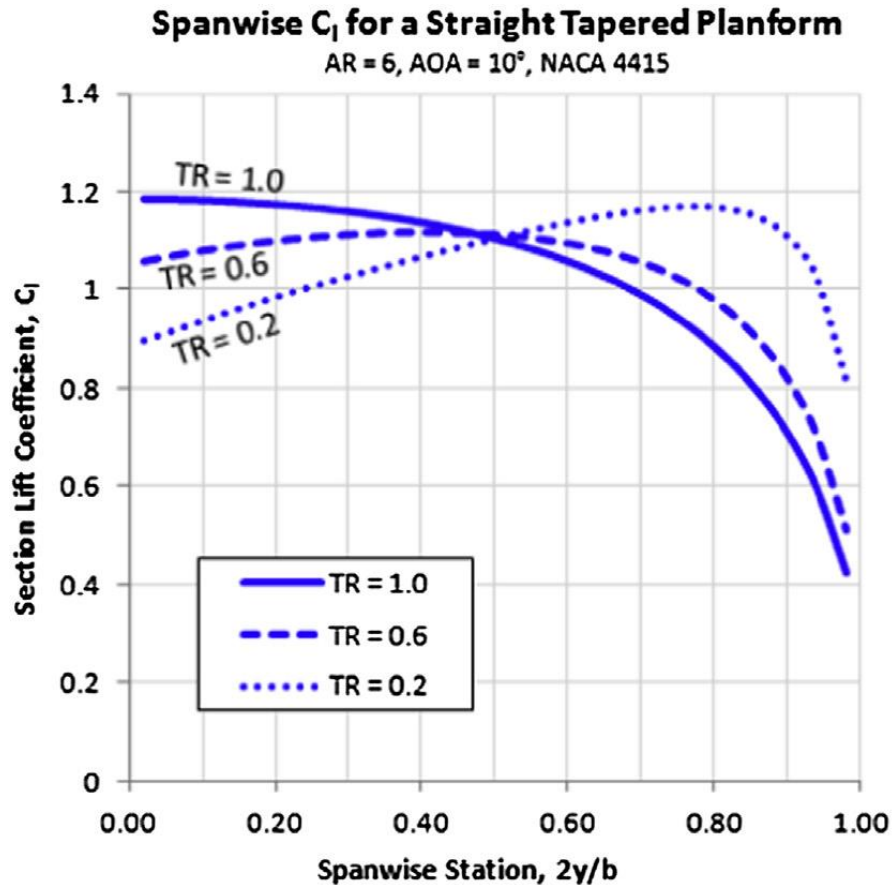
Wing performance in function of the main geometric parameters

- Effect of aerodynamic twist.
 - In the left image, the root airfoil stalls at a lower AOA than the tip.
 - In the right image, the root airfoil has a higher $C_{l_{max}}$ than the tip airfoil but stalls at the same AOA, the effective wash-out is zero.



Wing performance in function of the main geometric parameters

- Effect of taper ratio on the spanwise distribution of section lift coefficient (left image) and section lift force (right image)
- Tapering a wing planform gives a number of significant aerodynamic and structural advantages, but it can also cause problems if overdone.

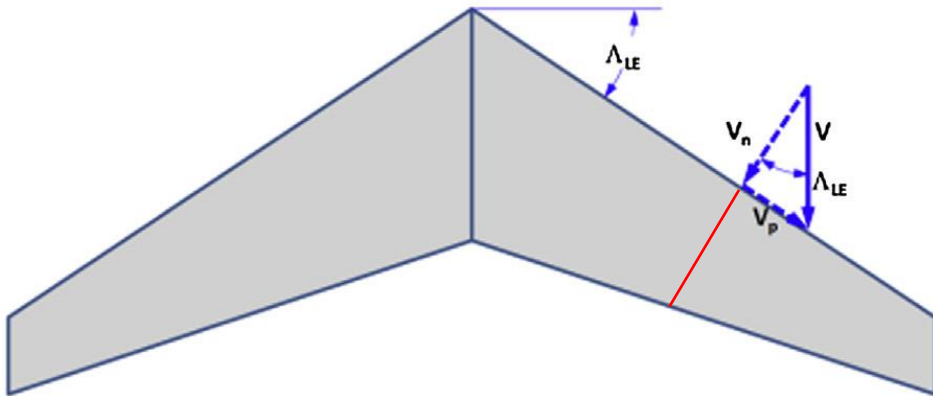


- Note that the spanwise distributions are different depending on the quantity used.
- If we use lift coefficient, the ideal case is a uniform distribution (straight line).
- If we use lift force, the ideal distribution is of elliptical shape.

Wing performance in function of the main geometric parameters

General knowledge as our focus is low speed aerodynamics for the moment.

- Sweep angle.
 - The main purpose of sweeping the wing backward (or forward) is to delay the onset of shock waves, reduce wave drag, and move the position of the MAC or CG.
 - In general, the maximum lift coefficient and lift curve slope are reduced with the sweep angle.



- The swept wing is a mechanism for reducing the large drag increase encountered at high-speed subsonic flight and at supersonic speeds.
- The flow over the wing (therefore the critical Mach number), depends on the velocity component perpendicular to the leading edge.
- By adding sweep, higher critical Mach numbers can be reached because the velocity component normal to the leading edge is lower than the freestream velocity.
- The velocity normal to the leading edge is equal to the freestream velocity multiplied by the cosine of the sweep angle (the local airfoil sees a lower velocity).

Wing performance in function of the main geometric parameters

- Sweep angle – Variation of minimum wing drag coefficient versus Mach number.

General knowledge as our focus is low speed aerodynamics for the moment.

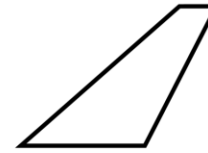
Sweep angle = 11°



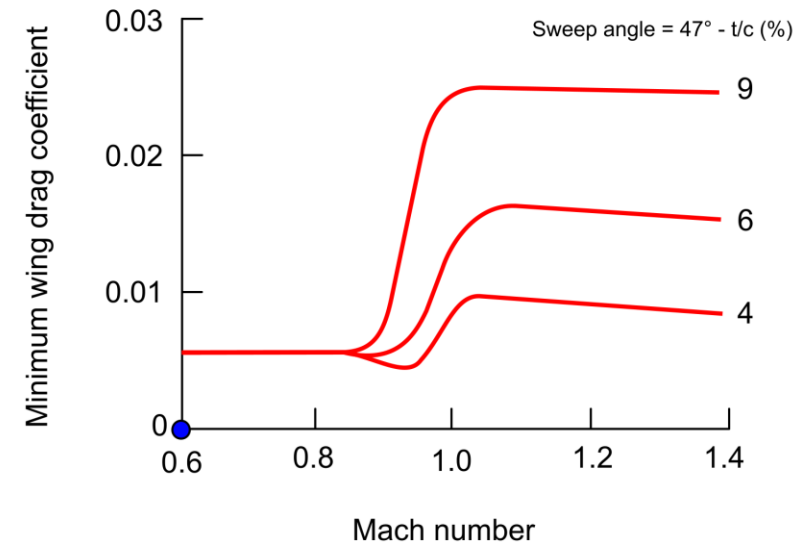
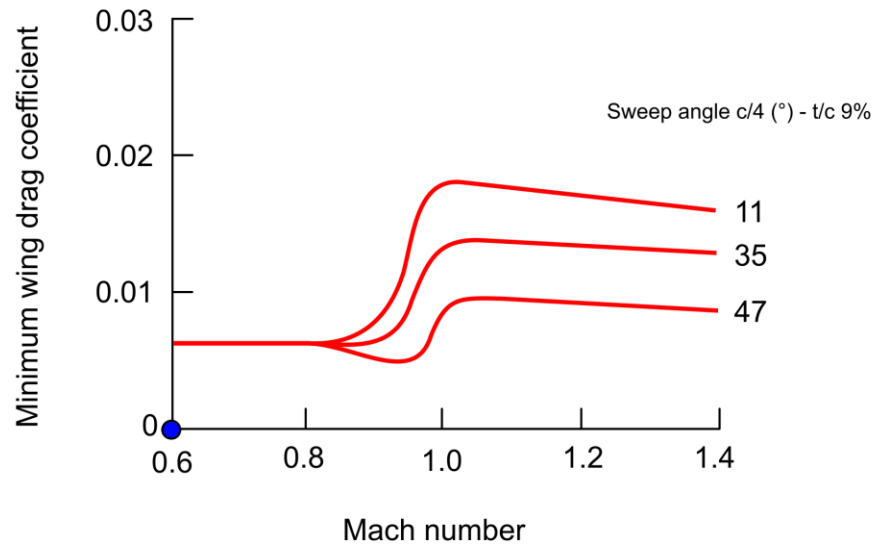
Sweep angle = 35°



Sweep angle = 47°



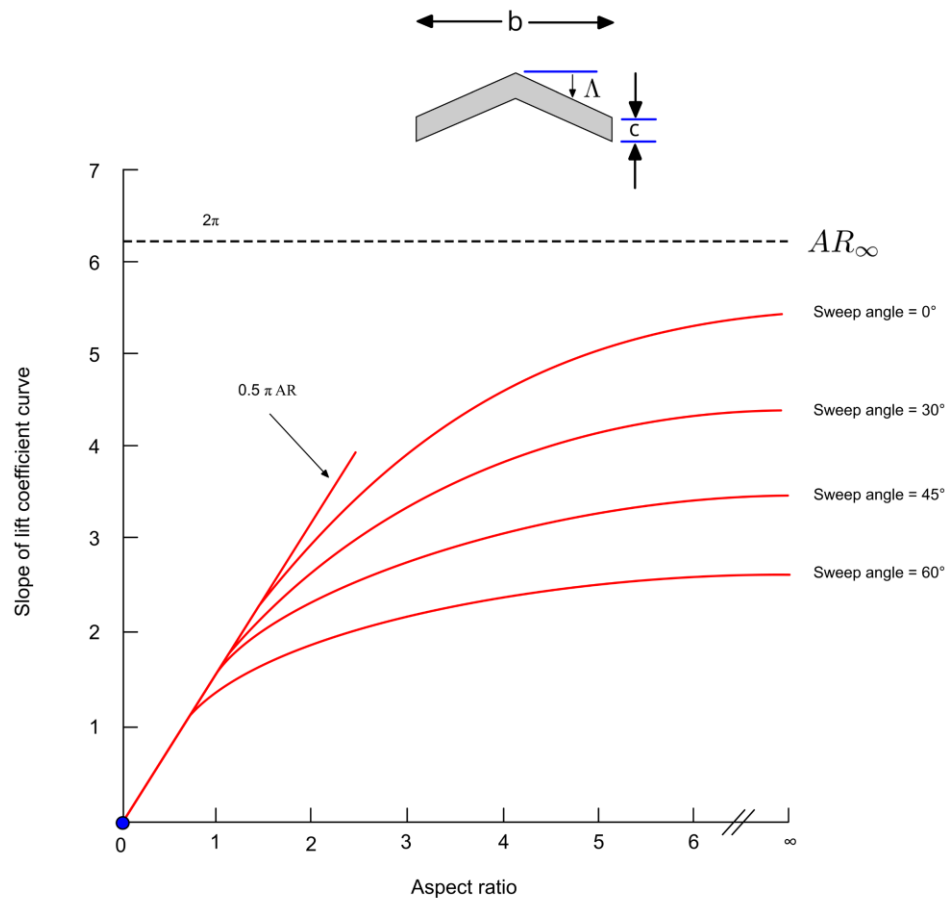
Aspect ratio = 3.5
Taper ratio = 0.2



Wing performance in function of the main geometric parameters

General knowledge as our focus is low speed aerodynamics for the moment.

- Influence of sweep angle on wing design.
- Sweep angle reduces $C_{L\alpha}$.
- In the figure, we illustrate general trends showing the effect of aspect ratio on the lift coefficient slope of wings with different sweep angle at subsonic speeds.



Theoretical variation of lift coefficient slope $C_{L\alpha}$ (or a) against aspect ratio for elliptical wings:

$$C_{L\alpha} = a = \frac{a_0}{1 + \frac{a_0}{\pi AR}}$$

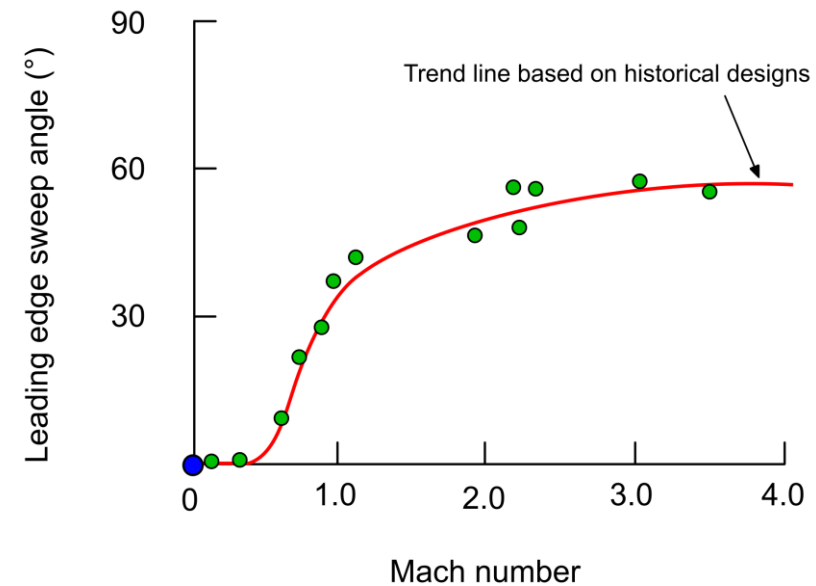
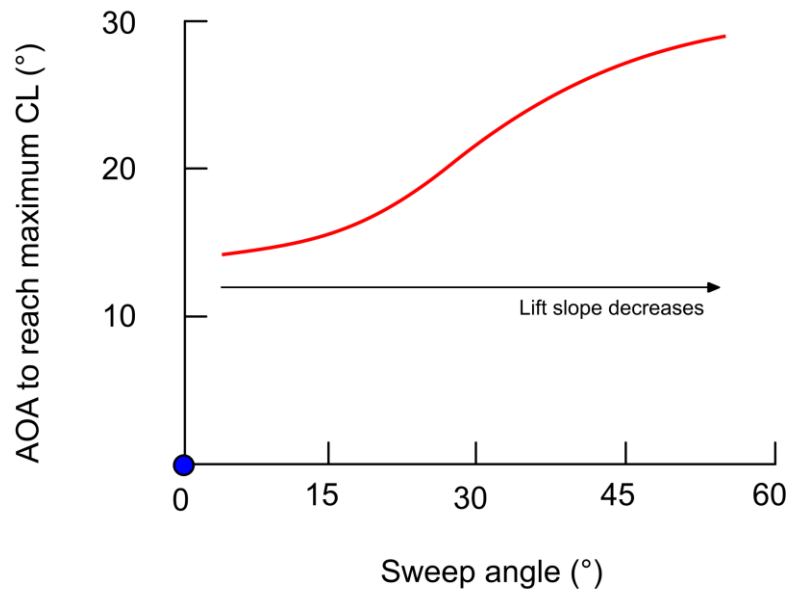
Airfoil lift curve slope

This relation represents the lift-curve slope for a wing with an elliptic lift distribution

Wing performance in function of the main geometric parameters

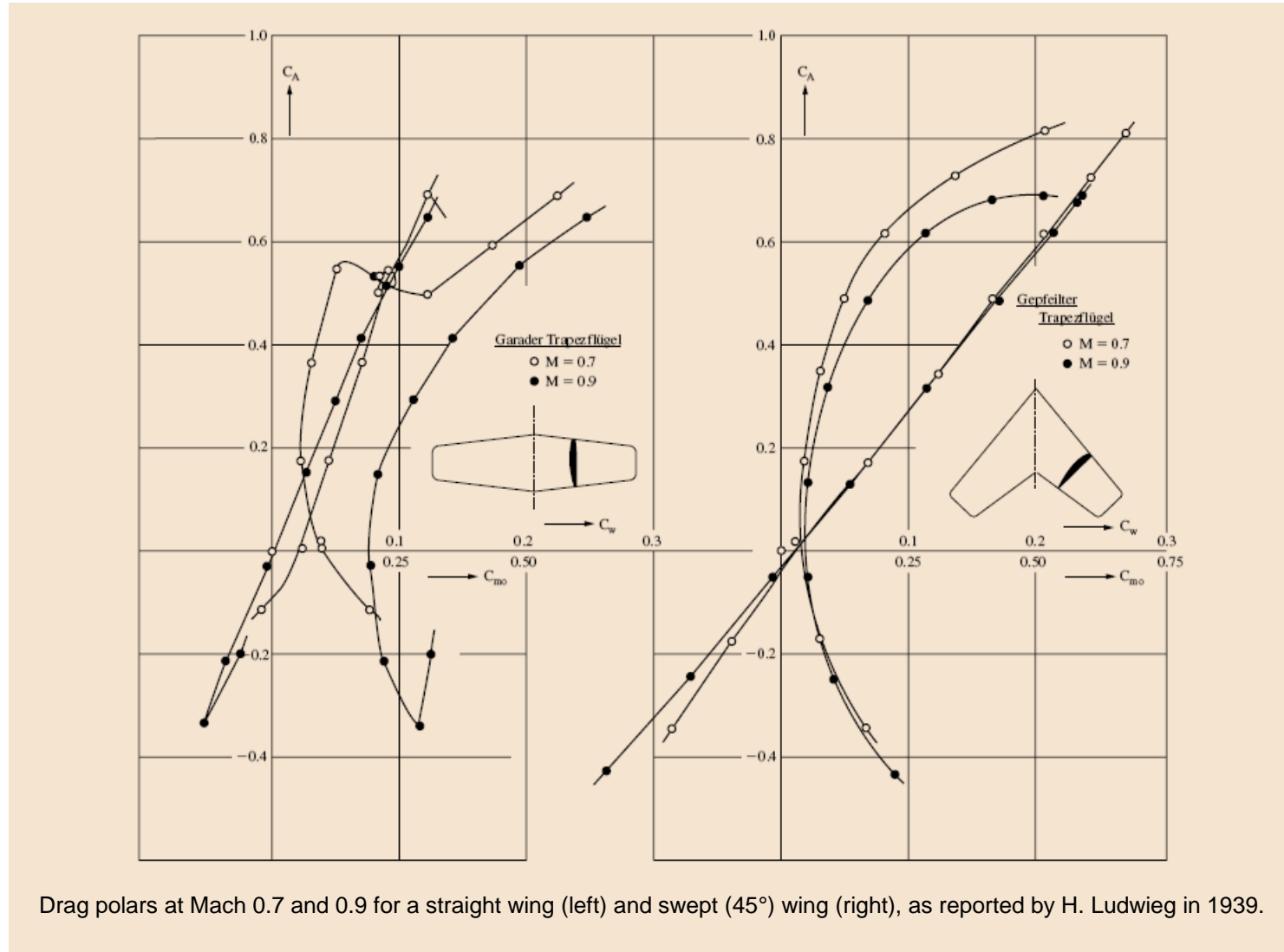
General knowledge as our focus is low speed aerodynamics for the moment.

- Influence of sweep angle on wing design.
- Disregarding the fact that the sweep angle decreases the lift curve slope, the sweep angle increases the AOA to reach maximum C_L .
- Wings designed for high speed are a good compromise of sweep angle, taper ratio, aspect ratio, and airfoil thickness.
- Over the years, as better engines became available (clean, cheap and efficient) and in the quest for higher speeds, the trend has been to increase the sweep angle (the whole wing or only the leading edge as in delta wings) to reduce the wave drag.



Wing performance in function of the main geometric parameters

- Experimental data – Influence of sweep angle on the aerodynamic performance of finite-span wings.

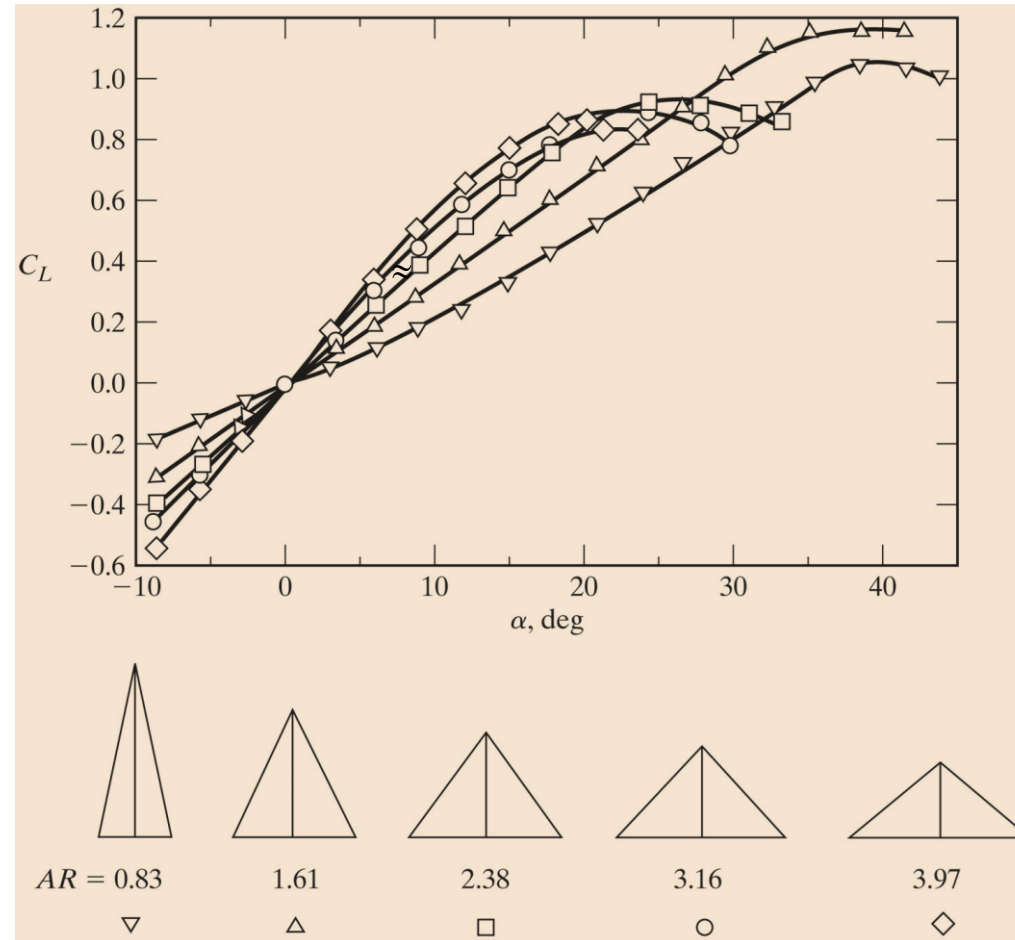


General knowledge as our focus is low speed aerodynamics for the moment.

Drag polars at Mach 0.7 and 0.9 for a straight wing (left) and swept (45°) wing (right), as reported by H. Ludwieg in 1939.

Wing performance in function of the main geometric parameters

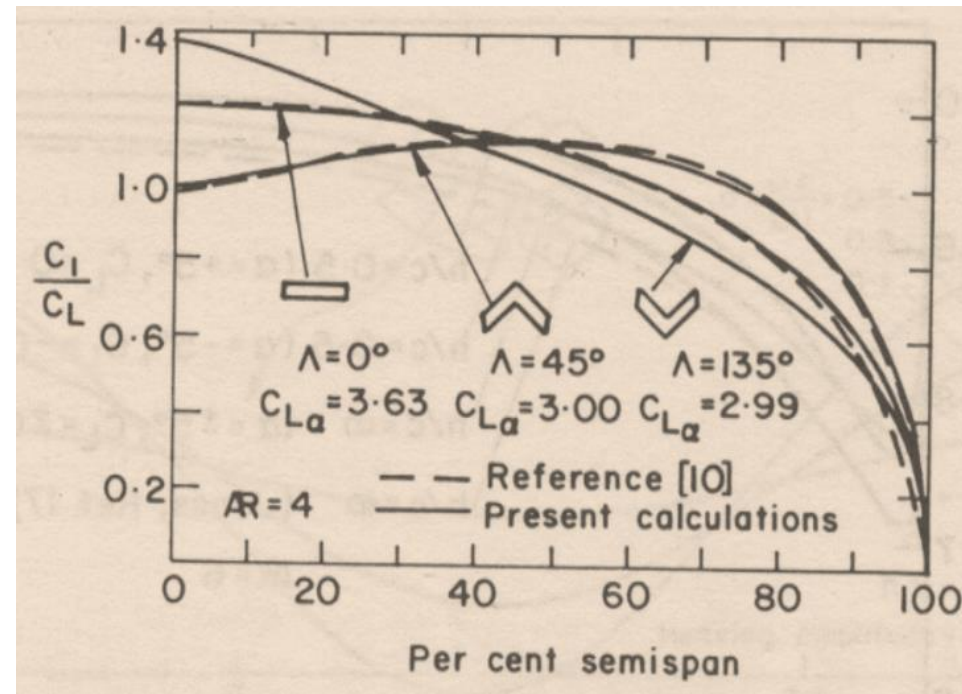
- Sweep angle – Delta wings.
- Experimental data – Lift coefficients for delta wings of various aspect ratios; $t = 0.12c$, $Re_c \approx 7 \times 10^5$



General knowledge as our focus is low speed aerodynamics for the moment.

Wing performance in function of the main geometric parameters

- In addition to reducing the lift, wing sweep changes the local section lift coefficient C_l .
- The lift slope of infinite wings is 2π , while the lift slope of a finite wing is zero at the tip and less than 2π at the root and along the wingspan. This is due to the downwash of the trailing vortices.
- Increasing the aspect can increase the lift slope, but the maximum value will never be that of infinite span wings (airfoils).
- The figure below [1], illustrates the loss of lift near the wing tips of finite span wings.



General knowledge as our focus is low speed aerodynamics for the moment.

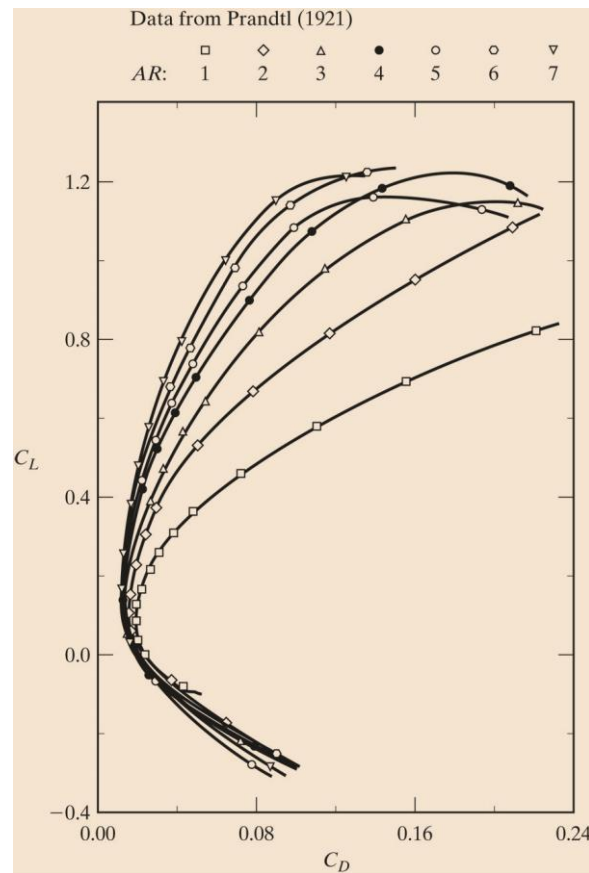
[1] J. Katz. Calculation of the Aerodynamic Forces on Automotive Lifting Surfaces. ASME. J. Fluids Eng. December 1985; 107(4): 438-443.

[2] Reference 10 in the figure: A. Donovan, H. Lawrence. Aerodynamic Components of Aircraft at High Speeds. Princeton Series Vol. VII, Princeton University Press, N.J., 1957.

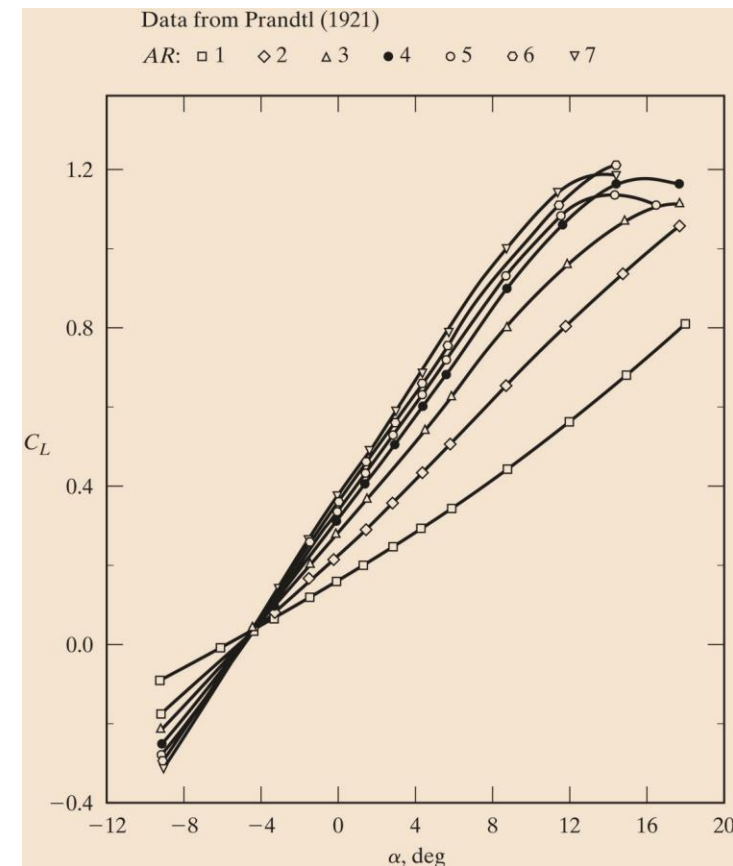
Wing performance in function of the main geometric parameters

- Experimental data – Effect of aspect ratio on the aerodynamic performance of a rectangular wing.

- Effect of the aspect ratio on the drag polar for rectangular wings (AR from 1 to 7): measured drag polars.



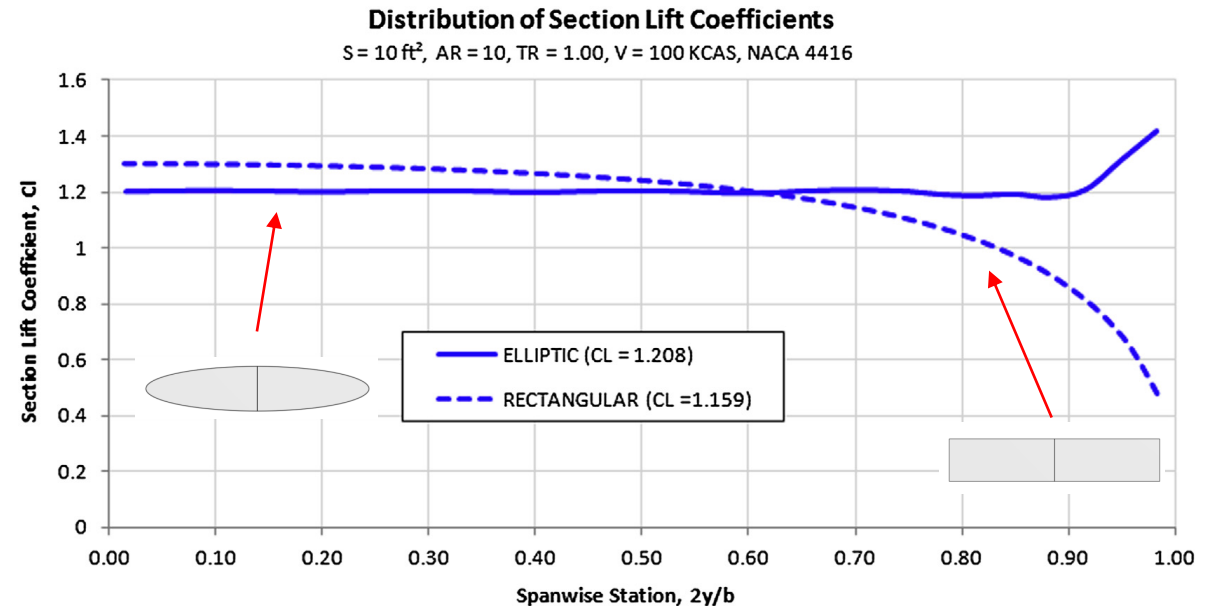
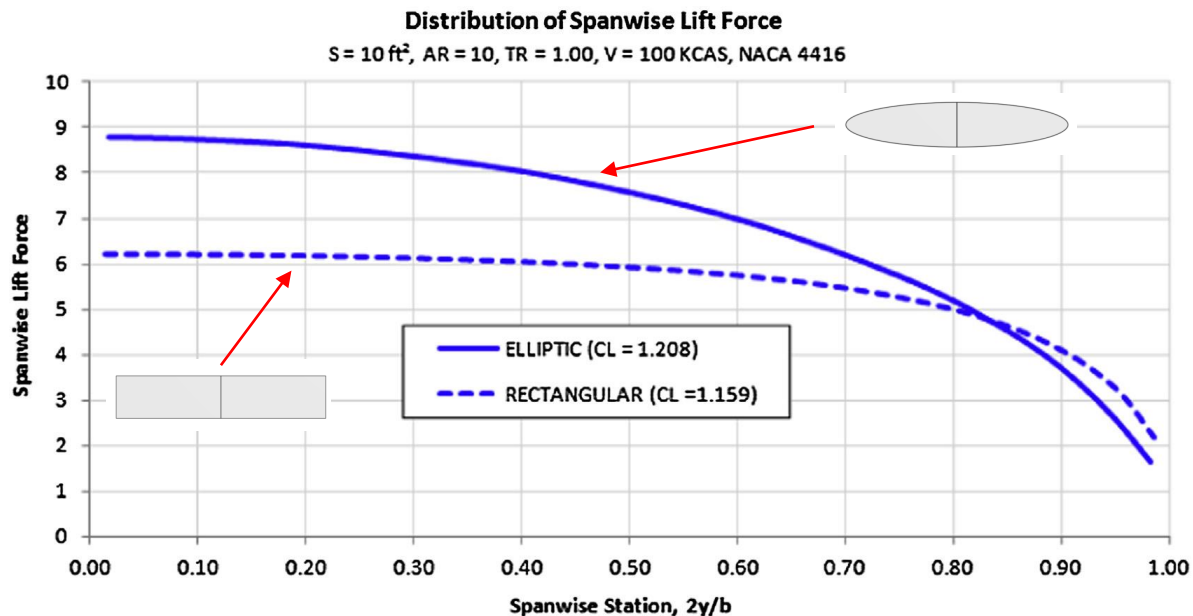
- Effect of the aspect ratio on the lift curve for rectangular wings (AR from 1 to 7): measured lift curves.



Wing performance in function of the main geometric parameters

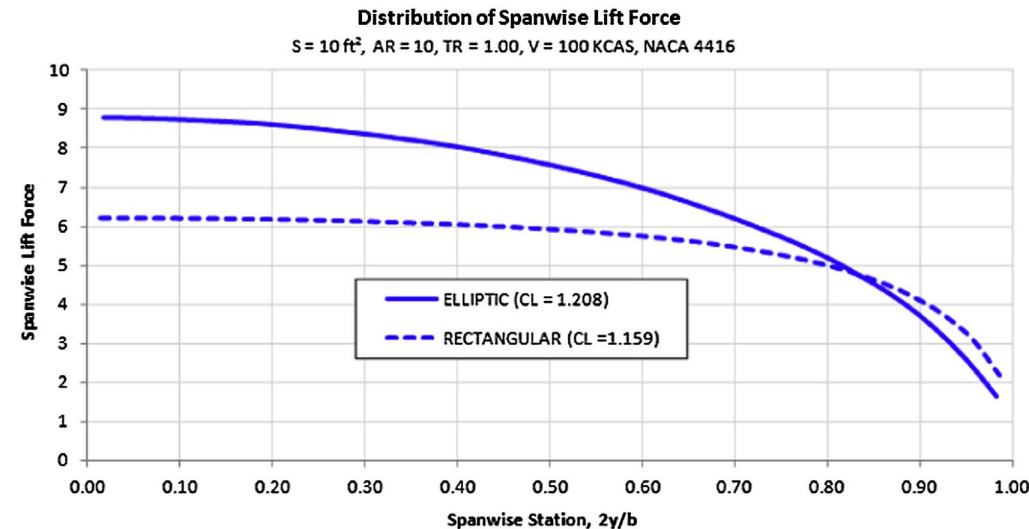
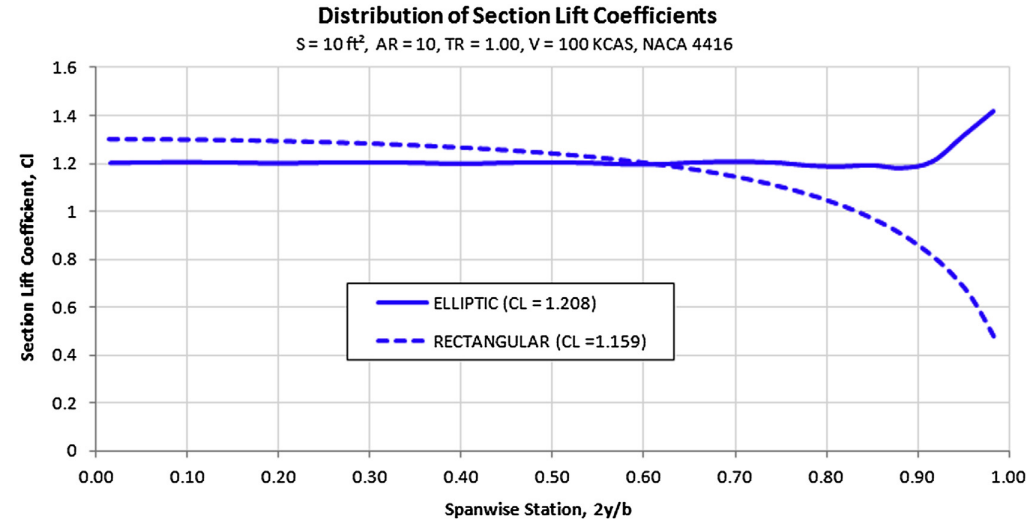
- Optimal lift distribution.
 - The optimal lift distribution (we are talking about force) is the elliptical one, as it generates the less possible induced drag and lower wing root bending moments.
 - If you think in terms of section lift coefficient, the distribution should be uniform.
 - However, an elliptical lift distribution have the drawback that the whole wing will stall at the same time.
 - Due to safety requirements, it is recommended to have a wing that first stall inboard, so we do not loose roll control. This can be achieved by adding geometrical/aerodynamic twist.

Note: The solutions shown were obtained using a vortex lattice method (VLM) solver.



Wing performance in function of the main geometric parameters

- Plots used to illustrate spanwise lift distribution.

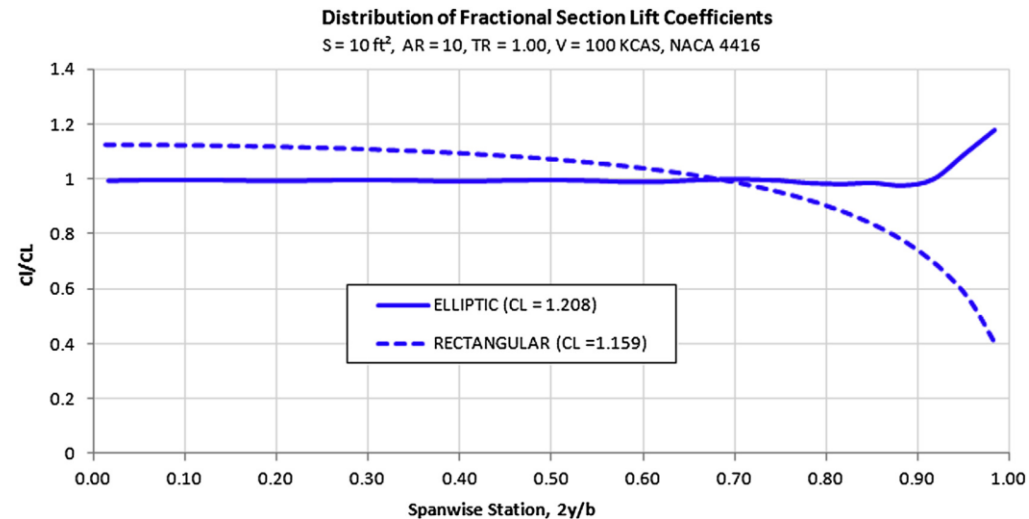
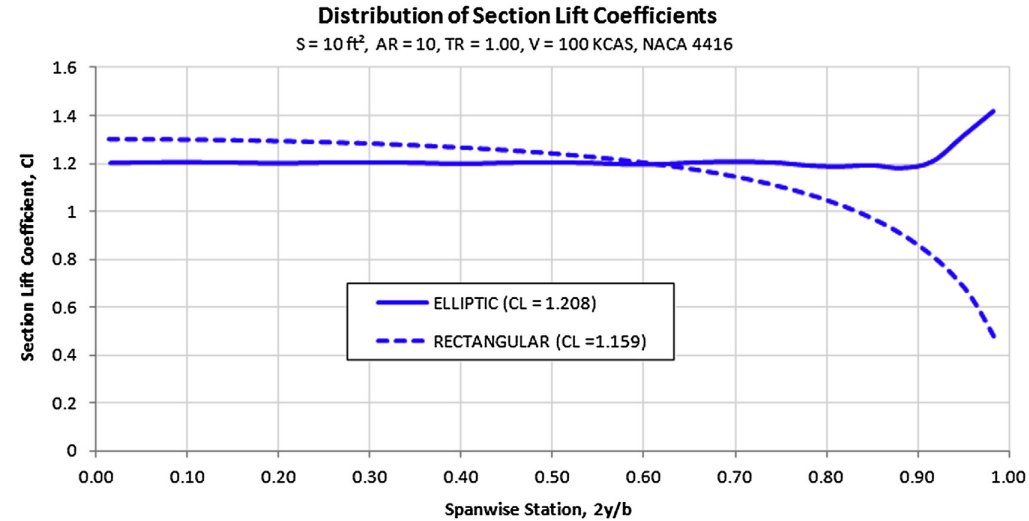


- Any of these plots can be used to illustrate spanwise lift distribution.
- You can use the actual span value, or you can normalize it.
- For minimum induced drag you should aim for:
 - **If you use lift coefficient distribution** (normalized or unnormalized), your goal is to obtain a uniform distribution (equivalent to that of an elliptical wing)
 - **If you use the lift force distribution**, your goal is to obtain an elliptical distribution.
- The elliptical lift distribution (or uniform lift coefficient distribution) might not be optimal in terms of stall characteristics towards the tips.
- Therefore, you will end up aiming for a little of aerodynamic or geometric twist towards the tips in order to delay stall.

- Notice that in the spanwise lift distribution plot (bottom figure), there is a loss in lift towards the tips. This is characteristic of finite span wings and is due to 3D effects.
- The high pressure in the bottom of the wing tends to move towards the top surface at the wing tips.

Wing performance in function of the main geometric parameters

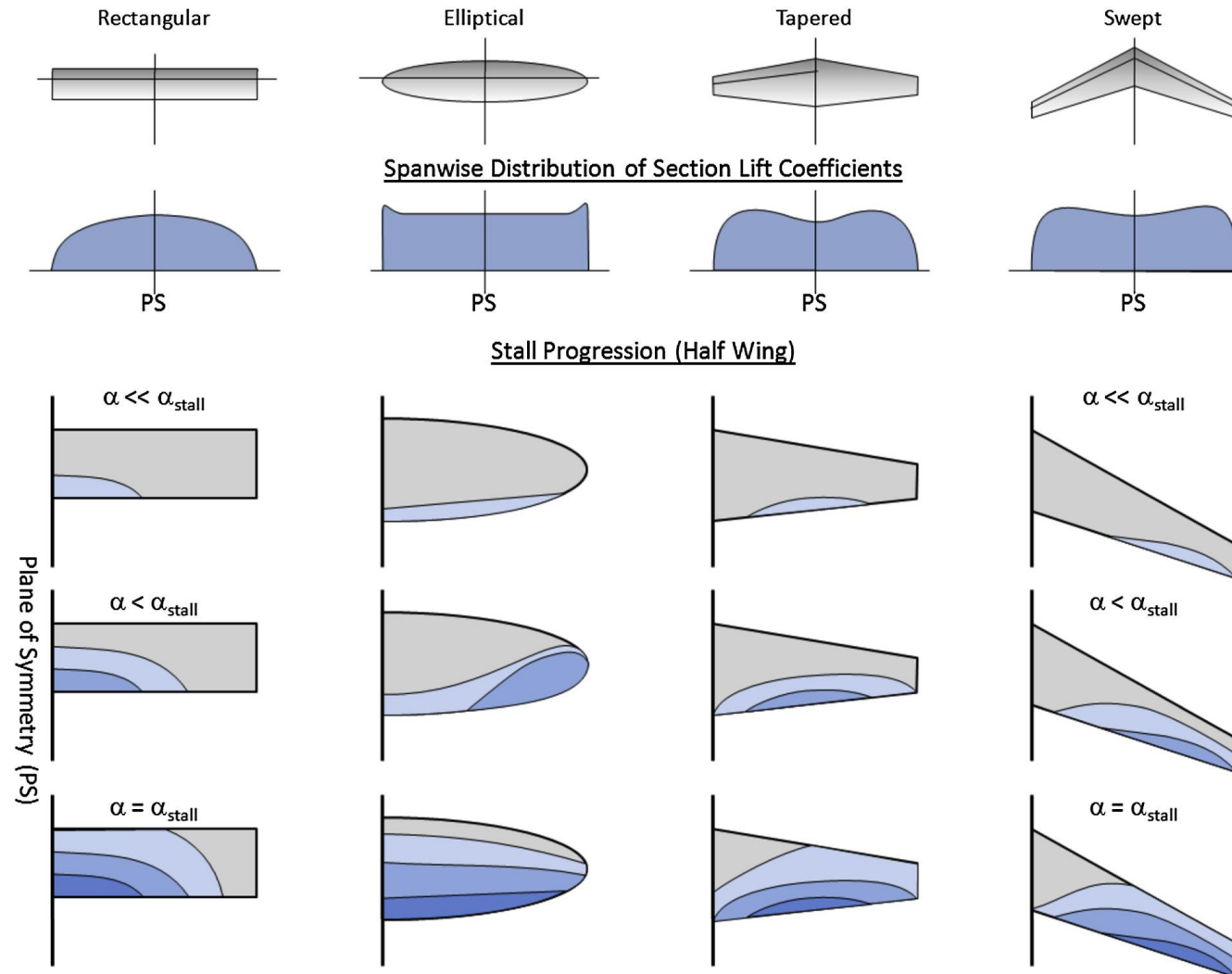
- Plots used to illustrate spanwise lift distribution.



- Any of these plots can be used to illustrate spanwise lift distribution.
- You can use the actual span value, or you can normalize it.
- You can use normalized or unnormalized lift coefficient distribution.
- The normalized lift coefficient distribution (bottom image) can give an indication of the excess or surfeit of lift in the current section; therefore, it can be used to design the wing's stall characteristics.

Wing performance in function of the main geometric parameters

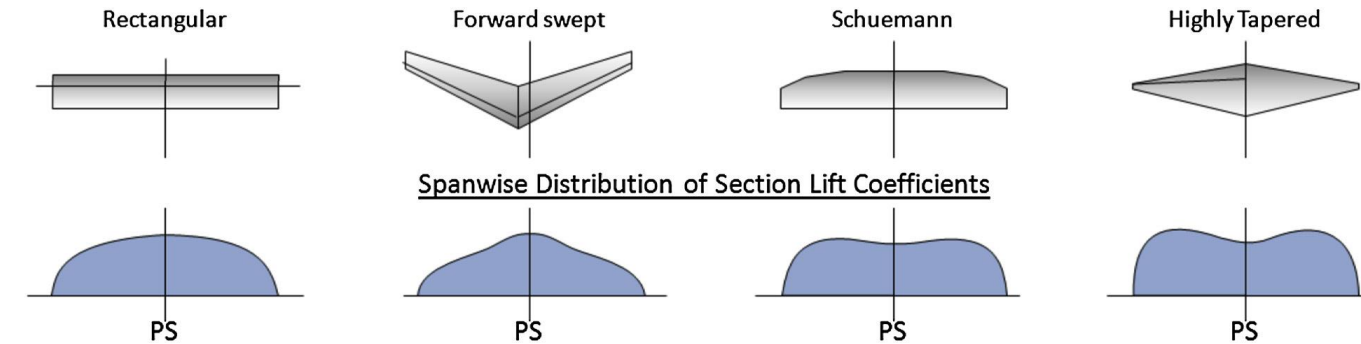
- Spanwise distribution of section **lift coefficient** and stall progression of different wing planforms.



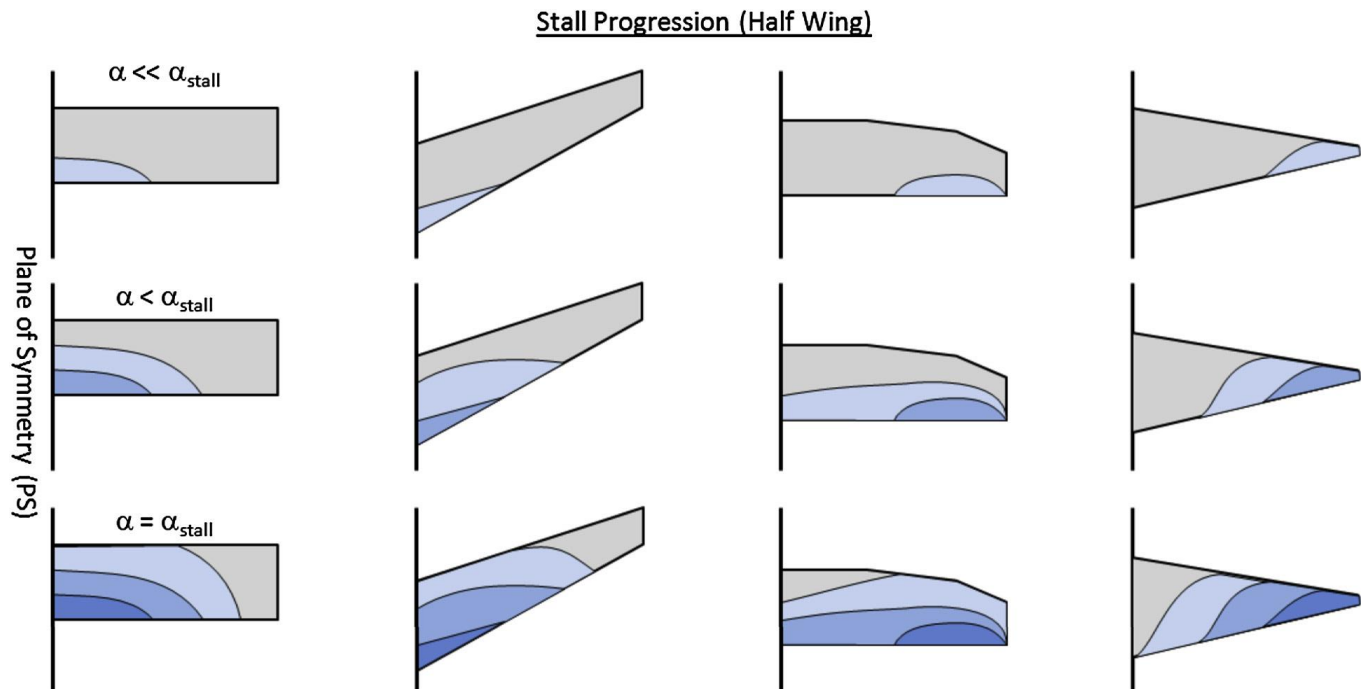
Neither geometrical twist nor aerodynamics twist

Wing performance in function of the main geometric parameters

- Spanwise distribution of section **lift coefficient** and stall progression of different wing planforms.

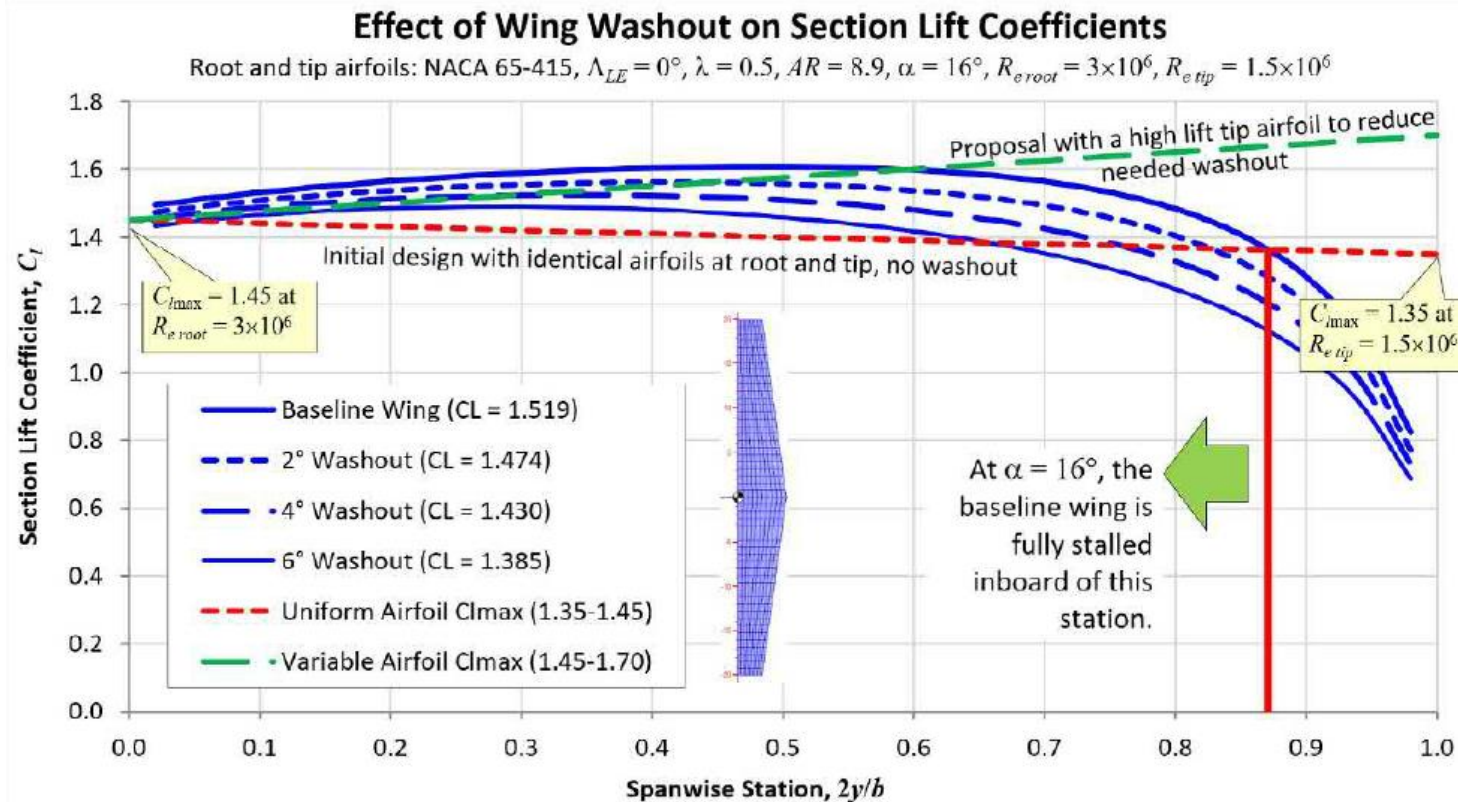


Neither geometrical twist nor aerodynamics twist



Wing performance in function of the main geometric parameters

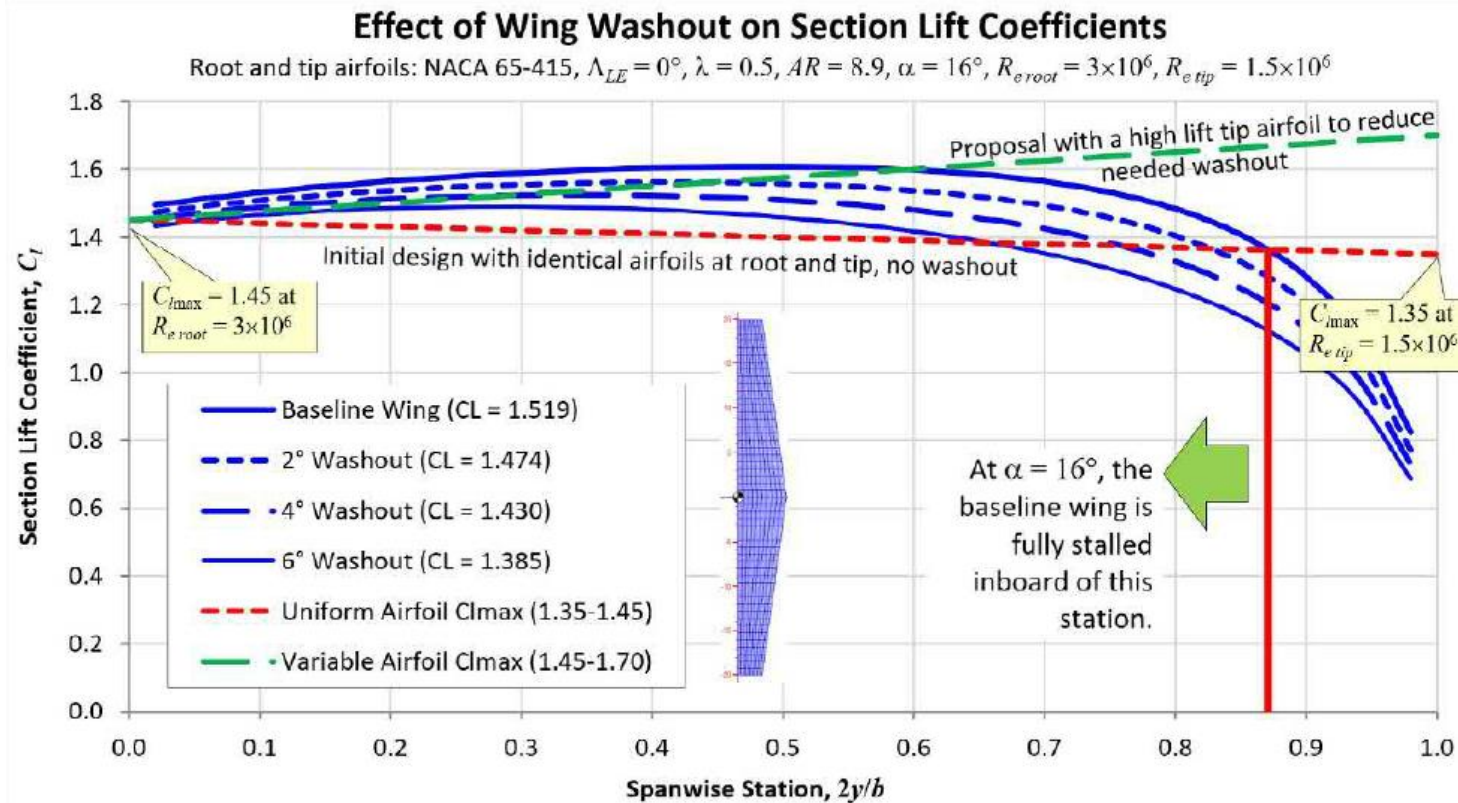
- The effect of wash-out on stall progression and spanwise lift distribution.
 - The baseline wing is more tip-loaded than the ones with wash-out and this will cause it to stall closer to the wingtip, which may cause roll off problems.
 - Wash-out is used to control stall progression and can be improved by selecting a high-lift airfoil at the tip.



- The baseline 2D curves are obtained by computing the cross-section $C_{l\ max}$.
- For a wing with taper ratio, each section have a different Reynolds number. Therefore, a different $C_{l\ max}$.
- Also, a wing with different cross-sections (aerodynamic twist) will have different $C_{l\ max}$.
- The location where the spanwise lift distribution touch the baseline curve, is where the wing stalls first and where the stall progression begins.
- This condition also corresponds to $C_{L\ max}$.
- This method to control stall progression is known as the critical section method.
- The airfoil $C_{l\ max}$ and spanwise lift distribution can be obtained from experimental measurements, linear methods (LLT, VLM, panel methods), or CFD simulations.

Wing performance in function of the main geometric parameters

- The effect of wash-out on stall progression and spanwise lift distribution.
 - Wash-out can also be used to achieve an optimal spanwise lift distribution.
 - By carefully tuning the angle of attack that each section sees, the induced drag can be reduced.
 - Remember, geometrical and aerodynamic twist can be used together.



- The baseline 2D curves are obtained by computing the cross-section $C_{l\ max}$.
- For a wing with taper ratio, each section have a different Reynolds number. Therefore, a different $C_{l\ max}$.
- Also, a wing with different cross-sections (aerodynamic twist) will have different $C_{l\ max}$.
- The location where the spanwise lift distribution touch the baseline curve, is where the wing stalls first and where the stall progression begins.
- This condition also corresponds to $C_{L\ max}$.
- This method to control stall progression is known as the critical section method.
- The airfoil $C_{l\ max}$ and spanwise lift distribution can be obtained from experimental measurements, linear methods (LLT, VLM, panel methods), or CFD simulations.

Wing performance in function of the main geometric parameters

- Most of the airfoil aerodynamic characteristics (2D) are inherited by wings (3D):
 - Airfoil shape – Curvature.
 - Reynolds number (sectional).
 - Mach number – Compressibility effects.
 - Stall mechanism and patterns.
 - Effect of early flow separation on lift and drag.
 - Effect of leading-edge separation bubbles on lift.
 - The effect of high lift devices (HLD) on lift and drag – Flaps and slats.
 - Effect of surface finish and leading-edge contamination on lift and drag.
- Therefore, it is of paramount importance to choose a good airfoil.
- As you might guess, designing/selecting wings is much more complex than two-dimensional cases (airfoils).
- And this is chiefly to 3D effects (wing tip vortex and spanwise velocity components), and the interaction of the wing with other aircraft components (fuselage, nacelles, pylons, and so on).

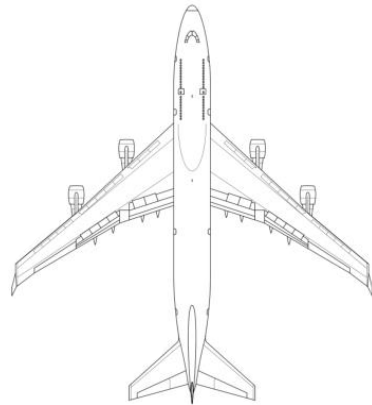
Different wing planforms used in history

Different wing planforms used in history

- Some of the different wing planforms used in history.
 - As you can see, there is no limitation regarding the shape of the wing.
 - Remember, when designing a wing your goal is to generate the required lift with the minimum drag.
 - You should also consider stability and structural issues.



Airbus 380



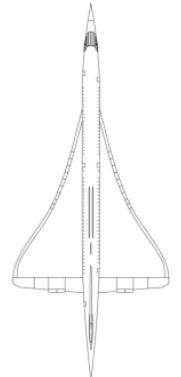
Boeing 747



Boeing 777



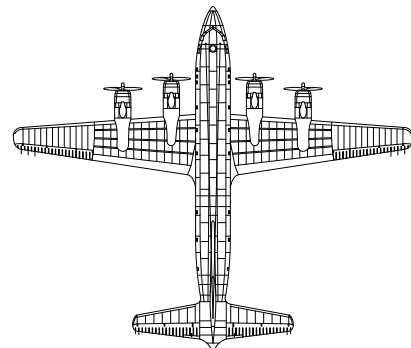
Boeing 737-800



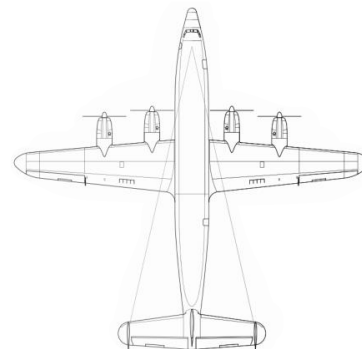
Concorde



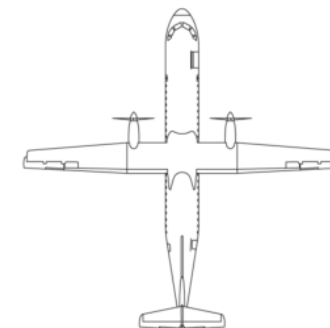
Douglas DC3



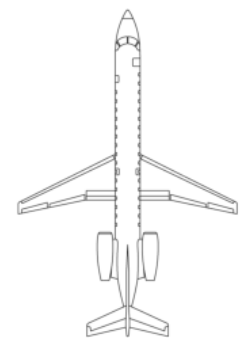
Douglas DC6



L49 Constellation



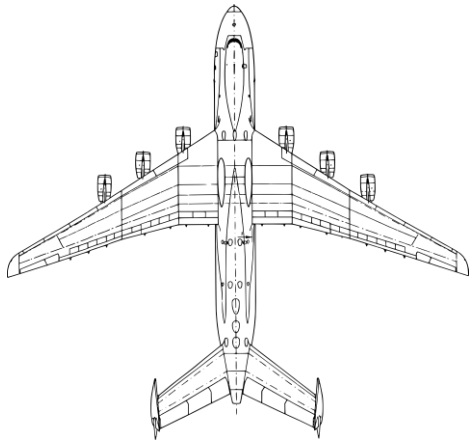
ATR 72



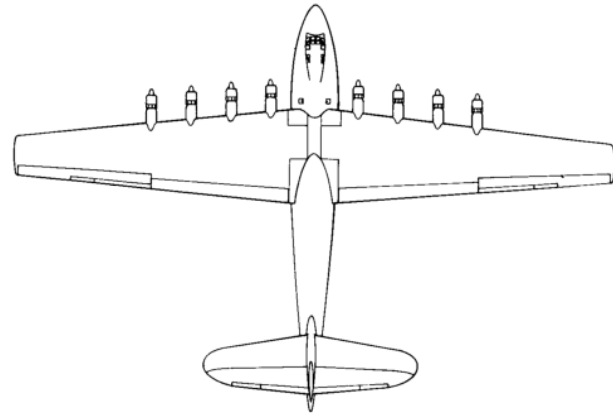
Embraer ERJ-145

Different wing planforms used in history

- Some of the different wing planforms used in history.
 - As you can see, there is no limitation regarding the shape of the wing.
 - Remember, when designing a wing your goal is to generate the required lift with the minimum drag.
 - You should also consider stability and structural issues.



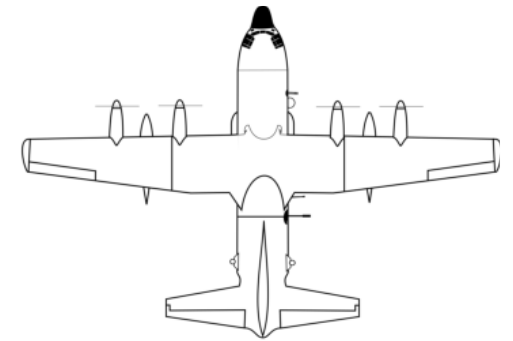
Antonov AN-225



Hughes H-4



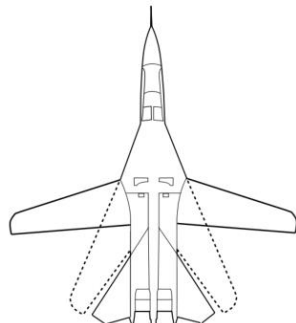
B52



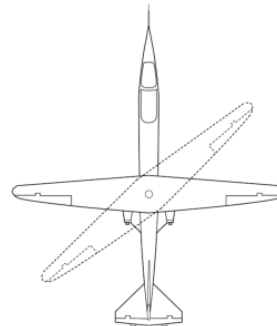
AC130



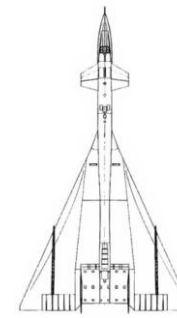
B-1B



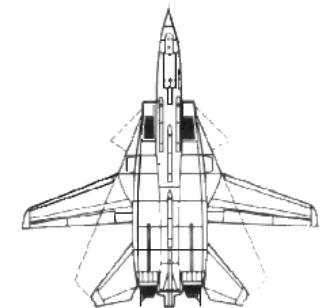
F-111



NASA AD-1



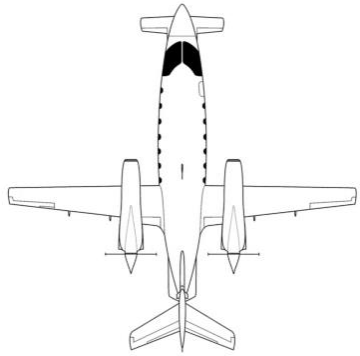
XB-70



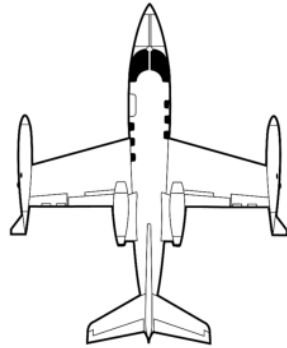
F14

Different wing planforms used in history

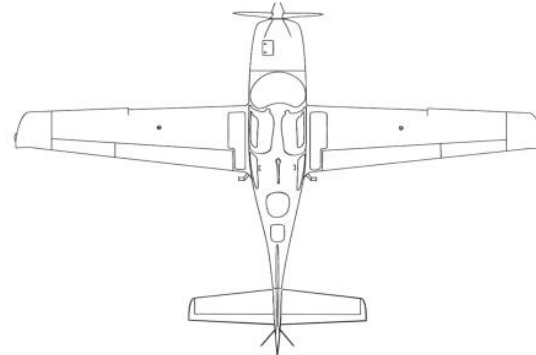
- Some of the different wing planforms used in history.
 - As you can see, there is no limitation regarding the shape of the wing.
 - Remember, when designing a wing your goal is to generate the required lift with the minimum drag.
 - You should also consider stability and structural issues.



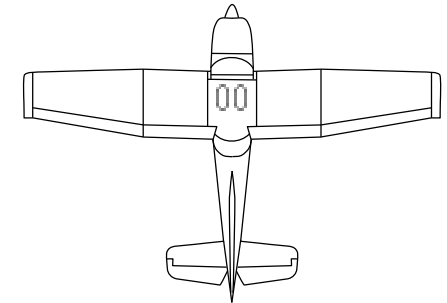
Piaggio P180
Avanti



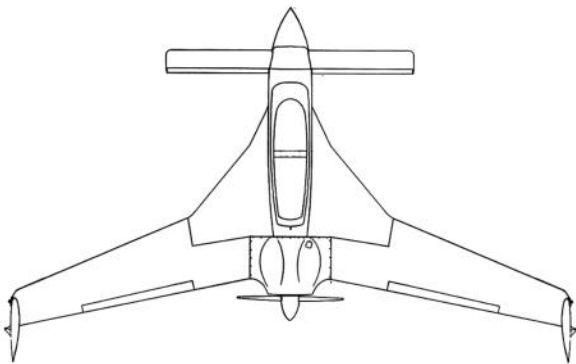
Learjet 25



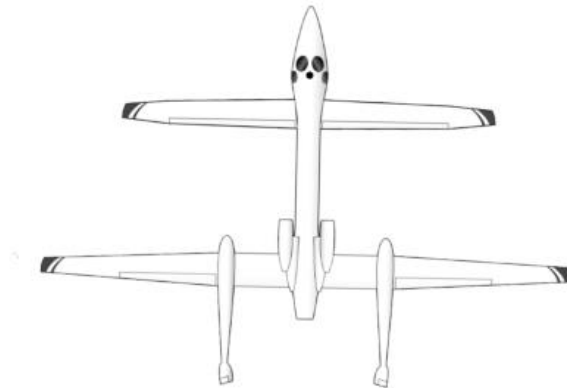
Cirrus SR22



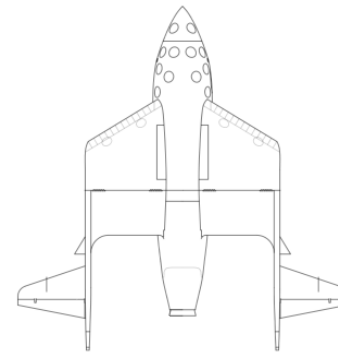
Cessna C172



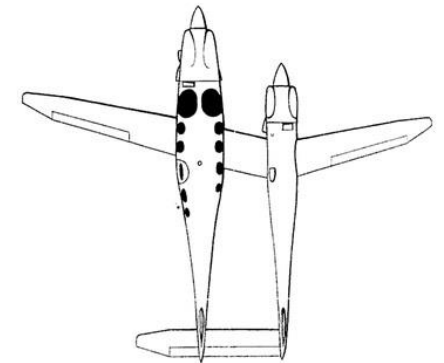
Rutan VariEze



Scaled Composites Proteus



Scaled Composites SpaceShipOne



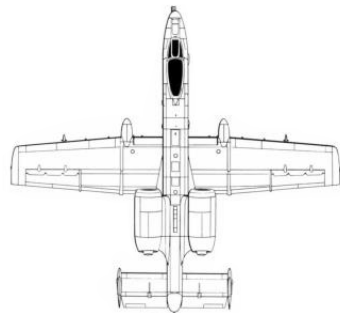
Rutan Boomerang

Different wing planforms used in history

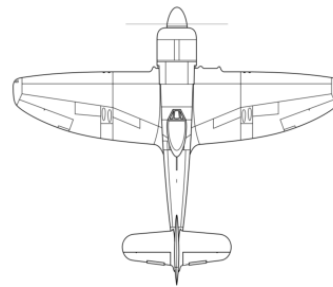
- Some of the different wing planforms used in history.
 - As you can see, there is no limitation regarding the shape of the wing.
 - Remember, when designing a wing your goal is to generate the required lift with the minimum drag.
 - You should also consider stability and structural issues.



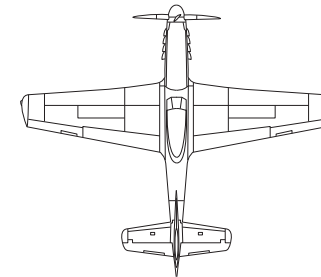
U2



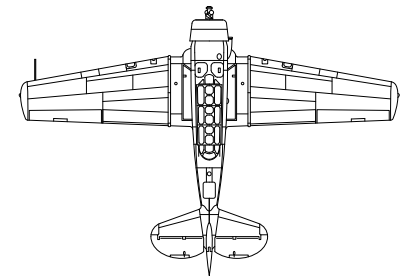
A10



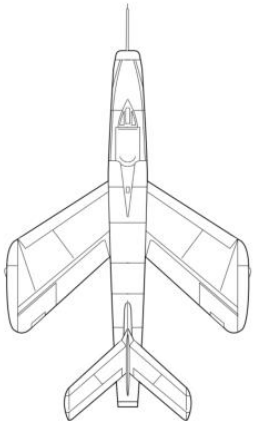
Hawker Tempest



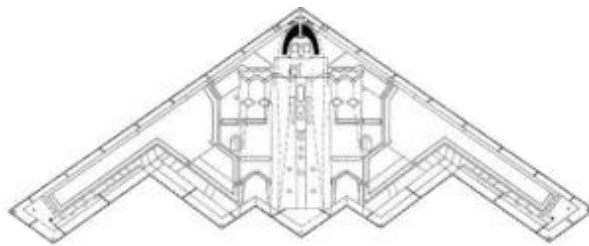
P-51 Mustang



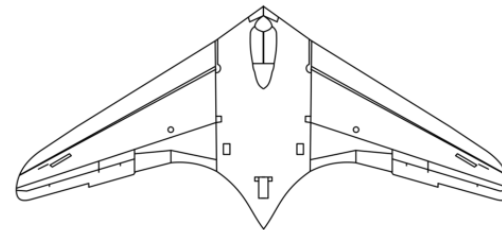
T-6G



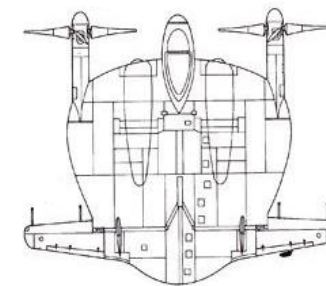
XF91



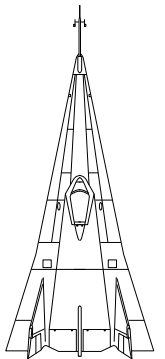
B2



Horten Ho 229



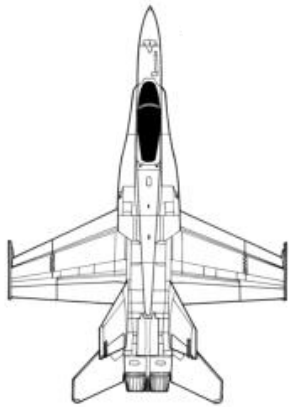
XF5U



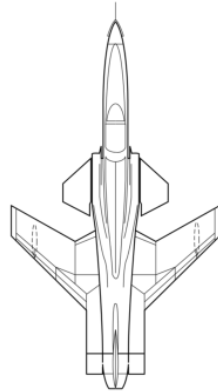
X-24B

Different wing planforms used in history

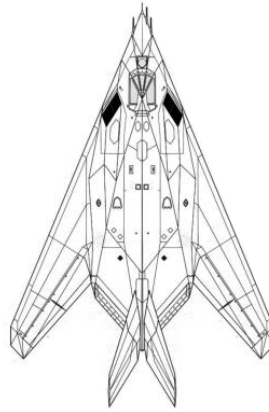
- Some of the different wing planforms used in history.
 - As you can see, there is no limitation regarding the shape of the wing.
 - Remember, when designing a wing your goal is to generate the required lift with the minimum drag.
 - You should also consider stability and structural issues.



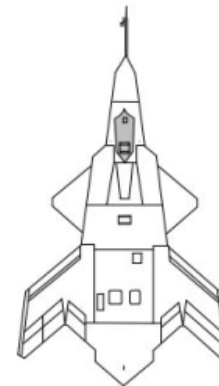
F18



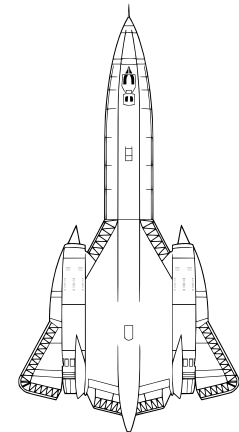
X29



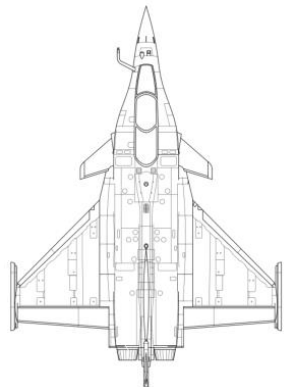
F117



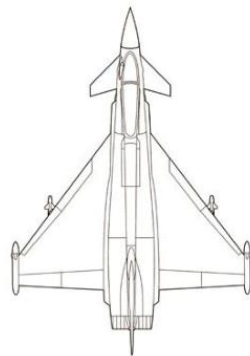
X36



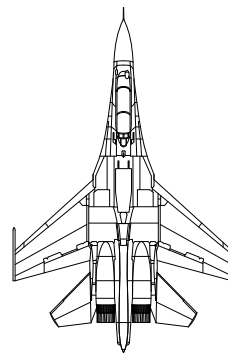
SR71



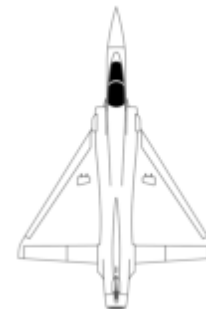
Dassault Rafale



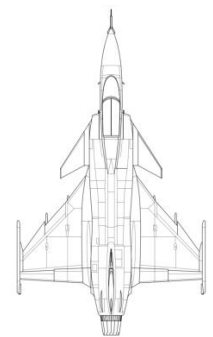
Eurofighter Typhoon



Sukhoi Su-30



Dassault Mirage
2000

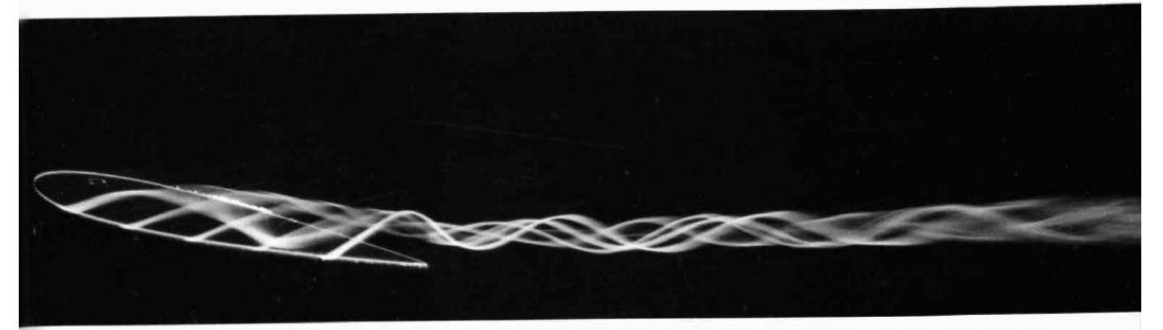
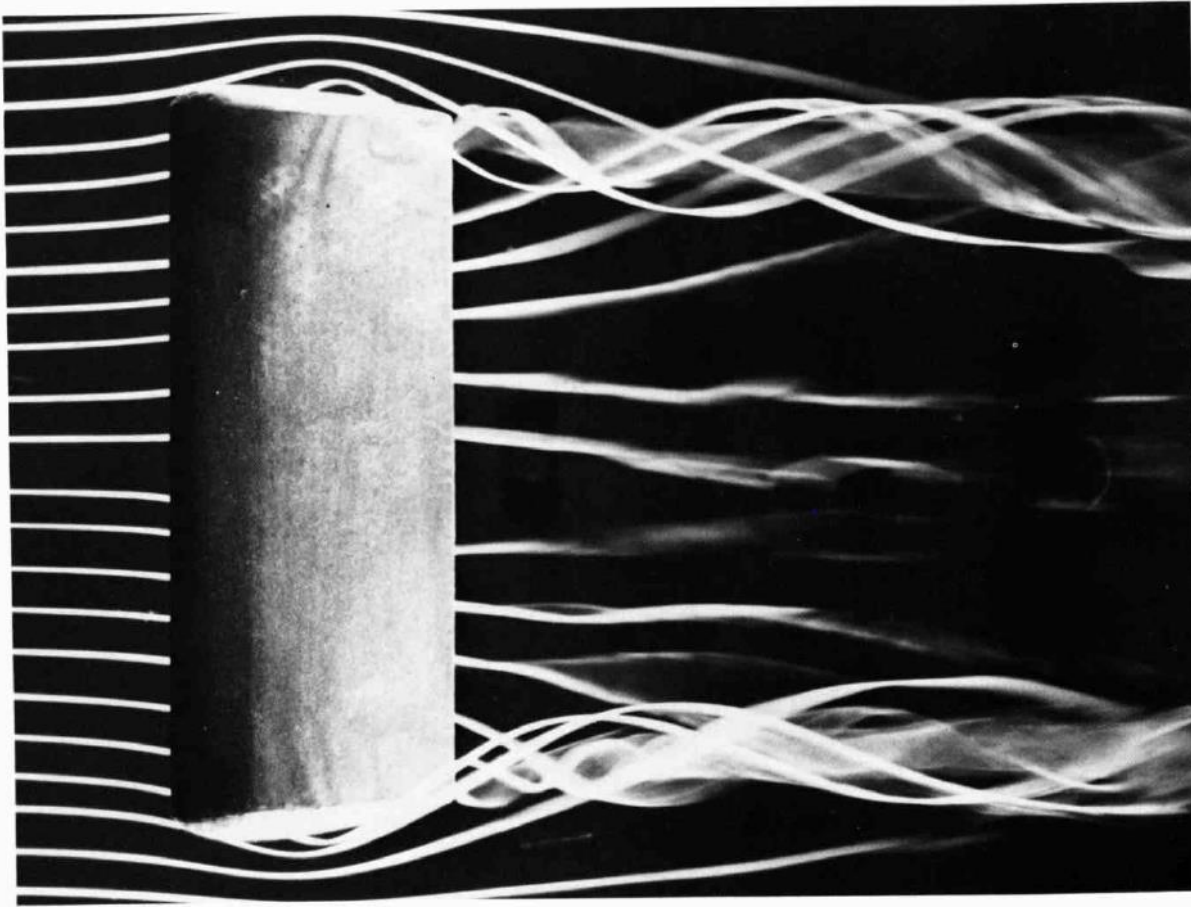


Saab JAS 39 Gripen

Finite-span wings features 3D world

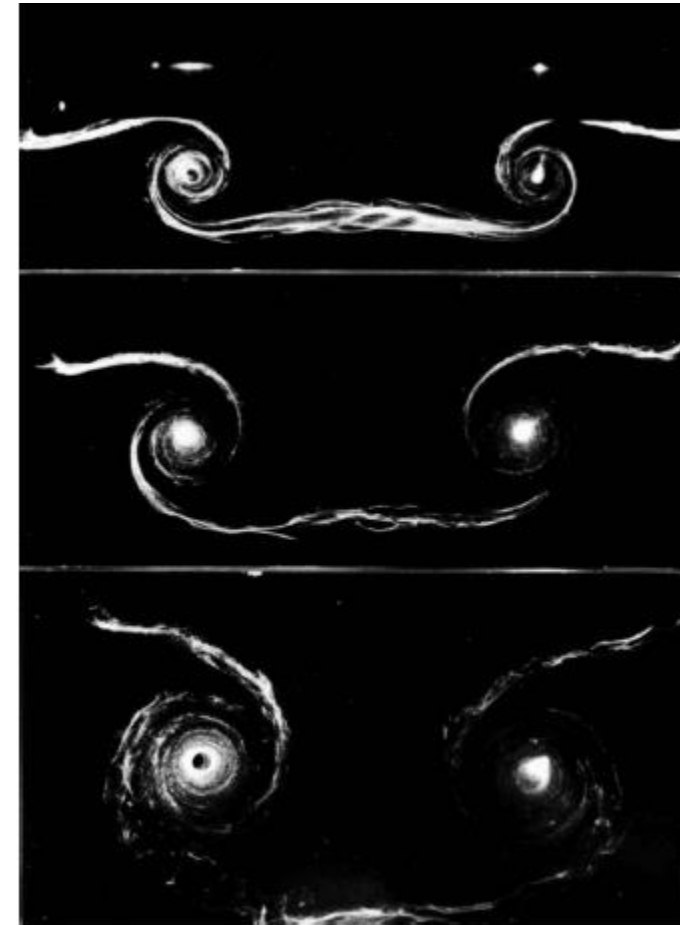
Finite-span wings features – 3D world

- Three-dimensional effects of finite-span wings – Wingtip and trailing edge vortices.



Finite-span wings features – 3D world

- Three-dimensional effects of finite-span wings – Visualization of the vortex sheet behind a rectangular wing.
- Wake rolling up behind the wing at 9° AOA is visualized at different planes behind the wing.



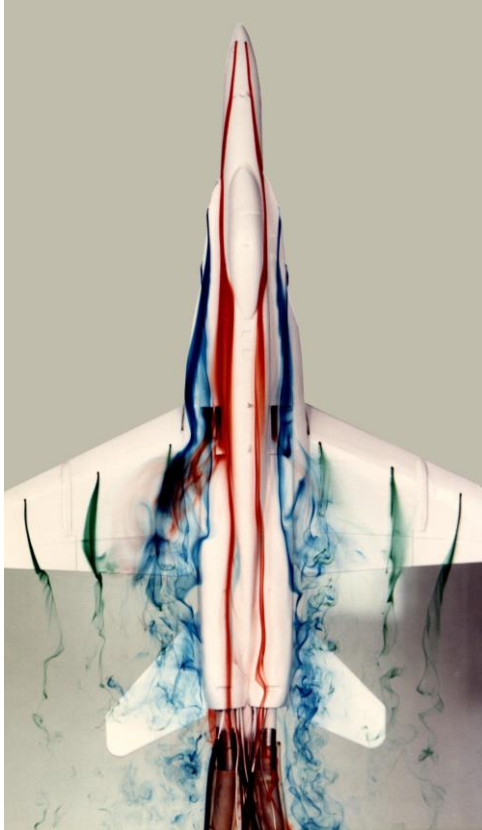
Finite-span wings features – 3D world

- Three-dimensional effects of finite-span wings – Wingtip vortices.

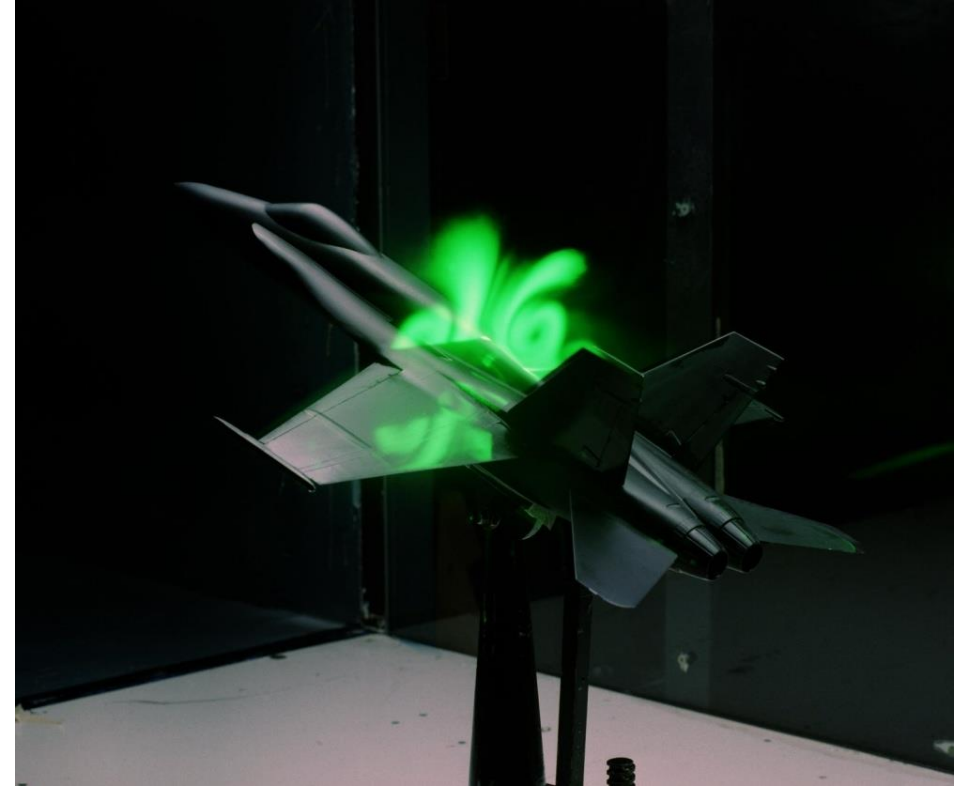


Finite-span wings features – 3D world

- Three-dimensional effects of finite-span wings – Visualization of vortical structures.



Vortices on a 1/48-scale model of an F/A-18 aircraft inside a Water Tunnel
Photo credit: NASA Dryden Flow Visualization Facility.
<http://www.nasa.gov/centers/armstrong/multimedia/imagegallery/FVF>
Copyright on the images is held by the contributors. Apart from Fair Use, permission must be sought for any other purpose.



Doppler Global Velocimetry (DGV) of F/A-18 – Visualization of vortical structures
Photo credit: NASA Langley Research Center.
<https://www.dvidshub.net/image/718184/doppler-global-velocimetry-f-18#.Uuj65GQ1jgo>
Copyright on the images is held by the contributors. Apart from Fair Use, permission must be sought for any other purpose.

Finite-span wings features – 3D world

- Interference effects and surface flow patterns visualization using fluorescent oil.

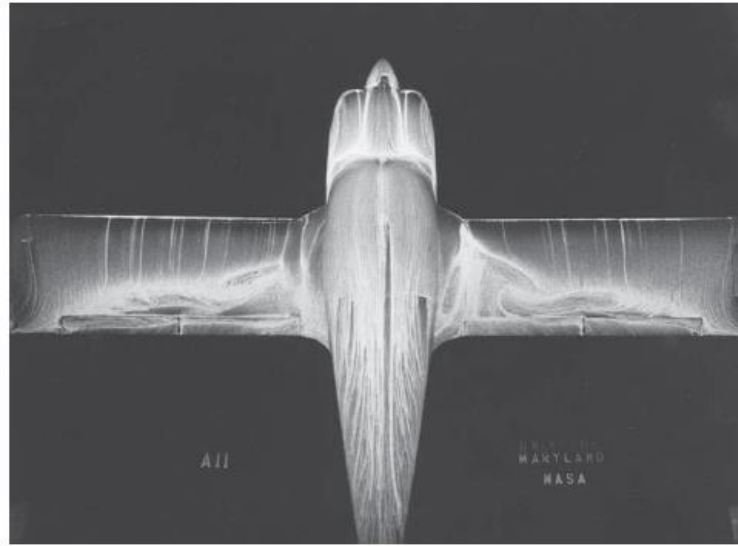


Finite-span wings features – 3D world

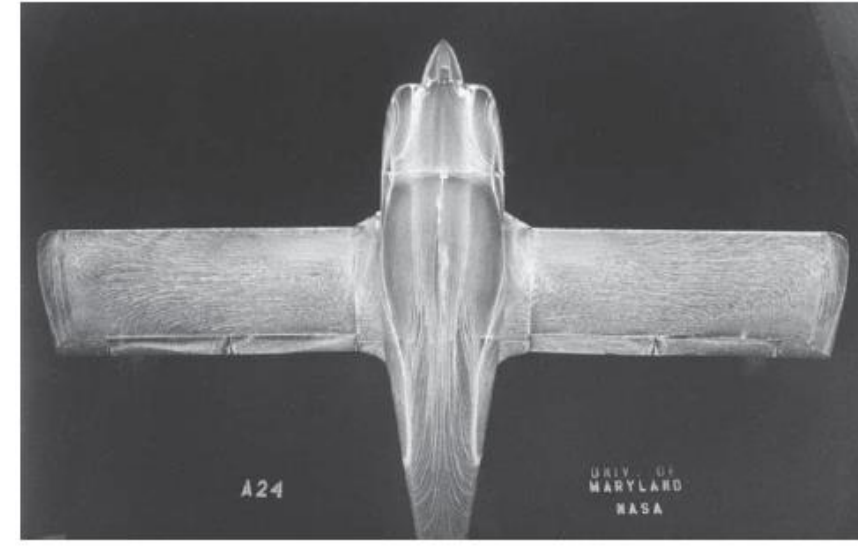
- Surface flow patterns visualization using fluorescent oil – Flow stall pattern on wing surface.



Below stall – Flow attached



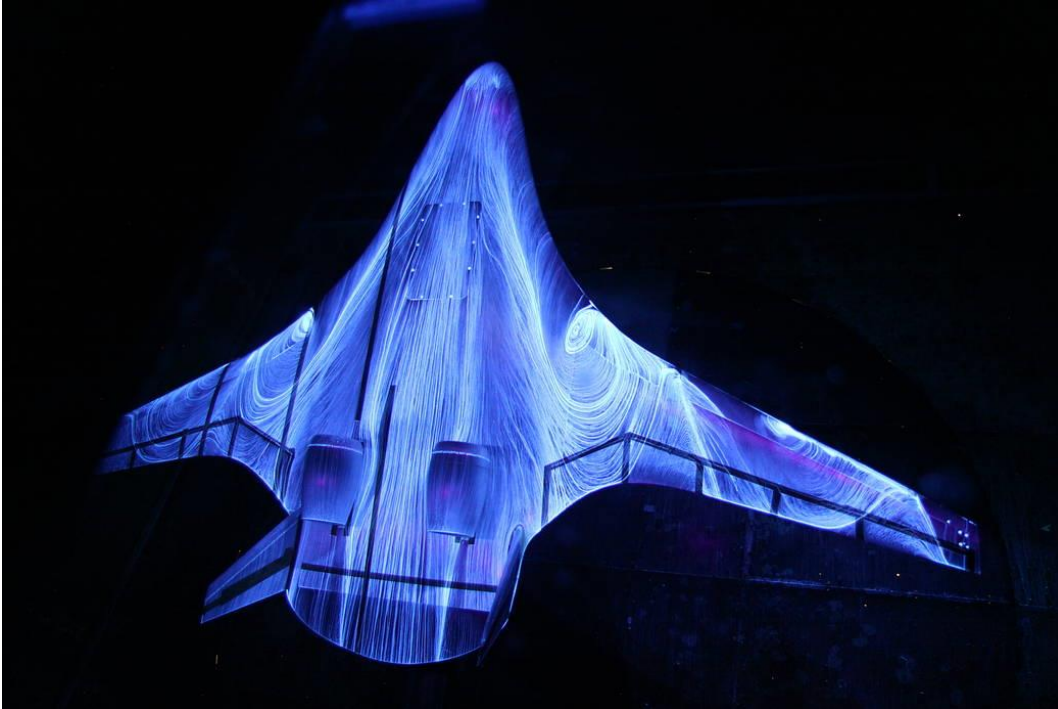
Near stall – Highly three-dimensional flow, it detaches close to the wing root.



Far beyond stall – The flow over the wing has separated.

Finite-span wings features – 3D world

- Surface flow patterns visualization using fluorescent oil – Wing/fuselage junction separation bubbles.

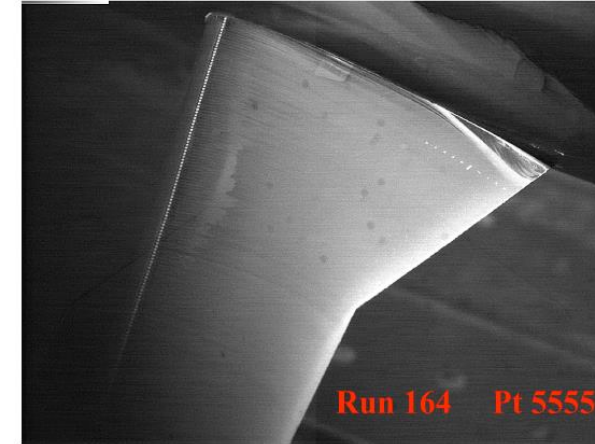


Surface flow patterns visualization using fluorescent oil

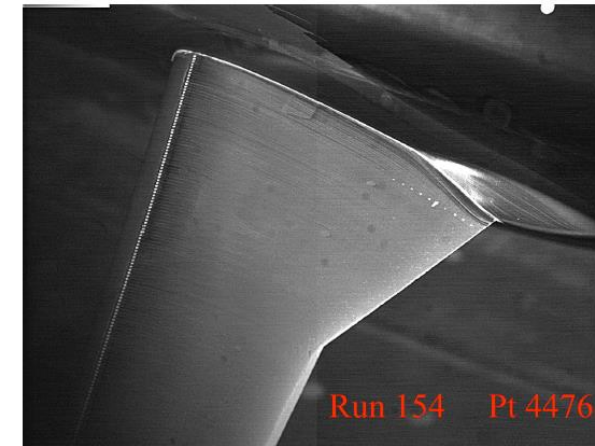
Photo credit: NASA Dryden Flow Visualization Facility.

https://www.nasa.gov/aero/flow_patterns_image.html

Copyright on the images is held by the contributors. Apart from Fair Use, permission must be sought for any other purpose.



a) Wing/Body configuration.



b) Wing/Body/Fairing configuration.

Figure 15. Surface oil flow visualization showing the effects of the FX2B fairing, $C_L = 0.5$, rear $\frac{1}{4}$ vie

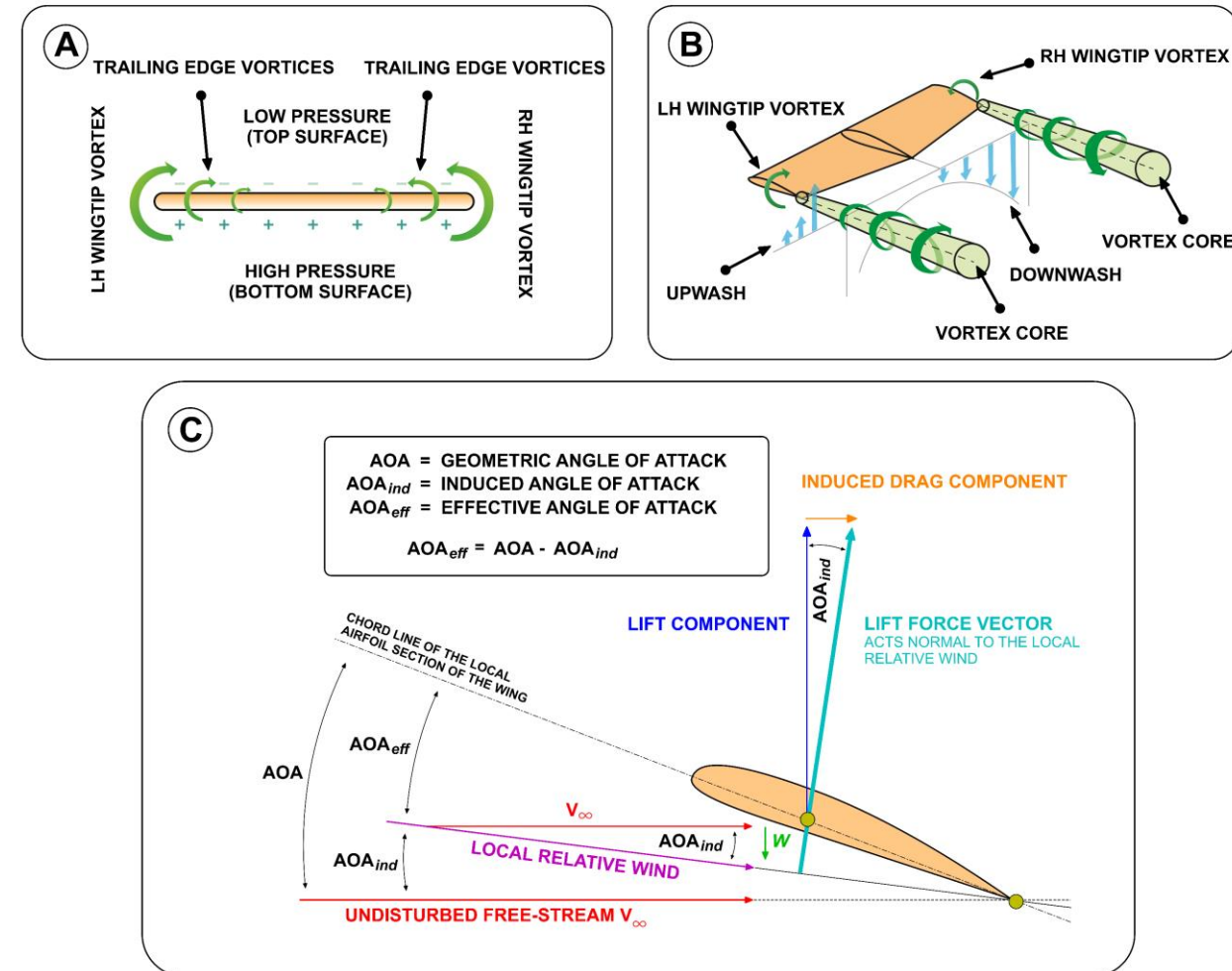
Photo credit: M. Gatlin, M. Rivers, S. Goodiff, R. Rudnik, M. Siltzmann. Experimental investigations of the DLR-F6 transport configuration in the national transonic facility. 26th AIAA conf, 2008.

Copyright on the images is held by the contributors. Apart from Fair Use, permission must be sought for any other purpose.

Lift-induced drag

Lift-induced drag

- On the origin of the lift-induced drag, downwash, and induced angle.
- Remember, lift-induced drag is a characteristic of finite-span wings.
- The flow moving from the high-pressure region to the low-pressure region will generate trailing edge vortices and wingtip vortices.
- This flow movement from the high-pressure region to the low-pressure region will also generate a downwash that will reduce the angle of attack that the airfoil effectively sees.
- This effect is particularly strong towards the wingtips.
- As a consequence of the downwash, every cross section of the wing will see a different angle of attack, the effective angle of attack.
- The downwash (w in the figure), will also incline backwards the lift component, giving raise to the lift induced-drag.
- The effective angle of attack is illustrated in the bottom figure.



Lift-induced drag

- To reduce the lift-induced drag we can:
 - As demonstrated by Prandtl, we can simply increase wings' aspect ratio **AR**.
 - Remember, **AR** is related to induced drag as follows,

$$C_{D_{ind}} = \frac{C_L^2}{\pi AR e}$$

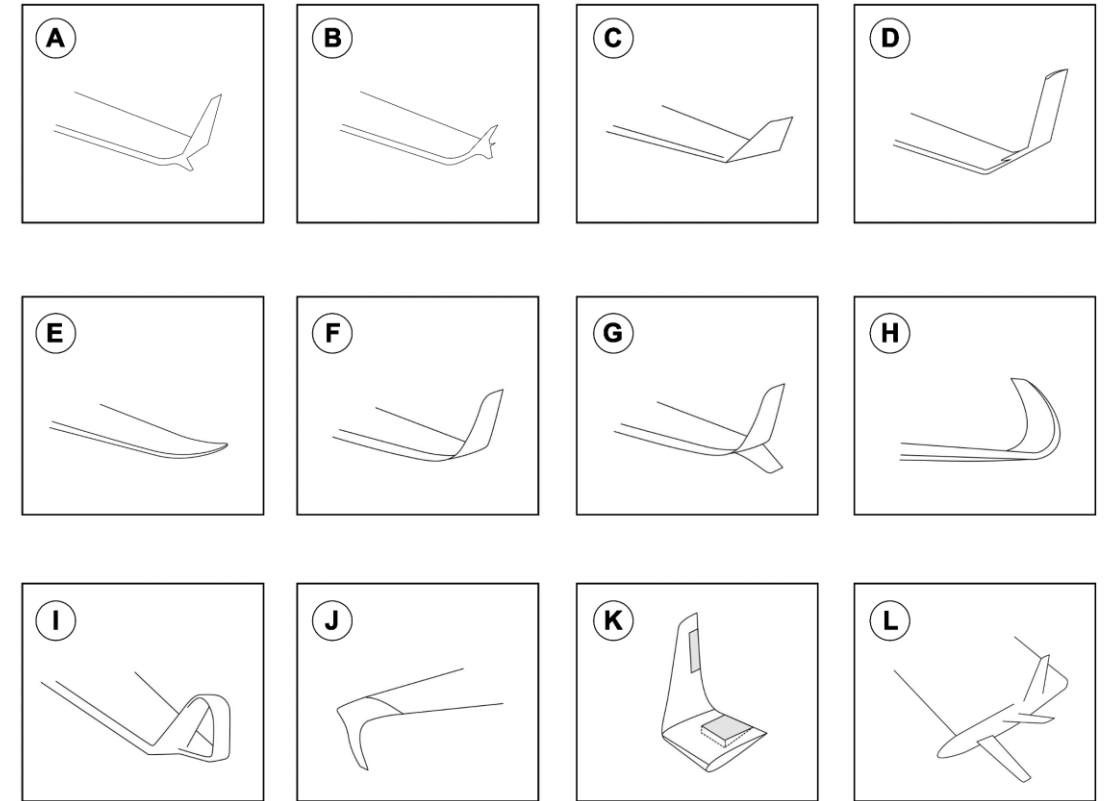
- The wing aspect ratio can be computed as follows,

$$AR = \frac{b^2}{S}$$

- By increasing the wingspan **b** we can increase the wing aspect ratio **AR**.
- Increasing the wing aspect ratio **AR** is the simplest way to reduce the lift induced drag.
- However, increasing the **AR** can have negative effects, such as, increased root bending moment, increased structural weight, poor handling qualities (low roll rate), airport operational problems, flutter, and so on.

Lift-induced drag

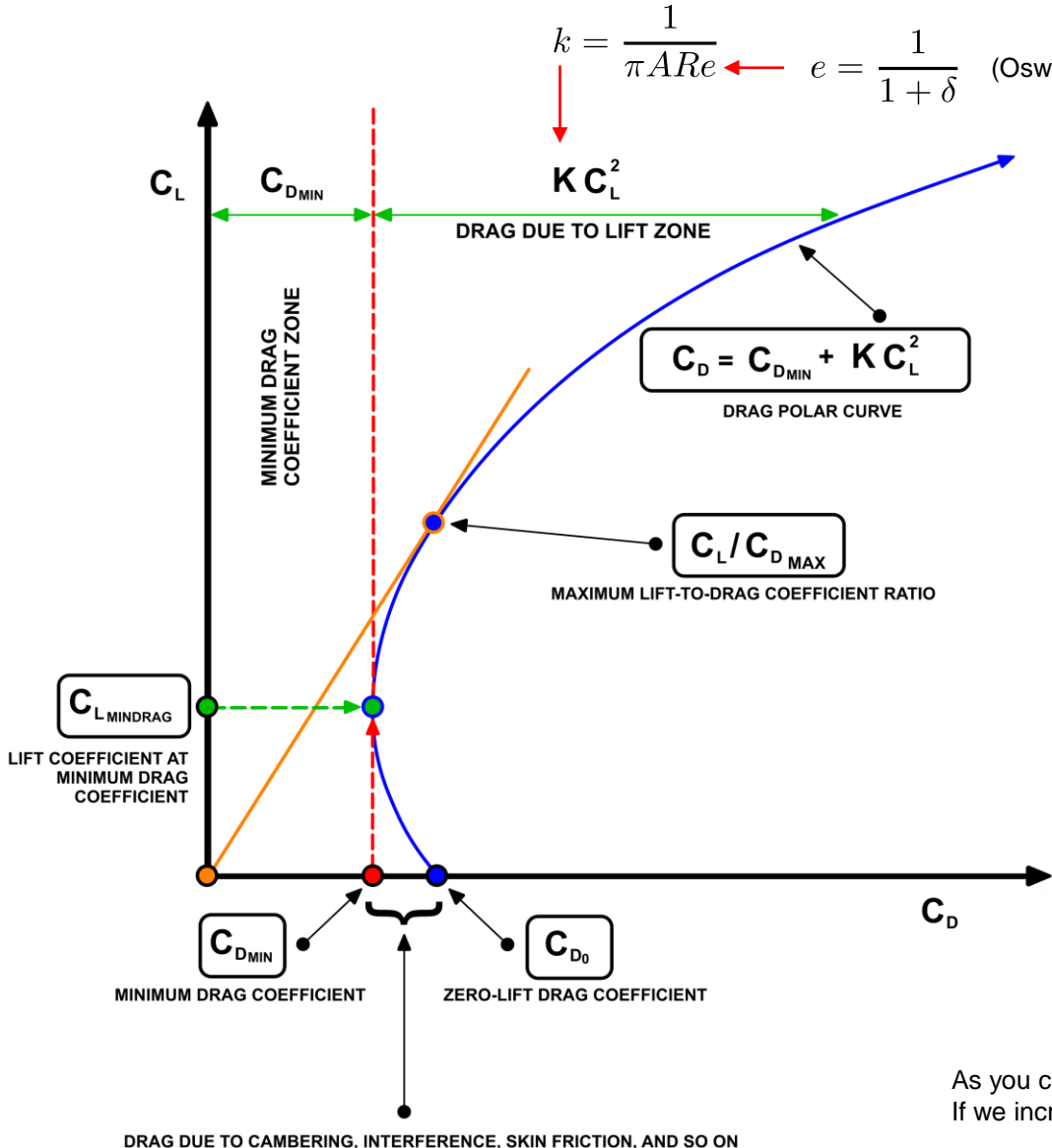
- To reduce the lift-induced drag we can:
 - Add wingtip devices that artificially increase the wingspan by modifying the pressure distribution at the wingtips.
 - One of such wingtip devices are known as winglets, as illustrated in the figure.
 - Other options:
 - Planform design.
 - Use of geometrical and aerodynamic twist.
 - Nonplanar systems different from winglets (closed loop surfaces and box wings).
 - Wingtip modifications (hoerner wingtip, drooped wingtip, wingtip feathers).
 - Multiple lifting surfaces.
 - And of course, larger AR.



- A. Whitcomb Winglet**
- B. Tip Fence**
- C. Canted Winglet**
- D. Vortex Diffuser**
- E. Raked Tip**
- F. Blended Winglet**
- G. Blended Split Winglet**
- H. Sharklet**
- I. Spiroid Winglet**
- J. Downward Canted Winglet**
- K. Active Winglet**
- L. Tip Sails**

Lift-induced drag

- Drag polar, lift-induced drag coefficient and induced drag factor.



- The induced drag factor δ is zero only for elliptical wings.
- For the rest of the wings is a number larger than zero and usually between 0.02 and 0.2.
- Basically, it penalizes the wing.
- The larger the number is, the more induced drag the wing will produce.
- It can be used as indication to determine how far we are from the elliptical distribution.
- The induced drag factor can also be used to compute the Oswald span efficiency e , which is another metric indicating how far we are from an elliptical lift distribution.
- A value of e equal to 1 is an indication of a perfect elliptical lift distribution.

Induced drag factor.

$$C_{D_{ind}} = \frac{C_L^2}{\pi A R e} = \frac{C_L^2}{\pi A R} (1 + \delta)$$

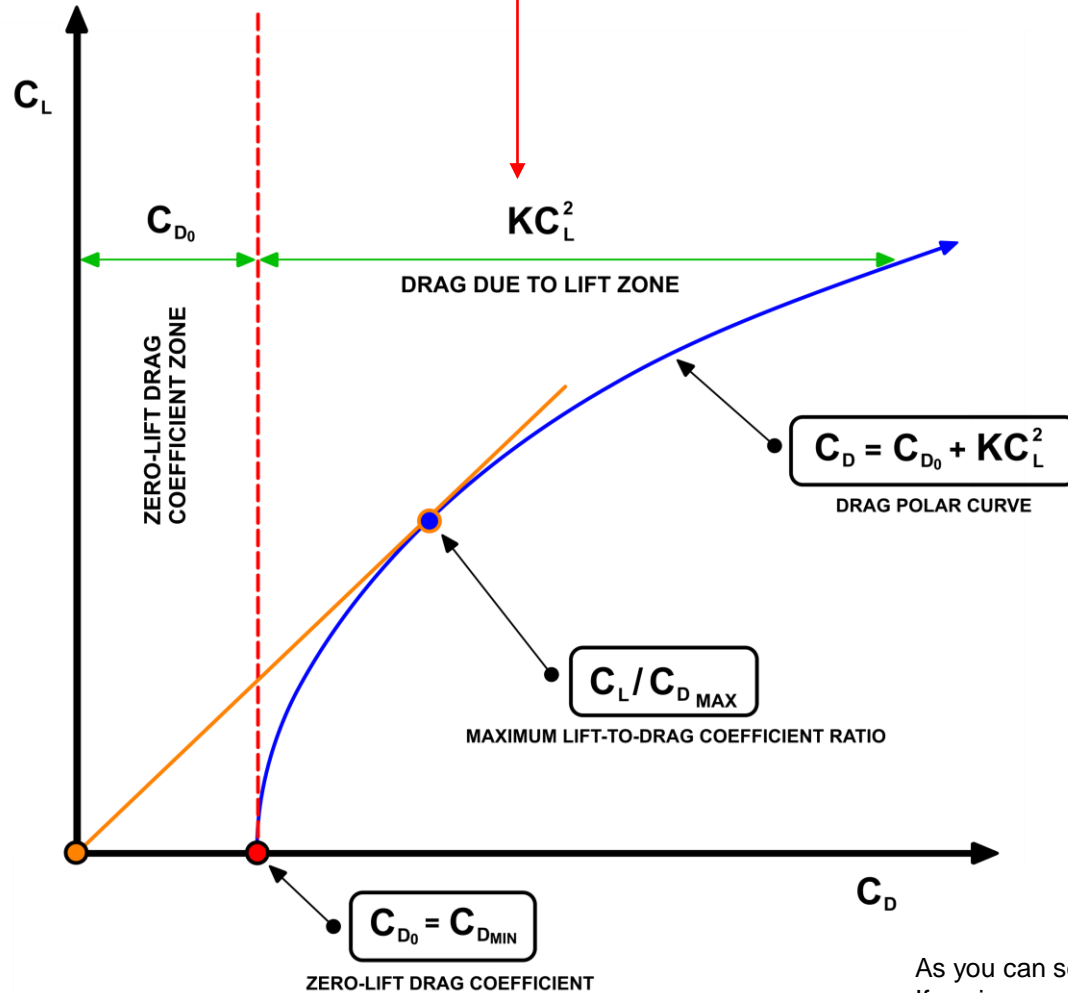
$e = \frac{1}{1 + \delta}$ (Oswald span efficiency)

As you can see, the lift-induced drag depends on the aspect ratio. If we increase the aspect ratio, we will reduce the lift-induced drag.

Lift-induced drag

- Drag polar, lift-induced drag coefficient and induced drag factor.

$$k = \frac{1}{\pi A R e} \leftarrow e = \frac{1}{1 + \delta} \quad (\text{Oswald span efficiency})$$



- The induced drag factor δ is zero only for elliptical wings.
- For the rest of the wings is a number larger than zero and usually between 0.02 and 0.2.
- Basically, it penalizes the wing.
- The larger the number is, the more induced drag the wing will produce.
- It can be used as indication to determine how far we are from the elliptical distribution.
- The induced drag factor can also be used to compute the Oswald span efficiency e , which is another metric indicating how far we are from an elliptical lift distribution.
- A value of e equal to 1 is an indication of a perfect elliptical lift distribution.

$$C_{D_{ind}} = \frac{C_L^2}{\pi A R e} = \frac{C_L^2}{\pi A R} (1 + \delta)$$

Induced drag factor. δ


$$e = \frac{1}{1 + \delta} \quad (\text{Oswald span efficiency})$$

As you can see, the lift-induced drag depends on the aspect ratio. If we increase the aspect ratio, we will reduce the lift-induced drag.

Lift-induced drag


- There are different drag polar models that are typically used to represent the total drag of finite-span wings or aircrafts.

$$C_D = C_{D_{min}} + k_1 C_L^2 + k_2 (C_L - C_{L_{mindrag}})^2 + \Delta C_{D_M}$$

Wave drag 

$$C_D = C_{D_{min}} + k(C_L - C_{L_{mindrag}})^2 + \Delta C_{D_M}$$

$$C_D = C_{D_0} + k C_L^2 + \Delta C_{D_M} \quad \text{where} \quad k = \frac{1}{\pi A R e} = \frac{(1 + \delta)}{\pi A R} \quad \text{and} \quad C_{D_0} \approx C_{D_{min}}$$



This is the most common drag polar found in literature

- Sometimes, the following assumptions are taken in the polars,

$$C_L = C_L - C_{L_{mindrag}}$$

$$C_{L_{mindrag}} \approx 0$$

$$C_{D_0} \approx C_{D_{min}}$$

$$k_2 \approx 0$$

Lift-induced drag

- Illustration showing the effect of changing $C_{L_{mindrag}}$ and $C_{D_{min}}$ on the drag polar.

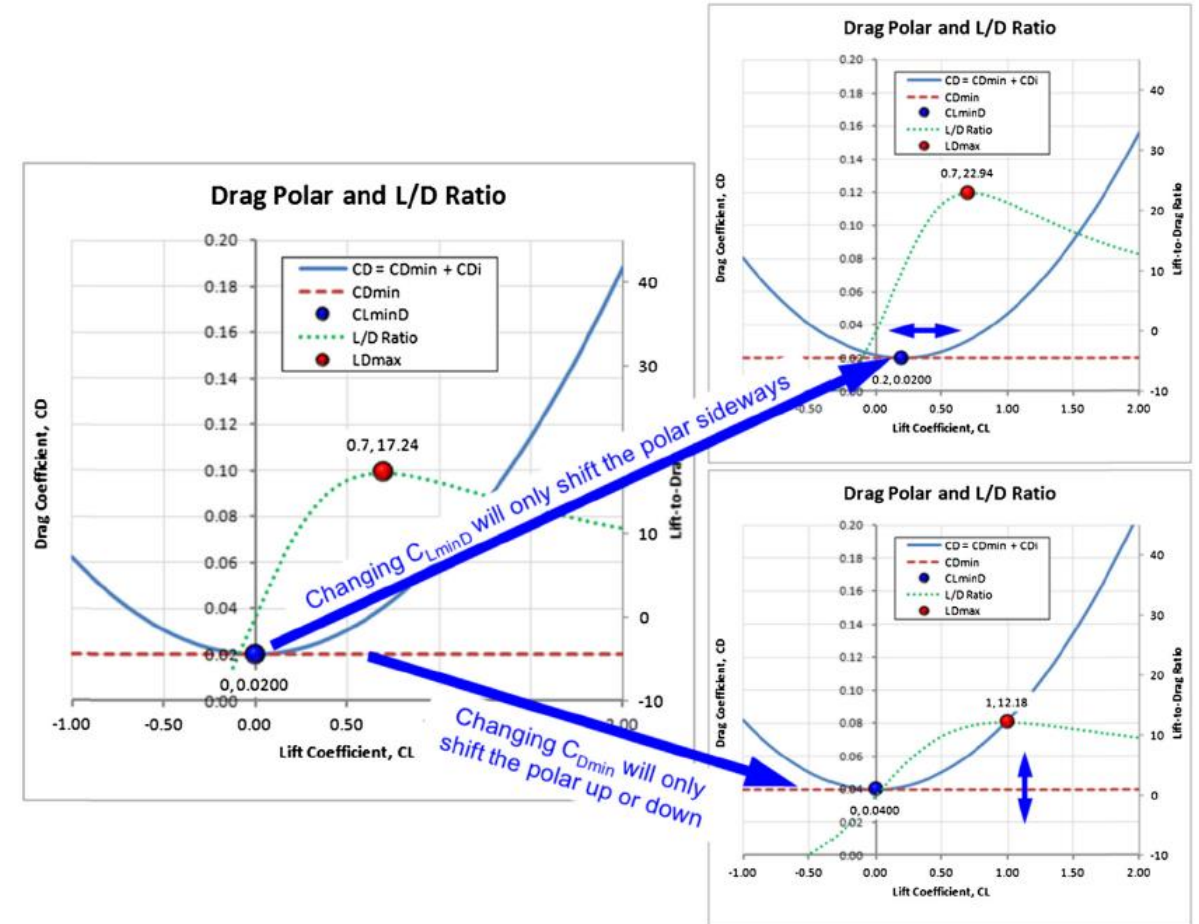
- The following quadratic model is widely found in literature, however, is not very accurate.

$$C_D = C_{D_0} + kC_L^2$$

- A more accurate quadratic model of the total drag is the following,

$$C_D = C_{D_{min}} + k(C_L - C_{L_{mindrag}})^2$$

- Have in mind that these quadratic models do not capture the drag bucket seen in airfoils.
- You will rarely see the drag bucket when plotting the polars of finite span wing (3D wings). This is due to three-dimensional effects, wing surface roughness, or freestream disturbances, among many factors.



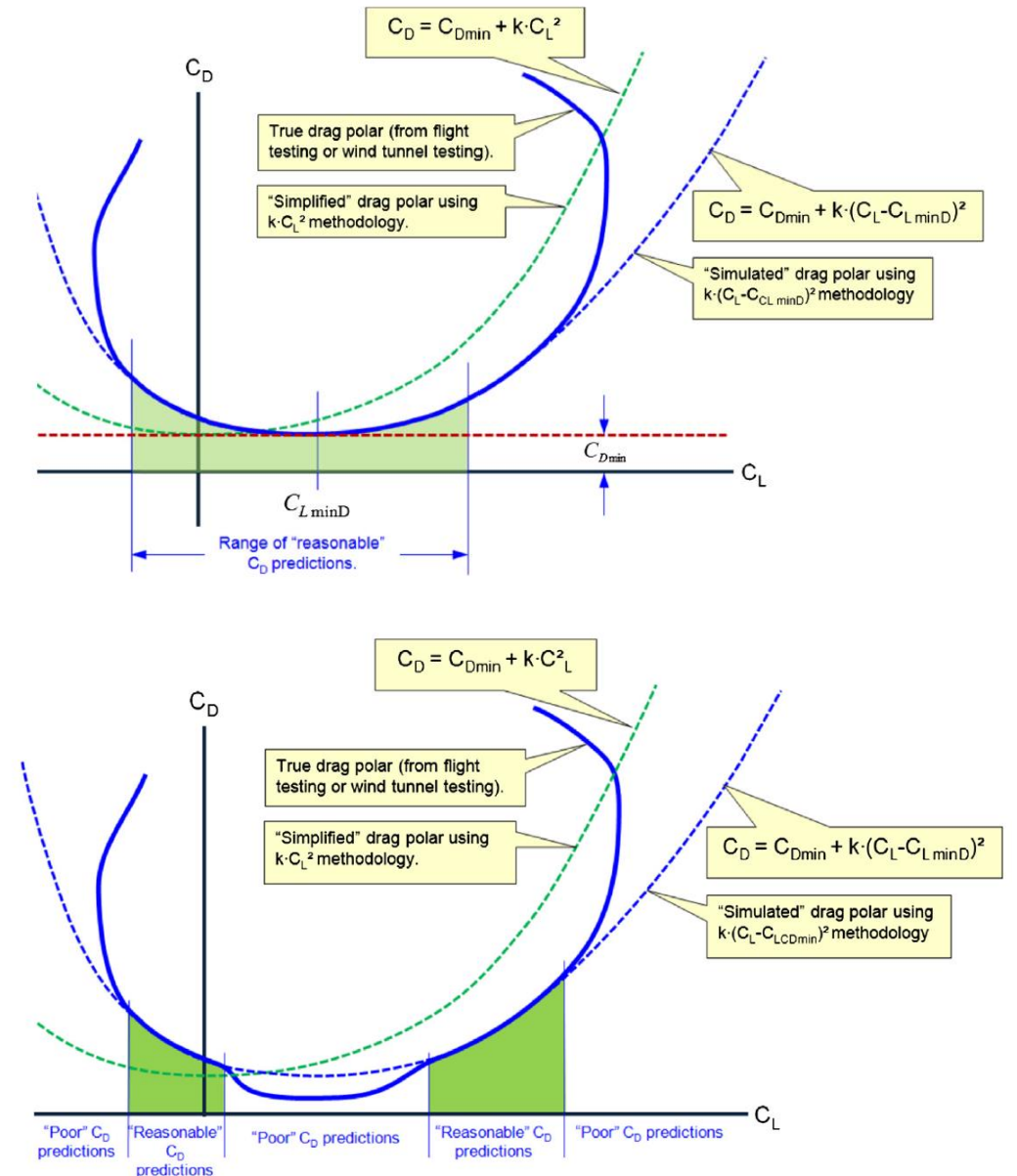
Lift-induced drag

- Curve fitting the true drag polar.
- These models are important because they are used to predict the aircraft performance.
- Therefore, we must be aware of their limitations.
- For example, if the wing features a camber, the simplified drag polar model,

$$C_D = C_{D0} + kC_L^2$$

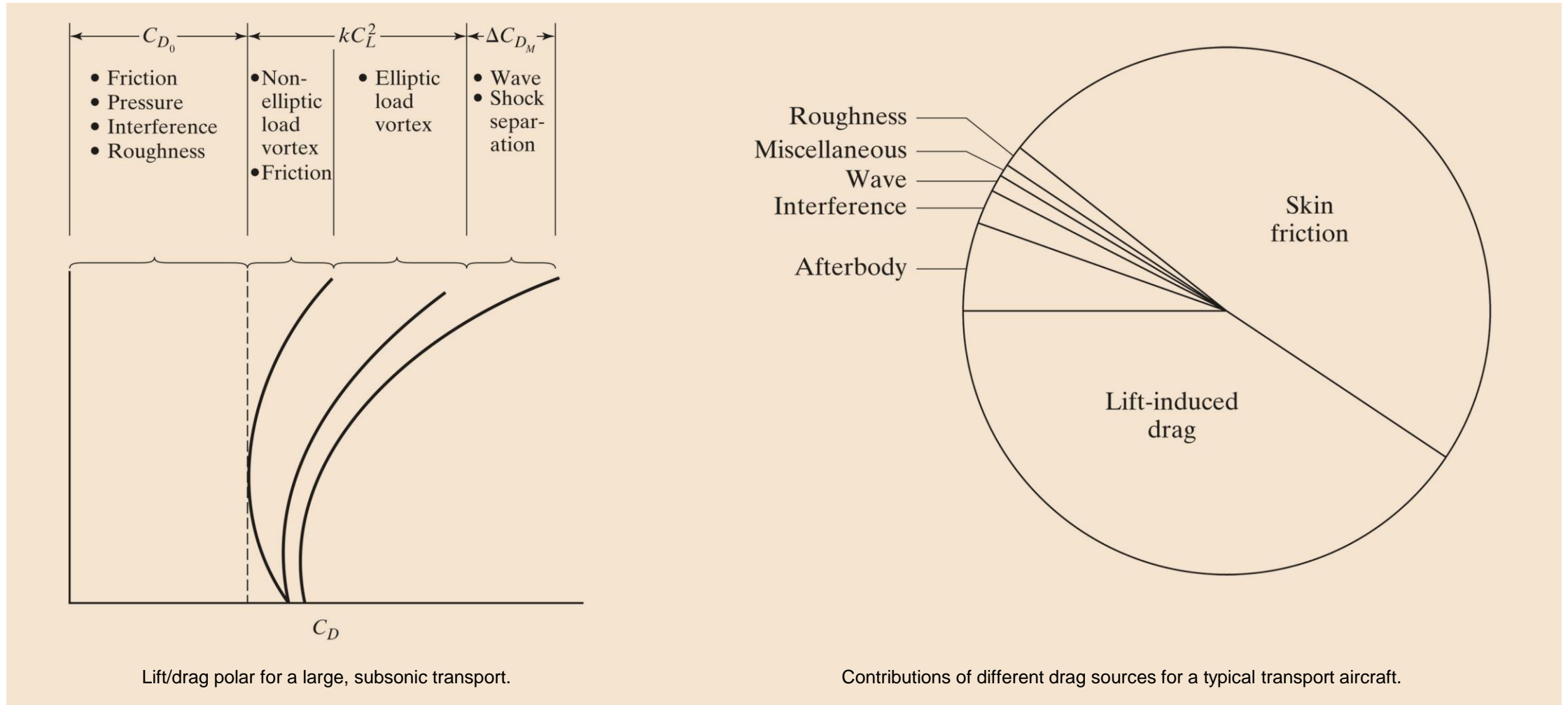
is not longer a valid representation of the drag polar.

- Also, in the presence of the drag bucket, these methods are not very accurate.
- Therefore, they must be used with care or must be corrected.



Lift-induced drag

- Lift/drag polar for a large, subsonic transport – Contribution of different drag sources for a typical transport aircraft.

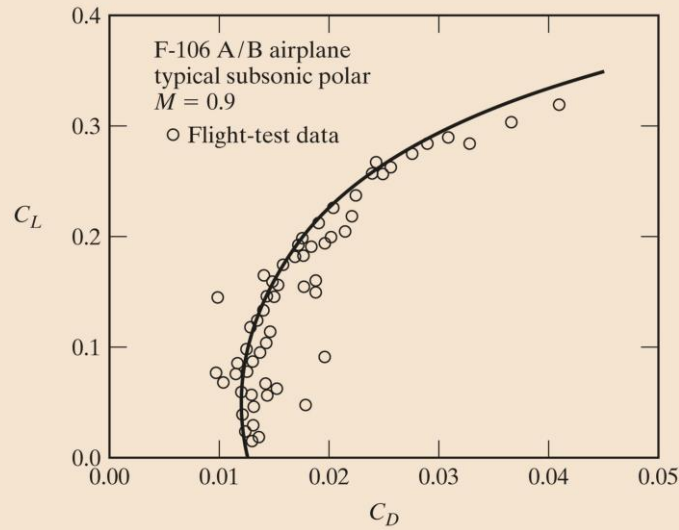


Lift/drag polar for a large, subsonic transport.

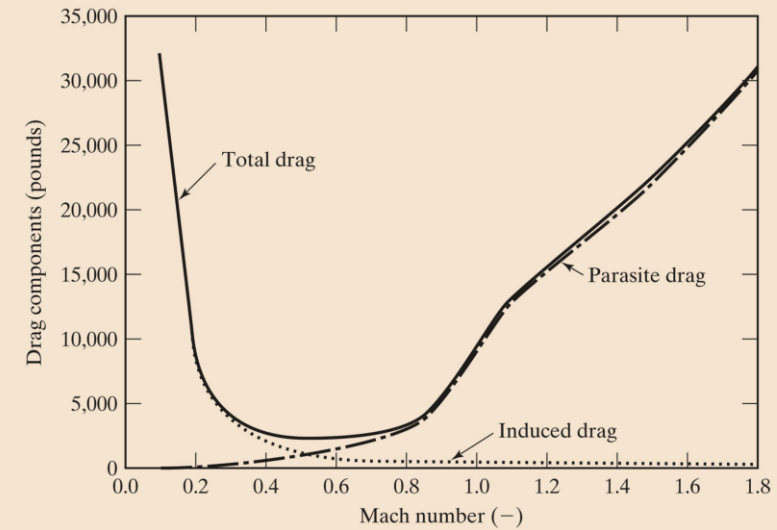
Contributions of different drag sources for a typical transport aircraft.

Lift-induced drag

- Flight data for different aircrafts.



Flight data for a drag polar for F-106A/B aircraft at a Mach number of 0.9.



Drag components for an F-16C flying in steady, level, unaccelerated flight at 20,000 ft.

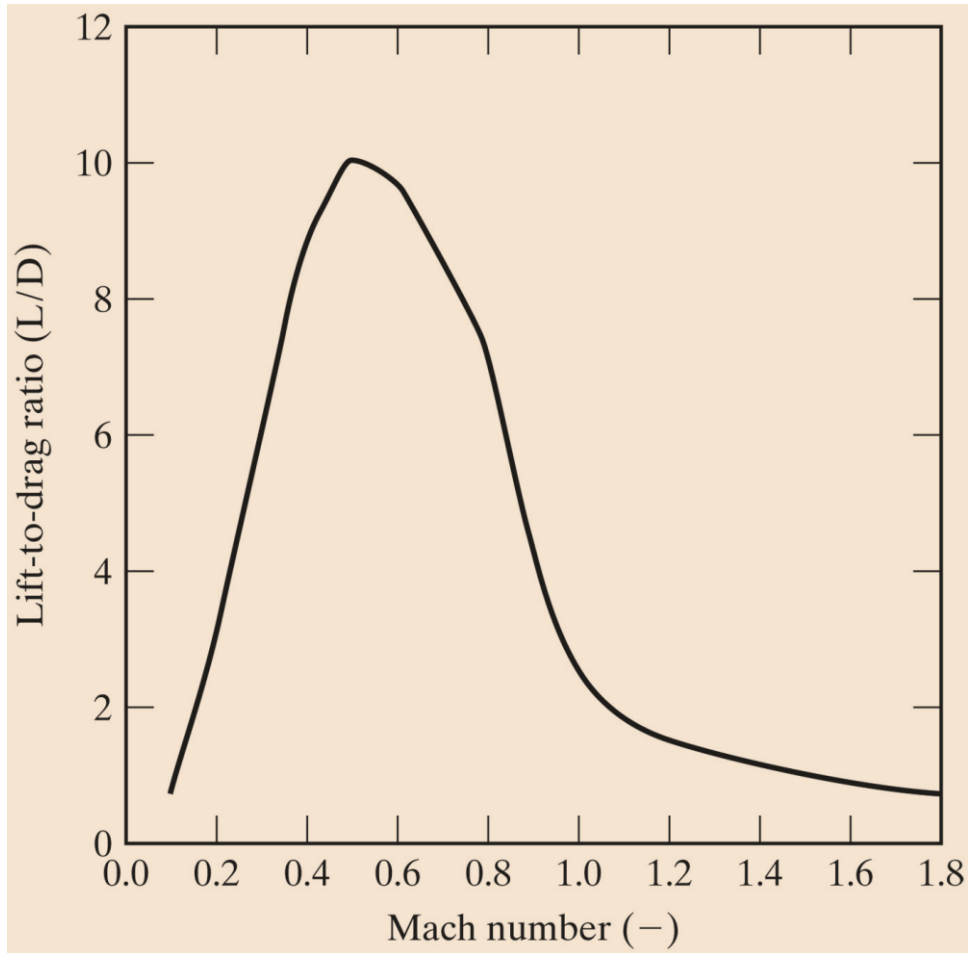
- The following equation correlates well the drag polar data in the left figure (the solid line in figure),

$$C_D = C_{D_{min}} + k_1 C_L^2 + k_2 (C_L - C_{L_{mindrag}})^2 + \Delta C_{DM}$$

- From the drag polar flight data, notice that $C_{D_{min}} \rightarrow C_L \approx 0.07$ $C_{D_{min}} \approx 0.012$ $C_{L_{mindrag}} \approx 0.07$
- In the drag polar flight data, $C_{D_{min}}$ is slightly lower than C_{D_0} .

Lift-induced drag

- L/D ratio for an F-16C as a function of Mach number at 20,000 ft.



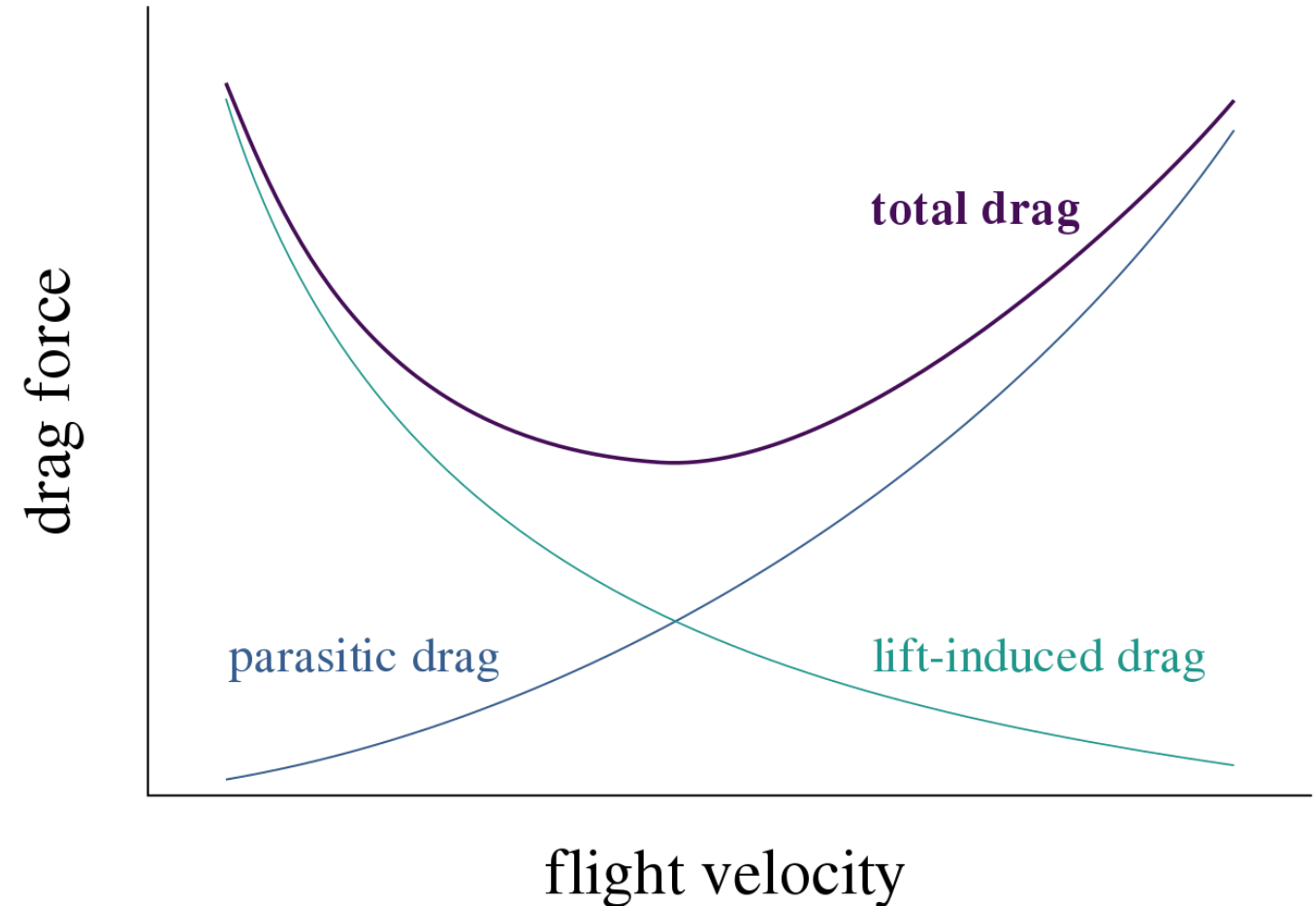
- Airplane performance is strongly related to L/D ratio.
- Many metrics of airplane performance are obtained in flight at L/D maximum.
- Performance conditions that occur at L/D max include:
 - Maximum range of propeller-driven airplanes.
 - Maximum climb angle for jet-powered airplanes.
 - Maximum power-off glide ratio (for jet-powered or for propeller-driven airplanes).
 - Maximum endurance for jet-powered airplanes.
- Therefore, when designing a wing, it is extremely important to have the L/D max as close as possible to cruise conditions (AOA and cruise velocity).
- You can take a look to Breguet equation (for range or endurance) to see the influence of L/D on aircraft performance.

$$\text{Performance} \leftarrow R = \frac{L}{D} \times \overset{\text{Propulsion}}{\eta} \times \ln \left(\frac{W_{Initial}}{W_{Final}} \right) \rightarrow \text{Structures + Materials}$$

Aerodynamics

Lift-induced drag

- The total drag of an airplane or a wing, is the parasitic drag plus induced drag.
- Recall that the parasitic drag is the drag not associated to lift production,
 - Form drag (or pressure drag) + skin friction drag
 - We can also add interference drag as another component.
- Recall also that lift-induced drag is a byproduct of lift generation in finite span wings.
- The drag breakdown of a typical transport aircraft shows that the lift-induced drag can amount to as much as 40% of the total drag at cruise conditions and 80–90% of the total drag in take-off configuration [1].
- Therefore, reducing lift-induced drag is of great interest in the aerospace industry.



Total drag in function of flight velocity

Photo credit: https://commons.wikimedia.org/wiki/File:Drag_curves_for_aircraft_in_flight.svg.
Apart from Fair Use, permission must be sought for any other purpose.

Drag polar comparison – Wing data against airfoil data

Drag polar comparison – Wing data against airfoil data

- Most of the airfoil aerodynamic characteristics (2D) are inherited by wings (3D):
 - Airfoil shape – Curvature effect on lift.
 - Reynolds number (sectional).
 - Mach number – Compressibility effects.
 - Stall mechanism and patterns.
 - Effect of early flow separation on lift and drag.
 - Effect of leading-edge separation bubbles on lift and drag.
 - The effect of high lift devices (HLD) on lift and drag – Flaps and slats.
 - Effect of surface finish and leading-edge contamination on lift and drag.
- Therefore, it is of paramount importance to choose a good airfoil.
 - If you choose a not so good airfoil, the wing performance will be heavily affected.
 - So, what is a good airfoil? This was addressed in the previous lecture.

Drag polar comparison – Wing data against airfoil data

- Due to three-dimensional effects, the behavior of wings is slightly different from that of airfoils.
 - The difference in the aerodynamic behavior is more evident when three-dimensional effects are larger.
 - Usually this is the case of low aspect ratio wings.
 - For very large aspect ratios, the behavior of wings is close to that of airfoils.
 - After all, airfoils can be seen as wings with infinity aspect ratio.
- As you might guess, designing/selecting wings is much more complex than two-dimensional cases (airfoils).
- In theory, we have infinite design variables.
 - Airfoils selection plus all wing's geometric parameters.
- Factors that affect the performance of wings:
 - Three-dimensional effects, such as wing tip vortex and spanwise velocity components.
 - Interaction of the wing with other aircraft components (fuselage, nacelles, pylons, and so on).
 - External disturbances, such as engine noise, vibrations, spanwise bending, boundary layer/wake interaction, shock waves, rain/ice, and so on.
 - Surface finish, interferences, discontinuities (such as control surfaces).

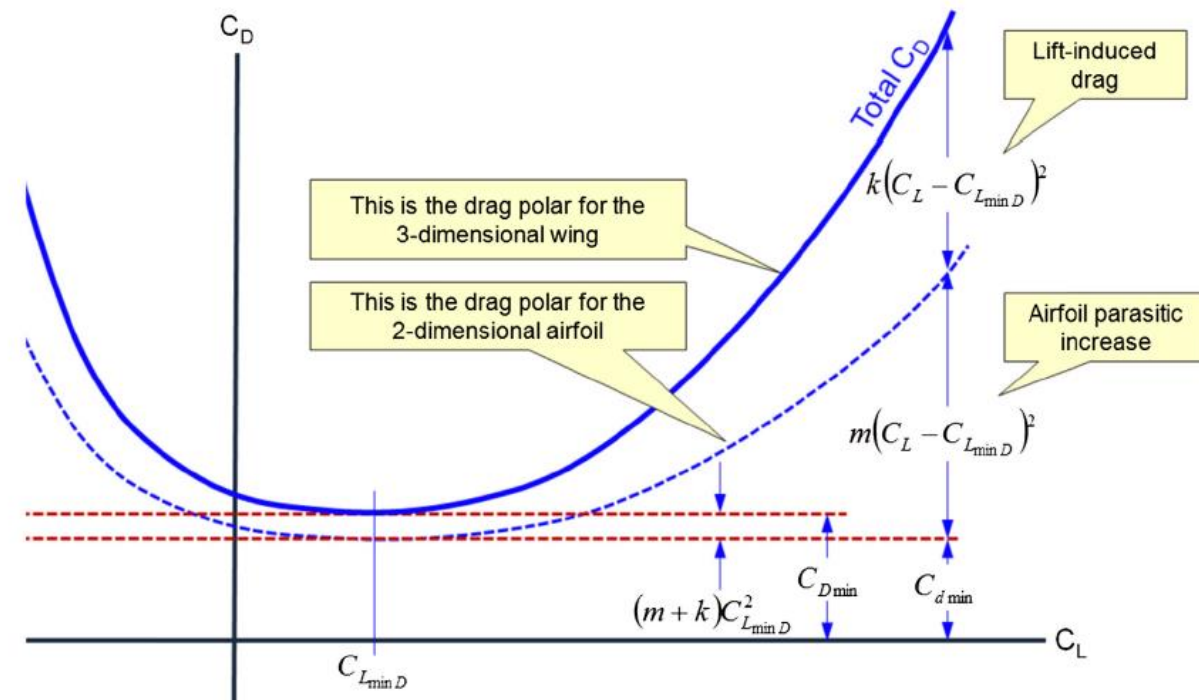
Drag polar comparison – Wing data against airfoil data

- Comparison between predicted and measured drag polar for a wing having a finite aspect ratio and an airfoil.
- The total drag of a wing is larger than that of an airfoil because of lift-induced drag and larger viscous drag.
- Remember, lift-induced drag is a consequence of three-dimensional effects.
- The equivalent drag polar model of an airfoil in a finite span wing can be expressed as follows,

$$C_D = C_{D_{min}} + m (C_L - C_{L_{mindrag}})^2 + k (C_L - C_{L_{mindrag}})^2 \quad \text{E1}$$

- Where m is a coefficient indicating the increment of the total drag of the airfoil.
- Expanding equation E1, the drag polar increases by a small factor (which shift the polar upwards),

$$(m + k) C_{L_{mindrag}}^2$$



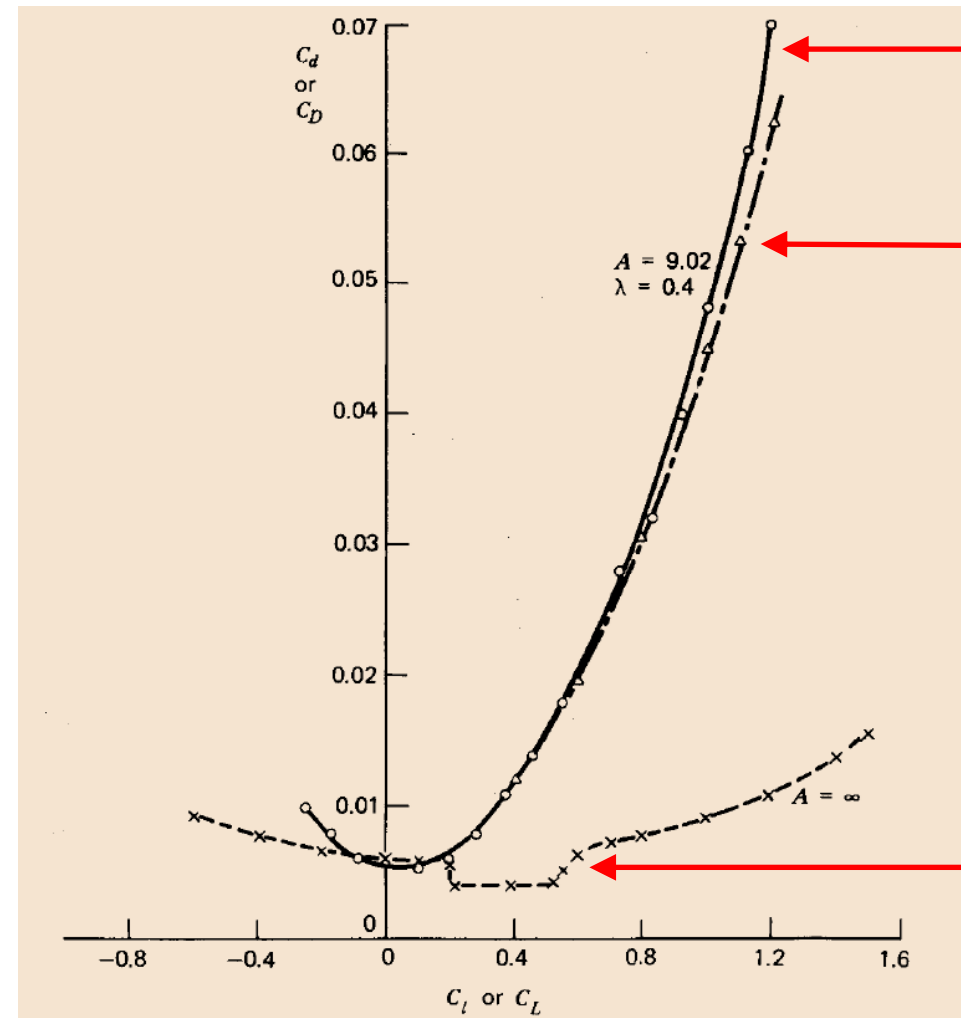
Drag polar comparison – Wing data against airfoil data

- Comparison between predicted and measured drag polar for a wing having a finite aspect ratio and an airfoil.

- Notice that the drag bucket is not present in the wing polars.
- This is due to three-dimensional effects, wing surface roughness, or freestream disturbances, among many factors.
- The wing will inherit most of the airfoil properties but mainly due to three-dimensional effects (lift induced drag), the two-dimensional behavior (viscous drag) is disguise or lost.

References:

- [1] Abbott, I., Von Doenhoff, A., Stivers, L. S., Summary of airfoil data. NACA Report 824. 1945.
- [2] J. Sivells, Experimental and calculated characteristics of three wings of NACA 64-210 and 65-210 airfoil sections with and without 2 degree washout. NACA-TN-1422, August 1947.
- [3] J. Sivells, S. Spooner, Investigation in the Langley 19-foot Pressure Tunnel of Two Wings of NACA 65-210 and 64-210 Airfoil Sections with Various Type Flaps. NACA-TR-942, January 1949.
- [4] Aerodynamics, Aeronautics, and Flight Mechanics, B. McCormick, John Wiley & Sons, 1995.



Wing data (references 2, 3)
Experimental total drag

Theoretical fitting (reference 4)

$$C_D = C_{D_{min}} + \frac{C_L^2}{\pi A Re}$$

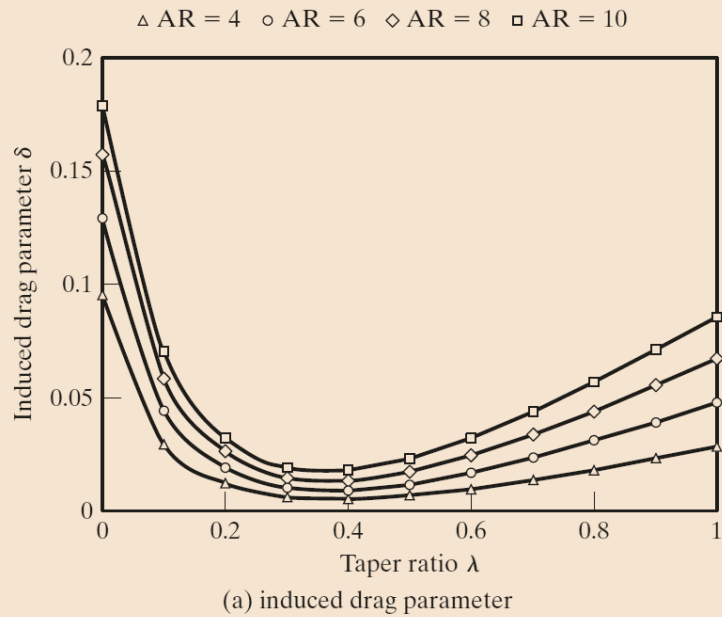
$$C_D = 0.0055 + 0.0394 C_L^2$$

Airfoil data (reference 1)
Profile drag.

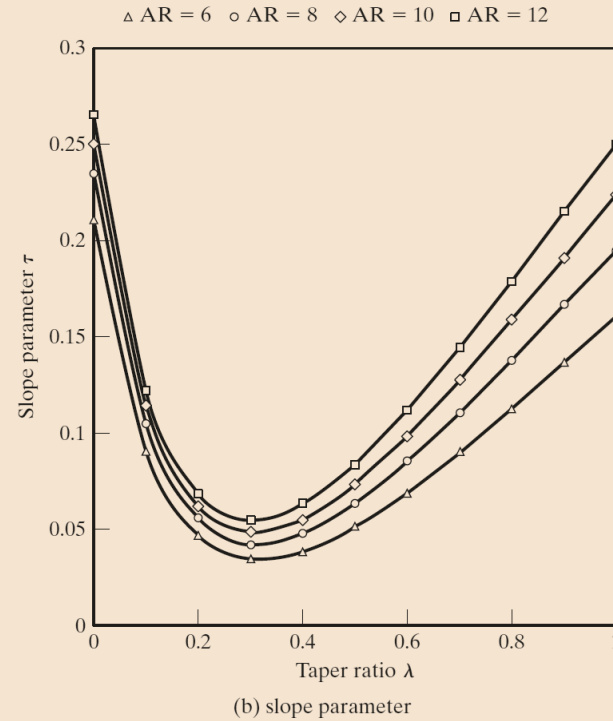
Effect of aspect ratio and taper ratio on induced drag

Effect of aspect ratio and taper ratio on induced drag

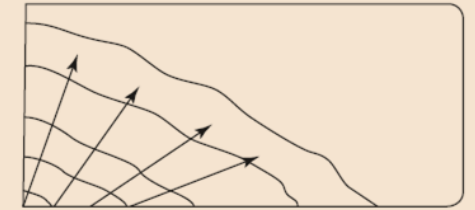
- Effect of aspect ratio and taper ratio on induced drag and lift curve slope.



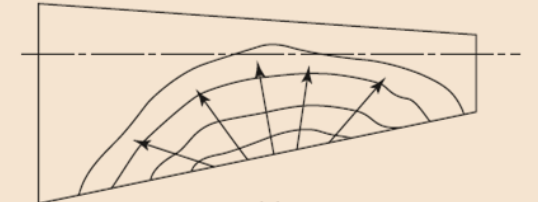
(a) induced drag parameter



(b) slope parameter



(a)



(b)



(c)

Typical stall patterns

$$C_{D_{ind}} = kC_L^2 = \frac{C_L^2}{\pi AR} (1 + \delta)$$

$$k = \frac{1}{\pi AR e} \quad e = \frac{1}{1 + \delta}$$

Oswald span efficiency

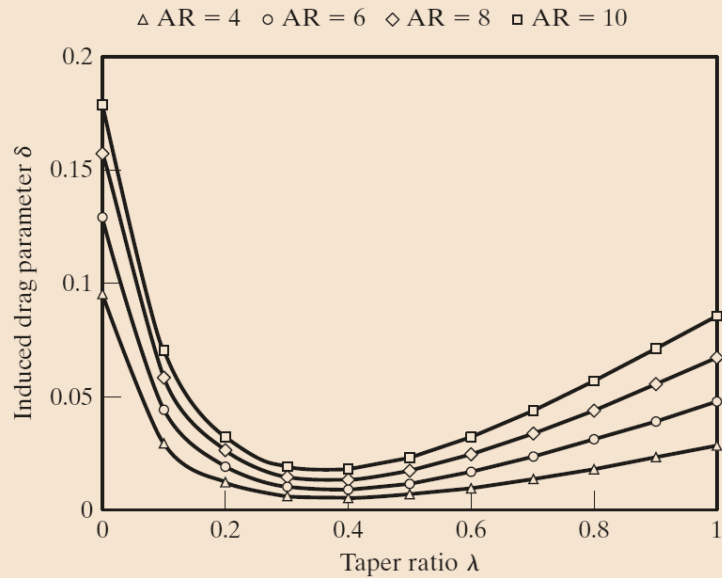
$$C_{L_\alpha} = a = \frac{a_0}{1 + \frac{a_0}{\pi AR} (1 + \tau)}$$

Correction factor for non-elliptical lift distribution

Airfoil lift curve slope

Effect of aspect ratio and taper ratio on induced drag

- Effect of aspect ratio and taper ratio on induced drag and lift curve slope.



(a) induced drag parameter

Correction factor for non-elliptical lift distribution

$$C_{D_{ind}} = kC_L^2 = \frac{C_L^2}{\pi AR} (1 + \delta)$$

$$k = \frac{1}{\pi AR e} \quad \leftarrow \quad e = \frac{1}{1 + \delta}$$

Oswald span efficiency

- In reference to the figure, the best induced drag parameter for different AR, corresponds to a wing with a taper ratio anywhere between 0.3 and 0.5.
 - A trapezoidal wing with this taper ratio approximates an elliptic platform shape and gives the best results for lift and drag.
- Recall that the induced drag parameter is zero only for elliptical wings.
- For the rest of the wings is a number larger than zero and usually between 0.02 and 0.2.
- The induced drag parameter penalizes the wing. It is an indication of how far we are from the elliptical lift distribution.
- The larger the induced drag parameter is, the more induced drag the wing will produce.
- A similar analysis can be conducted using the slope parameter showed in the previous slide.
- The slope parameter influences the wing's lift curve slope.

Effect of aspect ratio and taper ratio on induced drag

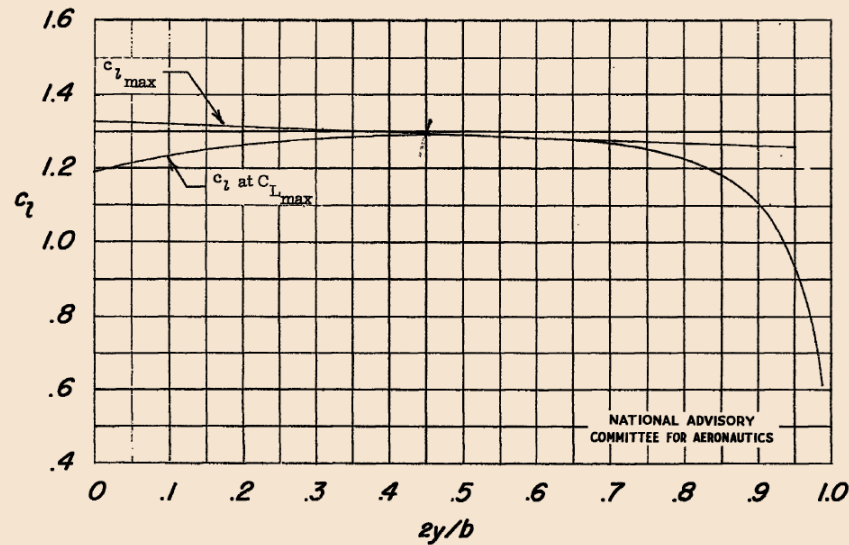
- Comparison of elliptical wing and a taper wing.
- By carefully designing the tapered wing, we can obtain the same lift distribution as the for the elliptical wing.



Effect of washout/washin on wing aerodynamic performance

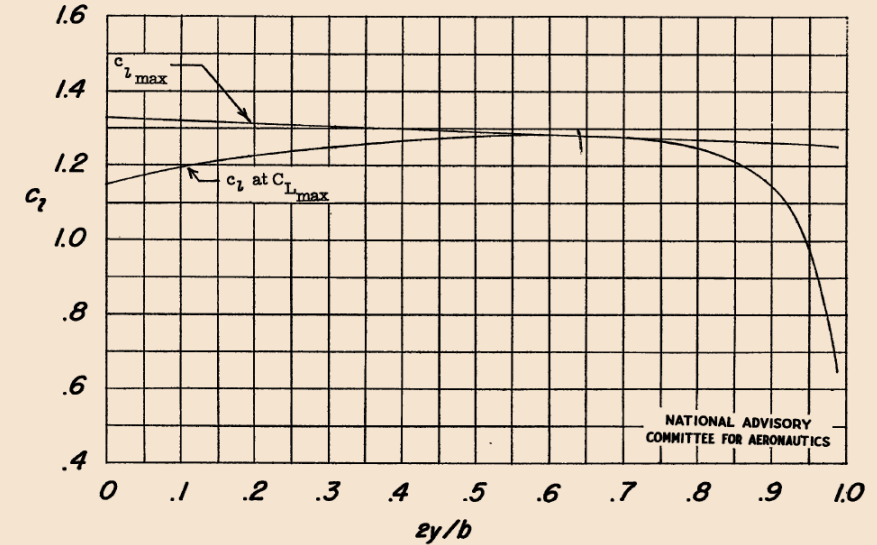
Effect of washout/washin on wing aerodynamic performance

- Spanwise variation of maximum section lift coefficient and section lift coefficient at maximum wing lift coefficient for wings of aspect ratio 9 and ratio of root chord to tip chord 2.5. Reynolds number approximately 4.4 millions [1].
- In the figure, by controlling the washout angle (left image), it is possible to change the lift distribution and the location where the wing first stalls.
- The method used in reference [1] to determine $C_{L,max}$ and the stall location is known as the critical section method [2, 3].



(b) NACA 65-210 sections, 2° washout.

Figure 6.- Continued.



(c) NACA 65-210 sections, 0° washout.

Figure 6.- Concluded.

Photo credit [1]. Copyright on the images is held by the contributors. Apart from Fair Use, permission must be sought for any other purpose.

[1] J. Sivells. Experimental and calculated characteristics of three wings of NACA 64-210 and 65-210 airfoil sections with and without 2 degree washout. NACA Technical Note No. 1422.

[2] S. Wakayama and I. Kroo. Subsonic Wing Planform Design Using Multidisciplinary Optimization. Journal of Aircraft, Vol. 32, No. 4, July-August 1995.

[3] E. Olson. Semi-Empirical Prediction of Aircraft Low-Speed Aerodynamic Characteristics. AIAA 2015-1679, 2015.

Effect of washout/washin on wing aerodynamic performance

- Spanwise variation of maximum section lift coefficient and section lift coefficient at maximum wing lift coefficient for wings of aspect ratio 9 and ratio of root chord to tip chord 2.5. Reynolds number approximately 4.4 millions [1].
- In the figure, by controlling the washout angle (left image), it is possible to change the lift distribution and the location where the wing first stalls.
- The method used in reference [1] to determine $C_{L_{max}}$ and the stall location is known as the critical section method [2, 3].

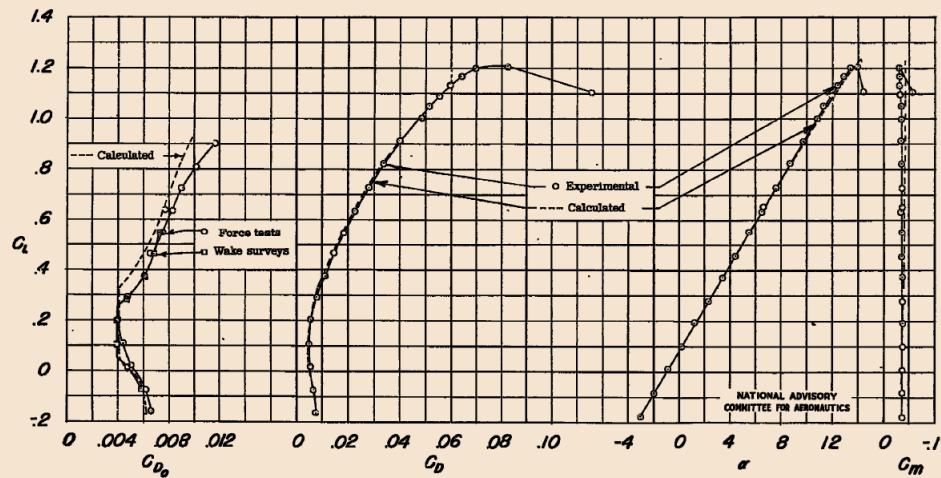


Figure 3.- Experimental and calculated characteristics of wing having NACA 65-210 airfoil sections. Washout, 2°; aspect ratio, 9; ratio of root chord to tip chord, 2.5; $R \approx 4.4 \times 10^6$; $M \approx 0.17$.

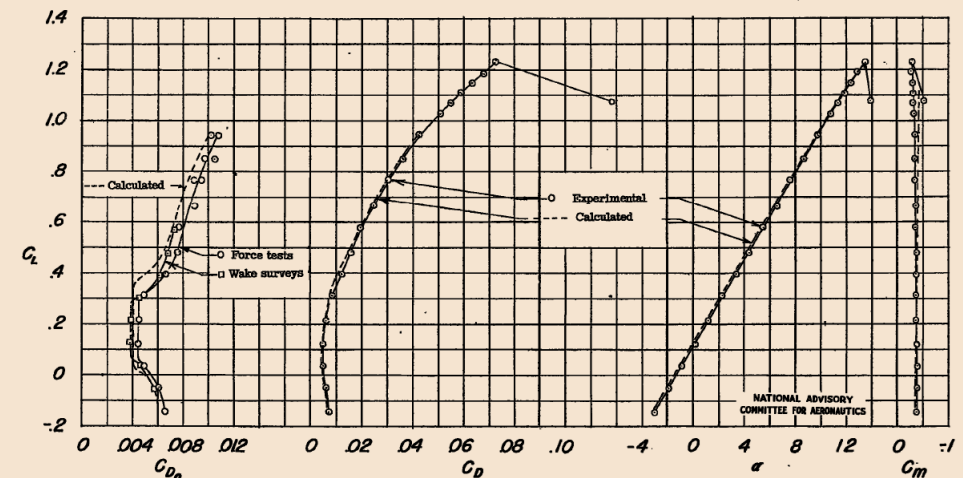


Figure 4.- Experimental and calculated characteristics of wing having NACA 65-210 airfoil sections. Washout, 0°; aspect ratio, 9; ratio of root chord to tip chord, 2.5; $R \approx 4.4 \times 10^6$; $M \approx 0.17$.

Photo credit [1]. Copyright on the images is held by the contributors. Apart from Fair Use, permission must be sought for any other purpose.

[1] J. Sivells. Experimental and calculated characteristics of three wings of NACA 64-210 and 65-210 airfoil sections with and without 2 degree washout. NACA Technical Note No. 1422.

[2] S. Wakayama and I. Kroo. Subsonic Wing Planform Design Using Multidisciplinary Optimization. Journal of Aircraft, Vol. 32, No. 4, July-August 1995.

[3] E. Olson. Semi-Empirical Prediction of Aircraft Low-Speed Aerodynamic Characteristics. AIAA 2015-1679, 2015.

Effect of washout/washin on wing aerodynamic performance

- The critical section method [1,2,3], together with linear methods, such as the LLT, VLM, or panel methods, is a cheat way to determine the maximum lift coefficient and stall progression of aircraft and wings.
- The maximum lift coefficient and stall progression of an aircraft or a wing is calculated using the critical section method as follows:
 - For increasing values of angle of attack, the lift coefficient at each location along the wing is compared to the maximum lift coefficient of that section, and a stall is declared when the maximum lift coefficient is first surpassed at any section.
 - The maximum lift coefficient for the aircraft or the wing is defined as the value achieved when the stalling condition is reached.

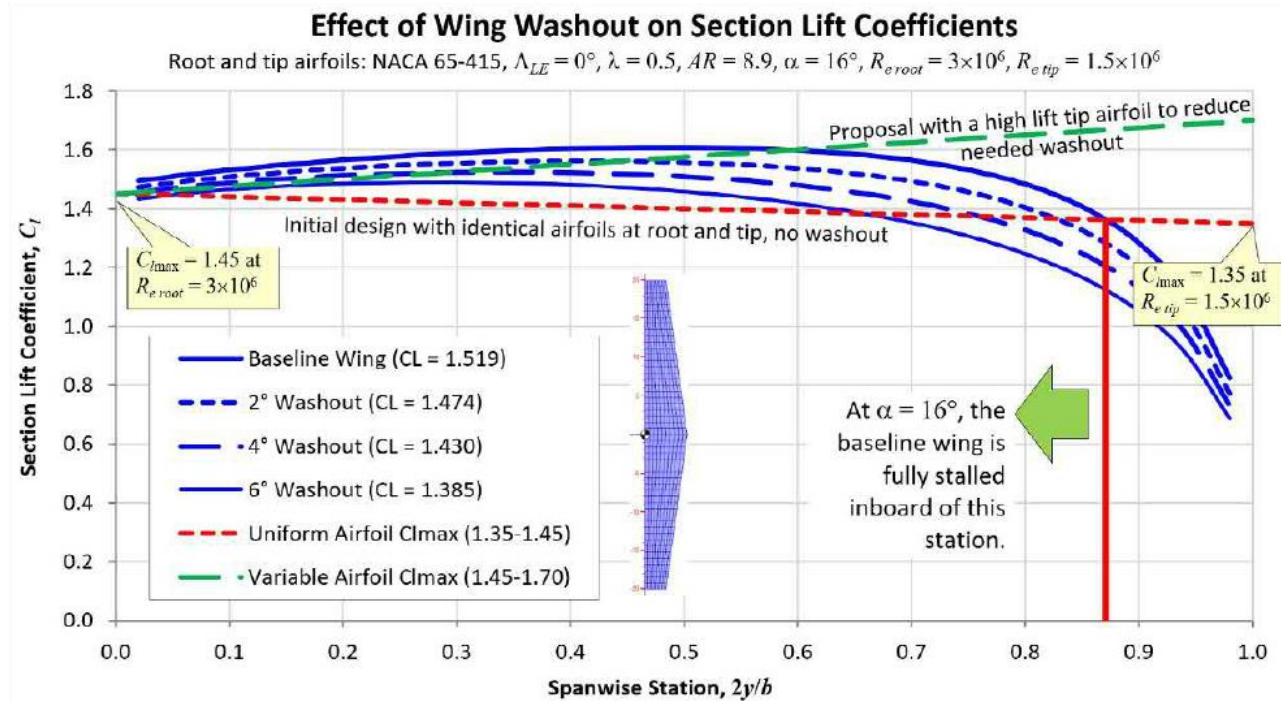


Photo credit: General Aviation Aircraft Design: Applied Methods and Procedures. Butterworth-Heinemann, 2016. Copyright on the images is held by the contributors. Apart from Fair Use, permission must be sought for any other purpose.

[1] J. Sivells. Experimental and calculated characteristics of three wings of NACA 64-210 and 65-210 airfoil sections with and without 2 degree washout. NACA Technical Note No. 1422.

[2] S. Wakayama and I. Kroo. Subsonic Wing Planform Design Using Multidisciplinary Optimization. Journal of Aircraft, Vol. 32, No. 4, July-August 1995.

[3] E. Olson. Semi-Empirical Prediction of Aircraft Low-Speed Aerodynamic Characteristics. AIAA 2015-1679, 2015.

Effect of washout/washin on wing aerodynamic performance

- The critical section method [1,2,3] is simple and computationally inexpensive, and gives surprisingly good results, probably because of the requirement to maintain good handling qualities at stall.
- Stall should not begin at the wingtips since this could cause undesirable pitch-up or roll.
- In the case of aft sweep, a conventional transport wing is prone to stall at the wingtips due to the effects of spanwise flow at higher angles of attack, so that aircraft designers modify airfoil sections on the inboard sections to degrade the C_{Lmax} of those sections and ensure stall beginning near the wing root.
- Some margin is provided against stalling the tip sections, so that the wing is designed to stall just below the point where the critical outer section reaches its C_{Lmax} .
- Studies have found that the critical section method can be too optimistic when studying sweep wings.
- So, corrections can be applied based on previous experience.
- For sweep wings and high-speed aerodynamics, a better alternative to the critical section method is the pressure difference rule [4].
- It is important to stress that both, the critical section method and the pressure difference rule need many solutions (different angles on attack, Reynolds number, and Mach number); and the only cost- and time-effective way to generate these solutions is by using surface panel methods and potential solvers.
- Predicting the maximum lift of finite span wings is not easy.

[1] J. Sivells. Experimental and calculated characteristics of three wings of NACA 64-210 and 65-210 airfoil sections with and without 2 degree washout. NACA Technical Note No. 1422.

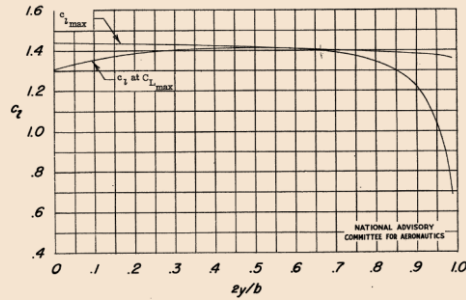
[2] S. Wakayama and I. Kroo. Subsonic Wing Planform Design Using Multidisciplinary Optimization. Journal of Aircraft, Vol. 32, No. 4, July-August 1995.

[3] E. Olson. Semi-Empirical Prediction of Aircraft Low-Speed Aerodynamic Characteristics. AIAA 2015-1679, 2015.

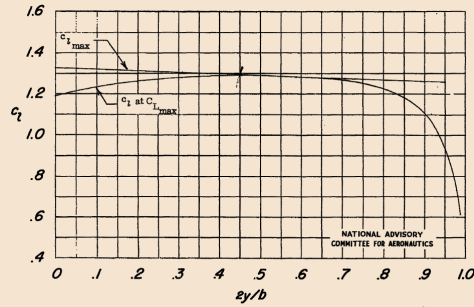
[4] W. O. Valerzo and V. D. Chin. Method for the prediction of wing maximum lift. Journal Aircraft, vol. 31, no. 1, 1994.

Effect of washout/washin on wing aerodynamic performance

- Prediction of C_{Lmax} and stall progression/patterns using the critical section method [1].

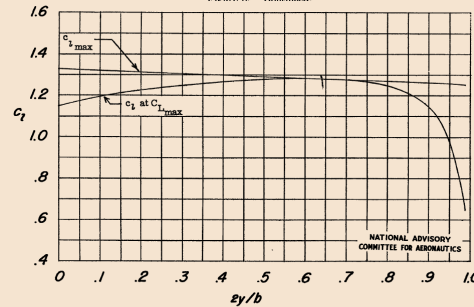


(a) NACA 64-210 sections, 2° washout.



(b) NACA 66-210 sections, 2° washout.

Figure 8 - Continued



(c) NACA 66-210 sections, 0° washout.

Figure 8 - Concluded.

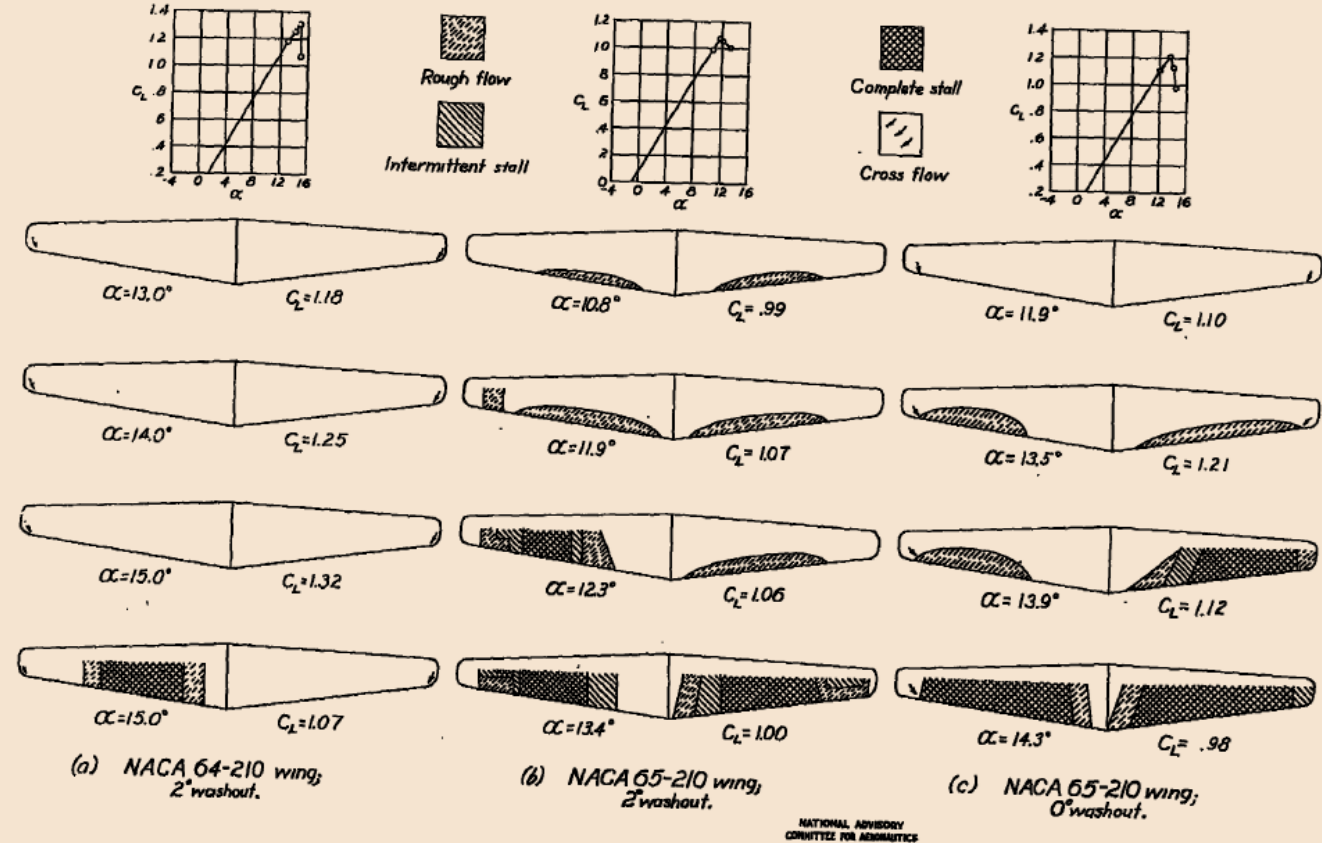
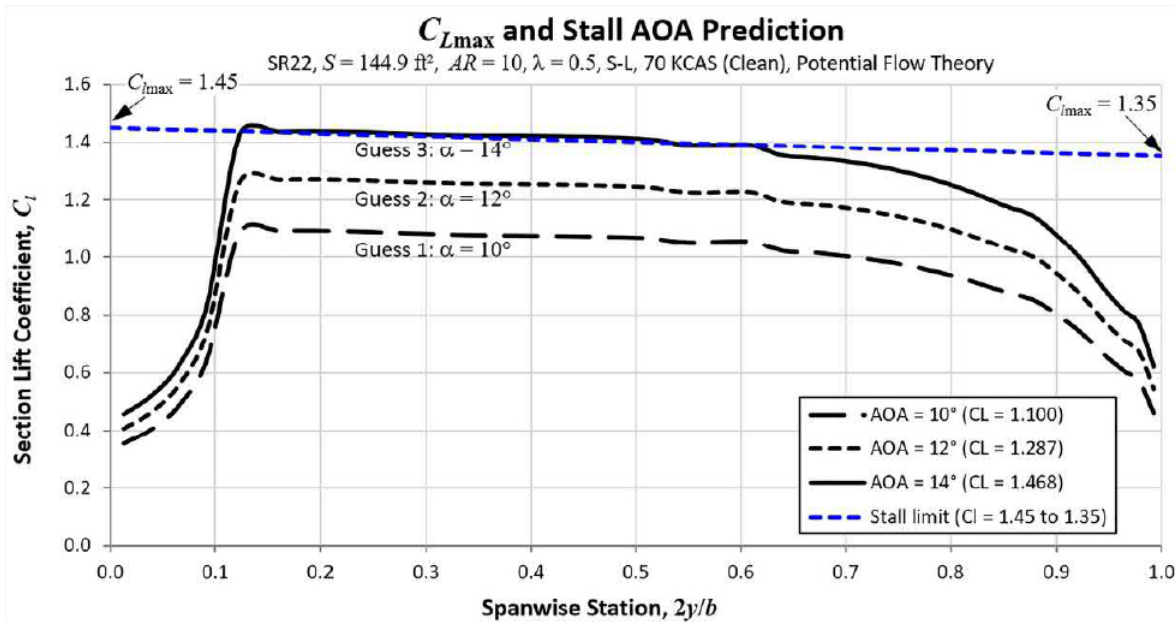


Figure 5.- Stalling characteristics of wings of aspect ratio 9 and ratio of root chord to tip chord 2.5.
 $R \approx 4.4 \times 10^6$; $M \approx 0.17$.

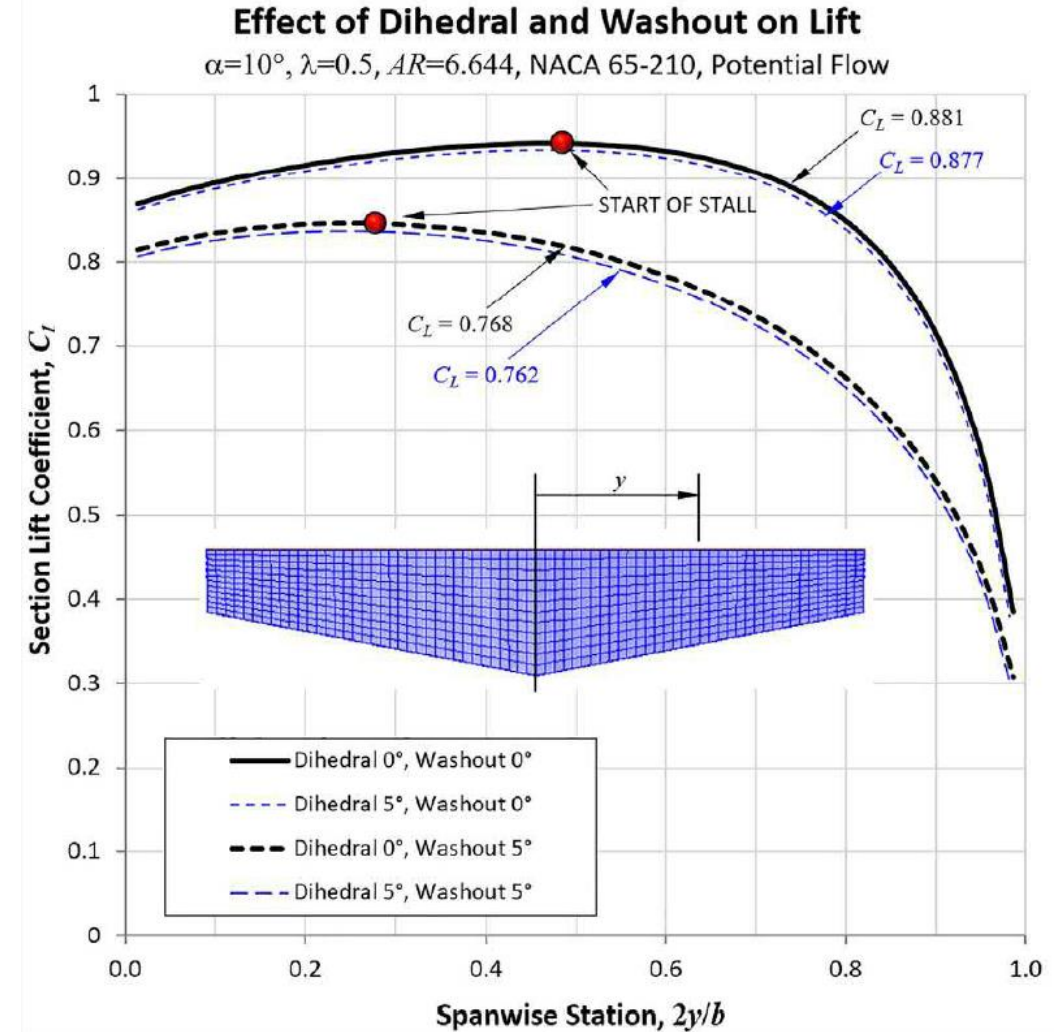
Effect of washout/washin on wing aerodynamic performance

- Lift distribution near stall predicted by potential flow and critical section method [1].
- The waviness in places is due to the discontinuity in the segment of the wing, which features a leading-edge extension.



Copyright on the images is held by the contributors. Apart from Fair Use, permission must be sought for any other purpose.

- Impact of washout and dihedral on the aerodynamics of a typical wing.



Copyright on the images is held by the contributors. Apart from Fair Use, permission must be sought for any other purpose.

High aerodynamic efficiency concepts

The otto Celera 500L

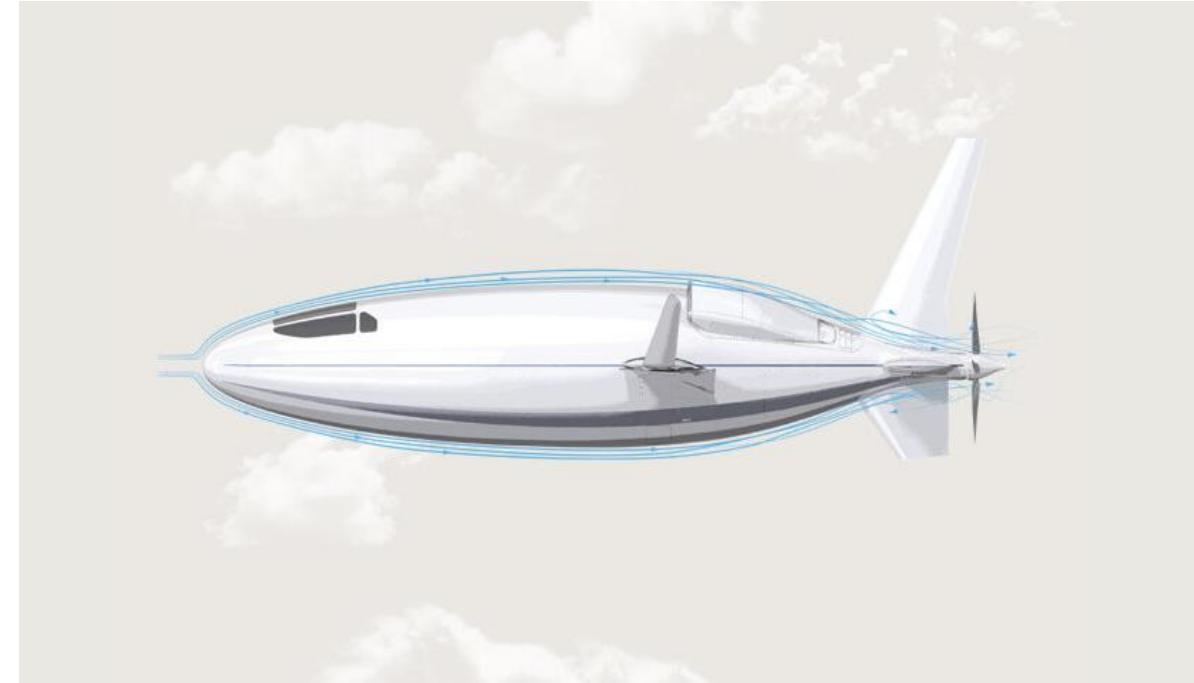
High aerodynamic efficiency concepts – The otto Celera 500L case

- Prolate spheroid fuselage to reduce flow separation and promote laminar boundary layer.
- The design of the Celera 500L fuselage takes advantage of an optimum length-to-width ratio to maximize laminar flow.
 - These benefits do not scale for large jet transports.



Old vs. new: Piper PA-31 (left aircraft) next to the Otto Celera 500L (right aircraft). Extensive use of laminar flow surfaces in the Otto Celera 500L results in approximately 59% reduction in drag compared to a similar sized conventional aircraft.

Photo credit: <https://edition.cnn.com/travel/article/celera-500l-business-aircraft-future/index.html>.



Prolate spheroid fuselage to reduce flow separation and promote laminar boundary layer.

Photo credit: <https://www.ottoaviation.com/technology>

High aerodynamic efficiency concepts – The otto Celera 500L case

- The Celera 500L makes extensive use of laminar flow surfaces which result in approximately 59% reduction of drag compared to a similar sized conventional aircraft.



High aerodynamic efficiency concepts – The otto Celera 500L case

- Other advanced aerodynamic concepts used in the Celera 500L:
 - Winglets, high aspect ratio wings, wing planform optimized for elliptical lift distribution, NLF airfoils, ventral fins, elliptical planform horizontal stabilizers, laminar flow control, pusher propeller, boundary layer ingestion, reduced excrescence and interference drag, among many.



High aerodynamic efficiency concepts – The otto Celera 500L case

- A 3D model can be found at the following link,
 - <https://sketchfab.com/3d-models/celera-500l-306092a41d174e719e83bd143a5ad042>



High aerodynamic efficiency concepts

The Honda HA-420 HondaJet

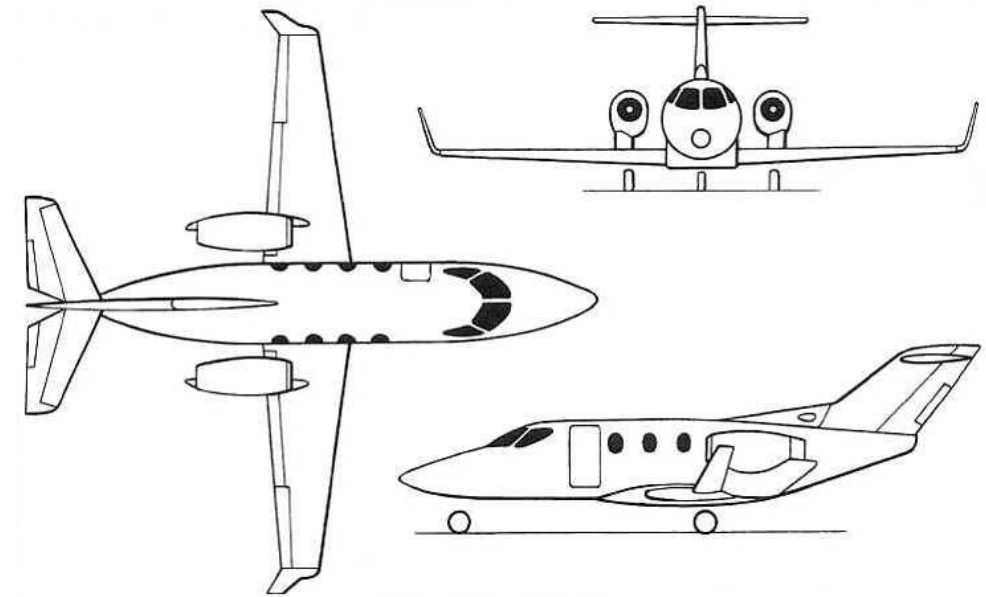
High aerodynamic efficiency concepts – The Honda HA-420 HondaJet

- The Honda HA-420 HondaJet is a light business jet produced by the Honda Aircraft Company.
- The HondaJet is an advanced, lightweight, business jet featuring an extra-large cabin, high fuel efficiency, and high cruise speed compared to existing small business jets.
- To achieve the high-performance goals, an over-the-wing engine-mount configuration, a natural-laminar-flow (NLF) wing, and a natural-laminar-flow fuselage nose were developed through extensive analyses and wind-tunnel tests.
- The wing is metal, having an integral, machined skin to achieve the smooth upper surface required for natural laminar flow.
- The fuselage is constructed entirely of composites; the stiffened panels and the sandwich panels are co-cured integrally in an autoclave to reduce weight and cost.



High aerodynamic efficiency concepts – The Honda HA-420 HondaJet

- The aircraft is a low-wing configuration with the engines mounted over the wing.
- The aircraft is 41.14 ft long, has a wingspan of 39.87 ft, and is 13.21 ft high at the top of the T-tail.
- Design maximum takeoff weight is about 9200 lb.
- The estimated maximum speed is about 420 knots at 30000 ft and the maximum range is about 1100 nm.
- The cabin is pressurized up to 8.7 psi to maintain an 8000 ft cabin altitude up to 44000 ft.
- The aircraft provides a very large cabin volume compared to those of other four-passenger seat arrangements and it is also possible to add two more passenger seats without sacrificing comfort.
- The aircraft is powered by two Honda HF-118 fuel-efficient turbofan engines, each rated at 1670 lb thrust at takeoff power.
- The engine is controlled by the Full Authority Digital Engine Control (FADEC) system.



Copyright on the images is held by the contributors. Apart from Fair Use, permission must be sought for any other purpose.

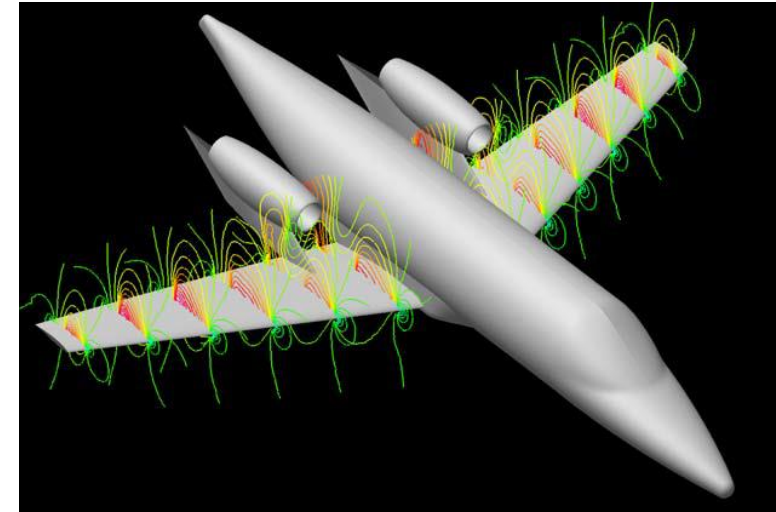
References:

M. Fujino. Development of the Honda Jet. 24th Congress of International Council of the Aeronautical Sciences, 29 August-3 September 2004, Yokohama, Japan

High aerodynamic efficiency concepts – The Honda HA-420 HondaJet

- **Over-the-wing Engine-Mount Configuration**

- Engine location was the major design decision in the development of the HondaJet configuration.
- In general, locating the engine nacelles over the wing causes unfavorable aerodynamic interference and induces a strong shock wave that results in a lower drag-divergence Mach number.
- Computational studies were conducted using a three-dimensional Euler solver.
- Experimental studies were conducted in the Boeing Transonic Wind Tunnel (BTWT) to validate the computational predictions.
- It was found that the shock wave is minimized and drag divergence occurs at a Mach number higher than that for the clean-wing configuration when the nacelle is located at the optimum position relative to the wing
- The over-the-wing engine mount configuration exhibits lower drag than does the conventional rear-fuselage engine mount configuration.
- By employing this optimum over-the-wing engine mount configuration, the cruise efficiency is higher than that of a conventional rear-fuselage engine-nacelle configuration and, in addition, the cabin volume is maximized.



Copyright on the images is held by the contributors. Apart from Fair Use, permission must be sought for any other purpose.

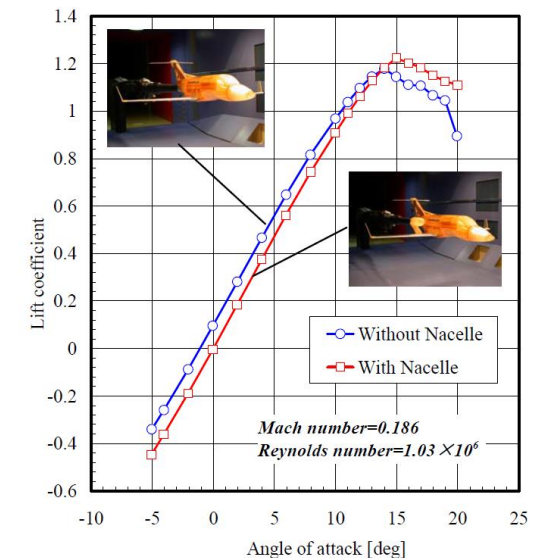
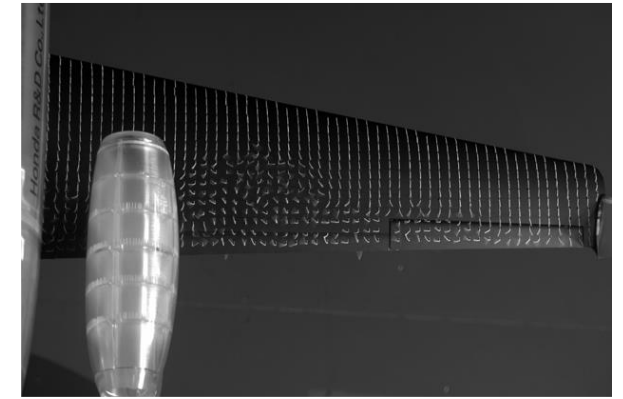
References:

M. Fujino. Development of the Honda Jet. 24th Congress of International Council of the Aeronautical Sciences, 29 August-3 September 2004, Yokohama, Japan

High aerodynamic efficiency concepts – The Honda HA-420 HondaJet

- **Wing design**

- Detail design studies were performed to minimize the induced drag with minimum wing weight.
- The study showed that the takeoff weight is minimized for a 1100 nm range aircraft when the wing geometric aspect ratio is 8.5 and a winglet having a height of 9% of the wingspan is installed.
- Because of the over-the-wing engine-mount configuration, the stall characteristics were carefully studied by computational analysis and low-speed wind-tunnel tests.
- From the computational analysis using a vortex-lattice method, and a three-dimensional panel method, a taper ratio of 0.38 and a washout of 5.1 degrees were chosen to provide good stall characteristics with minimum induced drag penalty.
- The zero-lift angle of the over-the-wing engine-mount configuration is about 1.2 degrees higher than that of the clean-wing configuration.
- The maximum lift coefficient of the over-the-wing engine-mount configuration is about 0.07 higher than that of the clean-wing configuration. Thus, there is no disadvantage with respect to the lift characteristics due to the nacelle installation over the wing.



Copyright on the images is held by the contributors. Apart from Fair Use, permission must be sought for any other purpose.

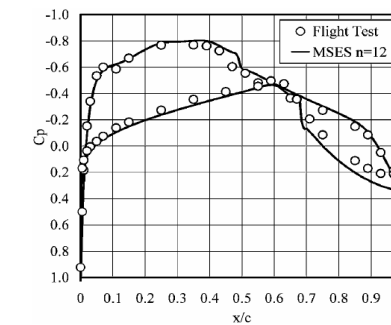
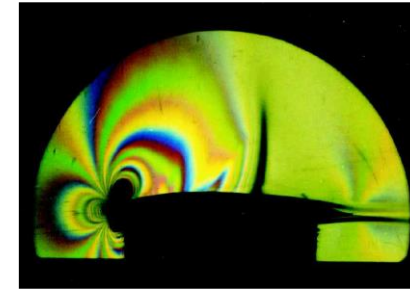
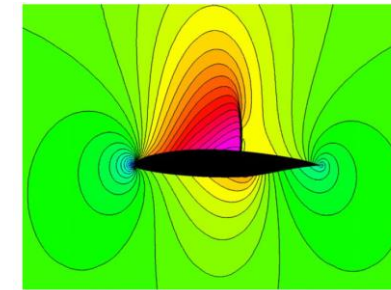
References:

M. Fujino. Development of the Honda Jet. 24th Congress of International Council of the Aeronautical Sciences, 29 August-3 September 2004, Yokohama, Japan

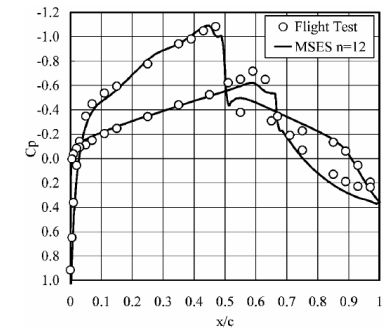
High aerodynamic efficiency concepts – The Honda HA-420 HondaJet

- **Natural-laminar-flow (NLF) airfoil**

- To satisfy the requirements of the HondaJet, a new natural-laminar-flow airfoil, the SHM-1, was designed using a panel code and inverse design using a conformal-mapping method.
- The pressure gradient on the upper surface is favorable to about 42-percent chord, followed by a concave pressure recovery, which represents a compromise between maximum lift, pitching moment, and drag divergence.
- The pressure gradient along the lower surface is favorable to about 63-percent chord to reduce drag.
- The leading-edge geometry was designed to cause transition near the leading edge at high angles of attack to minimize the loss in maximum lift coefficient due to roughness.
- The upper-surface trailing-edge geometry was designed to produce a steep pressure gradient and, thereby, induce a small separation. By the incorporation of this new trailing-edge design, the magnitude of the pitching moment at high speeds is greatly reduced.
- The airfoil exhibits a high maximum lift coefficient with docile stall characteristics and low profile-drag coefficients in cruise and climb.



a) $\alpha = 0.27$ deg, $Re = 13.6 \times 10^6$, and $M = 0.62$



b) $\alpha = -0.38$ deg, $Re = 16.2 \times 10^6$, and $M = 0.72$
Fig. 7 Comparison of theoretical and experimental (flight) pressure distributions.

Copyright on the images is held by the contributors. Apart from Fair Use, permission must be sought for any other purpose.

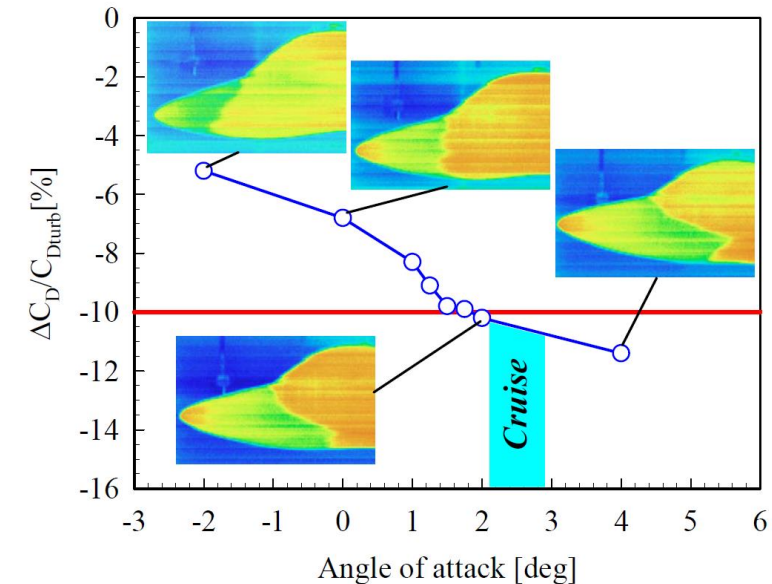
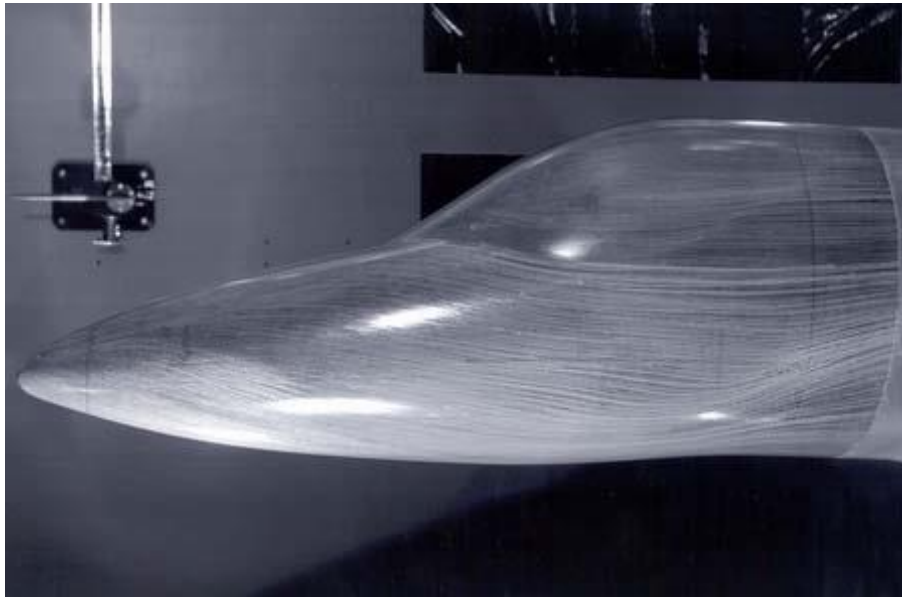
References:

M. Fujino. Development of the Honda Jet. 24th Congress of International Council of the Aeronautical Sciences, 29 August-3 September 2004, Yokohama, Japan

High aerodynamic efficiency concepts – The Honda HA-420 HondaJet

- **Natural-Laminar-Flow Fuselage Nose**

- A natural-laminar-flow, fuselage-nose shape was developed through extensive analysis and experiments to reduce the fuselage drag.
- Using a three-dimensional, panel code with an integral boundary-layer method the fuselage-nose contours were designed to maximize laminar-flow length by maintaining a favorable pressure gradient and minimizing crossflow.



Copyright on the images is held by the contributors. Apart from Fair Use, permission must be sought for any other purpose.

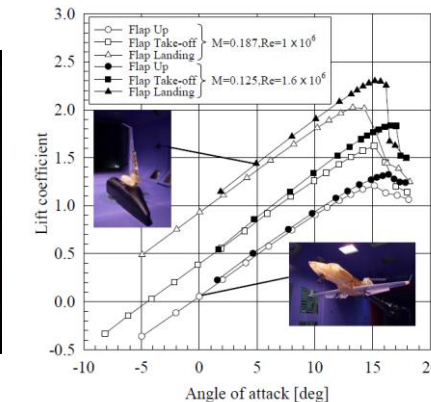
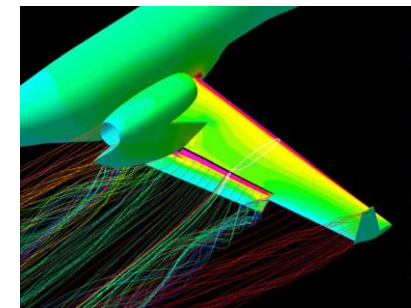
References:

M. Fujino. Development of the Honda Jet. 24th Congress of International Council of the Aeronautical Sciences, 29 August-3 September 2004, Yokohama, Japan

High aerodynamic efficiency concepts – The Honda HA-420 HondaJet

- **High lift system**

- A 30-percent-chord, double-slotted flap, which is deployed by a mechanical linkage, is employed to satisfy the stall-speed requirement as well as the high-speed requirement.
- The position of the vane with respect to the flap is fixed. The shapes of the vane and the flap as well as the gap and overlap were designed using a two-dimensional, multielement, panel code.
- The flap and vane shapes and positions were tested on a 1/3-scale, half-span model in the Honda Low-Speed Wind Tunnel and the results were compared with those from computational studies using a panel code.
- A test was also conducted using a 1/6-scale model in the Honda Low-Speed Wind Tunnel.
- The results for two Reynolds numbers allowed the full-scale maximum lift coefficient to be estimated more accurately using an analytical method that incorporated the pressure-difference rule.
- The maximum lift coefficient for the full-scale Reynolds number is estimated to be higher than 2.5, which satisfies the stall-speed requirement.



Copyright on the images is held by the contributors. Apart from Fair Use, permission must be sought for any other purpose.

References:

M. Fujino. Development of the Honda Jet. 24th Congress of International Council of the Aeronautical Sciences, 29 August-3 September 2004, Yokohama, Japan

High aerodynamic efficiency concepts – The Honda HA-420 HondaJet

- This paper is beautiful example of aerodynamic design and multidisciplinary design optimization in industry.
- We just reviewed the aerodynamic design aspects, but in the paper, the author also address the following topics:
 - Performance.
 - Flight Simulator.
 - Stability.
 - Aeroelasticity.
 - Structure.
 - Systems integration.
 - Ground tests.
 - Flight tests.
 - Wind tunnel testing.
 - Avionics.
- You are highly encouraged to read the paper.

Development of the HondaJet

Michimasa Fujino
Honda R&D Americas, Inc., Greensboro, North Carolina 27409

Keywords: *Airplane Design*

Abstract

The HondaJet is an advanced, lightweight, business jet featuring an extra large cabin, high fuel efficiency, and high cruise speed compared to existing small business jets. To achieve the high performance goals, an over-the-wing engine-mount configuration, a natural-laminar-flow wing, and a natural-laminar-flow fuselage nose were developed through extensive analyses and wind-tunnel tests. The wing is metal, having an integral, machined skin to achieve the smooth upper surface required for natural laminar flow. The fuselage is constructed entirely of composites; the stiffened panels and the sandwich panels are co-cured integrally in an autoclave to reduce weight and cost. The prototype aircraft has been designed and fabricated. Major ground tests such as structural proof tests, control-system proof test, system function tests, and ground vibration tests have been completed. The first flight was conducted on December 3, 2003, and flight testing is currently underway. The aerodynamic, aeroelastic, structural, and system designs and the ground tests performed during the development are described.

1 Introduction

The business jet is becoming a common tool for business people. Chartering business jets, however, is still expensive and the arrival of a new generation of small jets that are more affordable to operate than conventional jets is awaited. Market surveys and focus-group interviews, conducted in five major cities in the United States, show that demand for comfort, in particular, a large cabin, as well as high fuel efficiency are critical to the success of small business-jet development. The HondaJet (Fig.1) is designed to satisfy these needs. This new

aircraft has great potential to revolutionize air transportation.

A unique configuration, called an over-the-wing engine-mount configuration (OTWEM), was developed to provide a larger cabin than that of conventional configurations. By mounting the engines on the wing, the carry-through structure required to mount the engines on the rear fuselage is eliminated, which allows the cabin volume to be maximized. It was a technical challenge to employ an over-the-wing engine-mount configuration for a high-speed aircraft from both aerodynamic and aeroelastic standpoints. Extensive analytical and experimental studies, however, show that an over-the-wing engine-mount configuration reduces the wave drag at high speeds and achieves higher cruise efficiency when the nacelles are located at the optimum position [1].



Fig.1 HondaJet

To reduce drag and thereby achieve higher fuel efficiency, a new natural-laminar-flow (NLF) wing [2] and a natural-laminar-flow fuselage nose were developed through theoretical and experimental studies. By employing these advanced technologies, the specific range of the HondaJet is far greater than that of existing

References:

M. Fujino. Development of the Honda Jet. 24th Congress of International Council of the Aeronautical Sciences, 29 August-3 September 2004, Yokohama, Japan

High aerodynamic efficiency concepts – The Honda HA-420 HondaJet

- A 3D model can be found at the following link,
 - <https://sketchfab.com/3d-models/honda-private-jet-396a2651bf2b4409b34a6cf786b09ea9>

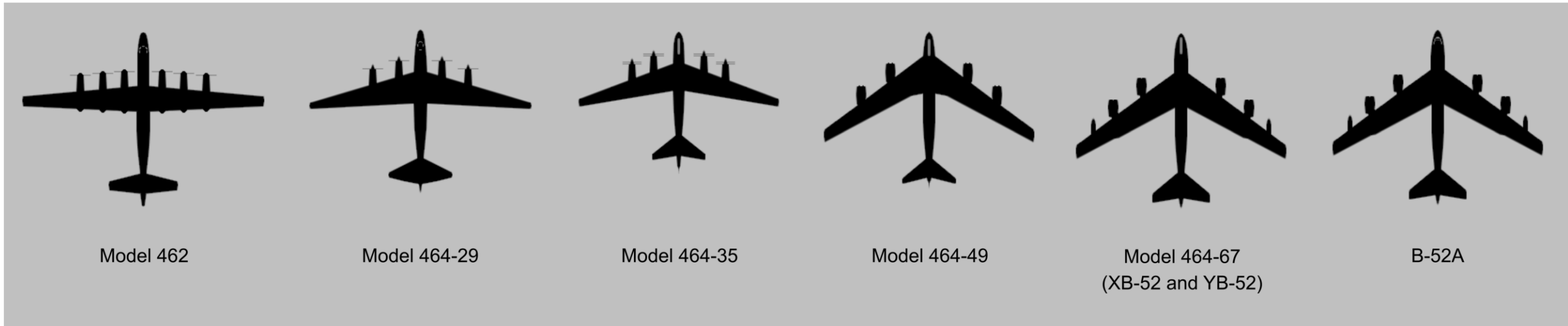


Design for speed

The evolution of the B-52

Design for speed – The evolution of the B-52

- Evolution of the B-52 according to the design speed requirements.
- Apart from the design speed requirements, there were also requirements on the ceiling, range, payload and engine type (among many other requirements).
- The final wings have a large aspect ratio, very large span, and 35-degree swept wing.



Model 462

Model 464-29

Model 464-35

Model 464-49

Model 464-67
(XB-52 and YB-52)

B-52A

1945
Cruise speed requirement
260 knots
480 km/h

1946
Cruise speed requirement
345 knots
645 km/h

1947
Cruise speed requirement
440 knots
800 km/h

1948
Cruise speed requirement
440 knots
800 km/h

Jet engines required

1950
Cruise speed requirement
440 knots
800 km/h

Jet engines required

1951
Cruise speed requirement
440 knots
800 km/h

Jet engines required

Side-by-side cockpit

Design for speed – The evolution of the B-52

- The B-52 in service today can reach cruise speeds as high as 650 mph (Mach 0.86).
- With a range of 7652 nautical miles (14160 km).
- A service ceiling of 50000 ft (15150 m).
- And a very large payload.
- It is expected to flight until 2040 and beyond.



[https://en.wikipedia.org/wiki/Boeing_B-52_Stratofortress#/media/File:B-52_Stratofortress_assigned_to_the_307th_Bomb_Wing_\(cropped\).jpg](https://en.wikipedia.org/wiki/Boeing_B-52_Stratofortress#/media/File:B-52_Stratofortress_assigned_to_the_307th_Bomb_Wing_(cropped).jpg)



https://commons.wikimedia.org/wiki/File:B-52s_arrive_at_Al_Udeid_Air_Base_3.jpg

Design for speed – The evolution of the B-52

- Do you notice something strange of wings? Or better, something missing?



https://www.boeing.com/resources/boeingdotcom/defense/b52_bomber/images/b_52_gallery_lrg_03_960.jpg



https://www.boeing.com/resources/boeingdotcom/defense/b-52_bomber/images/b_52_gallery_lrg_05_960.jpg

Design for speed – The evolution of the B-52

- The B-52 does not rely on ailerons for roll control (as many other large airplanes).
- Aileron activation would cause the wing to twist, undermining roll control with ailerons.
- Therefore, spoilers (or spoilerons) on each wing are responsible for roll control.



https://www.boeing.com/resources/boeingdotcom/defense/b-52_bomber/images/b_52_gallery_lrg_04_960.jpg



<https://theaviationgeekclub.com/wp-content/uploads/2018/05/B-52-Low-Level.jpg>

Design for speed – The evolution of the B-52

- A 3D model can be found at the following link,
 - <https://sketchfab.com/3d-models/boeing-b-52h-stratofortress-5497331214854040bd7de1e024b135af>



Wing design principles
How to compute/estimate the aerodynamic
characteristics of wings?

Wing design principles

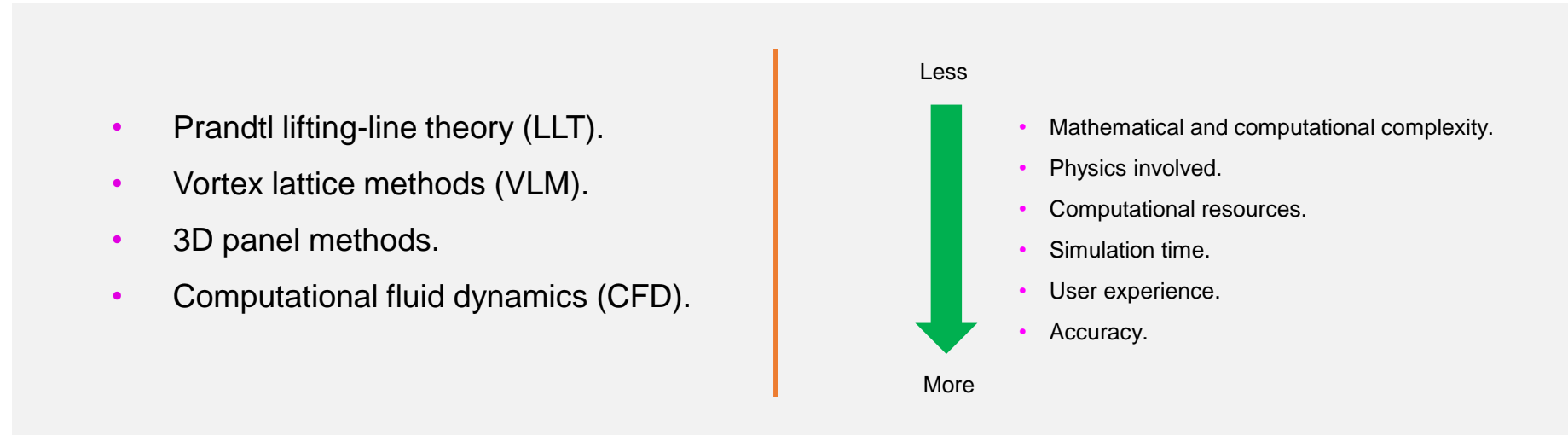
- When designing your wing always have in mind the following:
 - You need to design the wing in such a way that it generates the required lift.
 - We want a wing with low induced drag from the aerodynamic point of view.
 - This means a spanwise lift distribution as close as possible to the elliptical lift distribution.
 - We also want low viscous drag.
 - This strongly depends on the airfoil selection.
 - Satisfying the previous two requirements is not an easy task. If your wing generates the required lift, this is not a problem.
 - You can generate the required lift by changing any of the geometrical parameters of the wing, namely, aspect ratio, taper, span, sweep angle, geometrical/aerodynamic twist, and so on.
 - The wing first stalls inboard.
 - This can be verified by plotting the spanwise lift coefficient distribution.
 - The wing has gentle stall characteristics.
 - The wing does not generate large bending moments.

Wing design principles

- Things such as,
 - Dihedral/anedral angle.
 - High lift devices.
 - Wingtip devices.
 - And other operational requirements, such as, volume for fuel storage, roll rate, and so on, will come at a later stage.
- As you can see, to design a wing you have many possibilities.
- In fact, there are infinite combinations of the wing geometrical parameters.
- Therefore, the use of a fast and reliable tool is highly advisable.

How to compute/estimate the aerodynamic characteristics of wings?

- At this point, the question is, how do we compute the aerodynamic properties of wings?
- To do so, we can resort to the following methods:



- To design the wing, we can also use:
 - Semi-empirical methods (e.g., DATCOM).
 - Previous experience.
 - Experiments in wind tunnel.
 - Trail-and-error (worst approach).
- To estimate $C_{L_{max}}$ and stall progression, we can use the critical section method.

How to compute/estimate the aerodynamic characteristics of wings?

- When doing the initial design of your wing, you will be tempted to use CFD.
- However, CFD is too expensive to be used during the preliminary design phase.
 - CFD can be used to fine tune your design at a later stage.
- But if there is no other choice, or if you have enough time and resources, feel free to use CFD.

- Semi-empirical methods.
- Prandtl lifting-line theory (LLT).
- Vortex lattice methods (VLM).
- 3D panel methods.
- Computational fluid dynamics (CFD).

Less



More

- Mathematical and computational complexity.
- Physics involved.
- Computational resources.
- Simulation time.
- User experience.
- Accuracy.

References

References

- J. Sivells, Experimental and calculated characteristics of three wings of NACA 64-210 and 65-210 airfoil sections with and without 2 degree washout. NACA-TN-1422, August 1947.
- J. Sivells, R. Neely, Method for calculating wing characteristics by lifting-line theory using nonlinear section lift data. NACA-TN-1269, April 1947.
- J. Sivells, R. Neely, Method for calculating wing characteristics by lifting-line theory using nonlinear section lift data. NACA-TR-865, January 1947.
- J. Sivells, S. Spooner, Investigation in the Langley 19-foot Pressure Tunnel of Two Wings of NACA 65-210 and 64-210 Airfoil Sections with Various Type Flaps. NACA-TN-1579, May 1948.
- J. Sivells, S. Spooner, Investigation in the Langley 19-foot Pressure Tunnel of Two Wings of NACA 65-210 and 64-210 Airfoil Sections with Various Type Flaps. NACA-TR-942, January 1949.
- J. Sivells, An improved approximate method for calculating lift distributions due to twist. NACA-TN-2282, January 1951.
- J. Sivells, G. Westrick, Method for calculating lift distributions for unswept wings with flaps or ailerons by use of nonlinear section lift data. NACA-TR-1090, January 1952.

References

- J. Anderson, S. Corda, D. Van Wie, Numerical lifting line theory applied to drooped leading-edge wings below and above stall. J. Aircraft, Vol. 17, No. 12, 1981.
- C. Cone, The theory of induced lift and minimum induced drag of nonplanar lifting systems. NASA-TR-R-129, January 1962.
- H. Multhopp, Methods for calculating the lift distribution of wings (subsonic lifting-surface theory). Aeronautical research council R&M No. 2884, January 1950.
- R. Neely, T. Bollech, G. Westrick, R. Graham, Experimental and Calculated Characteristics of Several NACA 44-series Wings with Aspect Ratios of 8, 10, and 12 and Taper Ratios of 2.5 and 3.5. NACA-TN-1270, May 1947.
- L. Prandtl, Applications of Modern Hydrodynamics to Aeronautics. NACA-TR-116, January 1923.